APPENDIX IX

MATES IV

FINAL REPORT

Regional Modeling Analyses

Authors

Joe Cassmassi

Sang-Mi Lee

Xinqiu Zhang

Kalam Cheung

IX.1 Introduction

The MATES IV regional modeling analysis is presented in Chapter 4 of the main document. This appendix provides the analyses to complement and support the regional modeling demonstration. These include: characterization and validation of the meteorological input data, development of the MATES IV modeling emissions inventory, discussion of the development of the boundary conditions, model performance, and risk.

The Comprehensive Air Quality Model with Extensions enhanced with a reactive tracer modeling capability (CAMx RTRAC, Environ, 2006) provided the dispersion modeling platform and chemistry used to simulate annual impacts of both gaseous and aerosol toxic compounds in the Basin. The version of the RTRAC "probing tool" in CAMx used in the modeling simulations includes an air toxics chemistry module to treat the formation and destruction of reactive air toxic compounds.

Numerical modeling was conducted on a domain that encompassed the Basin and the coastal shipping lanes located in the Southern California Bight portions of the Basin using 2 km by 2 km computational grids. The domain was extended by 80 km to the east to include Coachella Valley and 10 km to the south to include the entire Orange County beyond the MATES III domain. An updated version of the 2012 AQMP emissions inventory for model year 2008, which included detailed source profiles of air toxic sources, provided mobile and stationary source input for the MATES III CAMx RTRAC simulations. Back-casting to the previous MATES modeling inventories was not performed due to the complications involved in the map projections and speciation profiles used in the inventory.

Grid-based, hourly meteorological fields were generated from the Weather Research Forecast (WRF) mesoscale model (Skamarock, 2008). The National Weather Service (NWS) North American Model (NAM) analysis field was employed as initial and lateral boundary values for the WRF modeling. Four dimensional data assimilation was performed using the NAM output enhanced with available upper and surface measurements. WRF was simulated for the period of July 1, 2012, to June 20, 2013, which provided the dispersion platform for the chemical transport modeling using CAMx.

IX.2 Background

MATES IV regional modeling analyses relied on the CAMx RTRAC model to simulate annual impacts of both gaseous and aerosol toxic compounds in the Basin. The 2000 MATES II analysis used the Urban Airshed Model with TOX (UAMTOX) chemistry to simulate the advection and accumulation of toxic compound emissions throughout the Basin. UAMTOX was simulated for 2 km by 2 km grid domain that overlaid the Basin. The analysis relied on the 1997-1998 emissions projection from the 1997 AQMP and meteorological data fields for 1997-1998 generated from objective analysis using a diagnostic wind model. These tools were consistent with those used in both the 1997 and 2003 AQMP attainment demonstrations.

For MATES III, the regional modeling dispersion platform and chemistry simulations progressed from the UAMTOX model to CAMx RTRAC. The second major change in the MATES III modeling analysis was the incorporation of the Mesoscale Meteorological Model 5 (MM5, Grell, 1994) to drive the meteorological data simulation. At that time, MM5 was the state-of-the-art meteorological model used in numerous regional modeling analyses, worldwide.   The transition to CAMx and MM5 was made based on suggestions from peer review for the 2003 AQMP modeling efforts.

During MATES III, MM5 was simulated for two periods to provide the dispersion profile for the CAMx simulations: April 1998 through March 1999 and all days in 2005. As for emissions, an updated version of the 2007 AQMP inventory for model year 2005 was used. This included detailed source profiles of air toxics and mobile and stationary sources for CAMx RTRAC simulations. An additional back-cast of the 2007 AQMP emissions inventory was generated for 1998 to re-simulate MATES II in a framework identical to the MATES III, which enabled a direct comparison of risk assessments of the two previous MATES studies.

The CAMx-MM5 modeling platform from MATES III was updated to the CAMx-WRF coupled system in MATES IV. The WRF, state-of-the-science meteorological modeling tool offers a variety of user options to cover atmospheric boundary layer parameterizations, turbulent diffusion, cumulus parameterizations, land surface-atmosphere interactions, which can be customized to specific geographical and climatological situations. SCAQMD performed extensive sensitivity tests and developments to improve the WRF performance for the South Coast Basin, of which geographical and climatological characteristics impose great challenges in predicting complex meteorological structures associated with air quality episodes. For MATES IV, CAMx with RTRAC algorithms continued to serve as the chemical transport platform, given the importance of tracking chemically active toxic elements individually to assess the contribution of each source category. The RTRAC algorithm provides a flexible approach for tracking the emission, dispersion, chemistry, and deposition of multiple gas- and particle-phase species that are not otherwise included in the model's chemistry mechanisms.

IX.3 CAMx Modeling Domain

Modeling was conducted on a domain that encompassed the South Coast Air Basin and the coastal shipping lanes located in the Southern California Bight portions of the Basin using a 2 km by 2 km grid. Figure IX-1 depicts the MATES IV modeling domain, which was extended by 80 km in the east and 10 km to the south beyond the MATES III domain, which was presented as the shaded area in the figure. The discrepancy of the two domains, other than the size, results from the map projection used in the grid configuration. MATES III employed a UTM coordinate map projection, an orthogonal grid system. MATES IV used a Lambert conformal map projection (reference point was located at 120° 30′ W and 37° N) which complements the meteorological simulations and more accurately represents the geographical setting. Offsets in the orientation of the domain and the shape of the computational grid make it impossible to compare the two modeling results directly on an individual grid level, but meaningful comparisons can be made when averaging results over an extended area, such as a countywide or Basin total. The total integrated risks for each county and the South Coast Basin total were presented in Chapter 4 and the modeling results section later in this Appendix. Concentrations

simulated for a specific location in the domain consisted of a nine-cell distance weighted average.
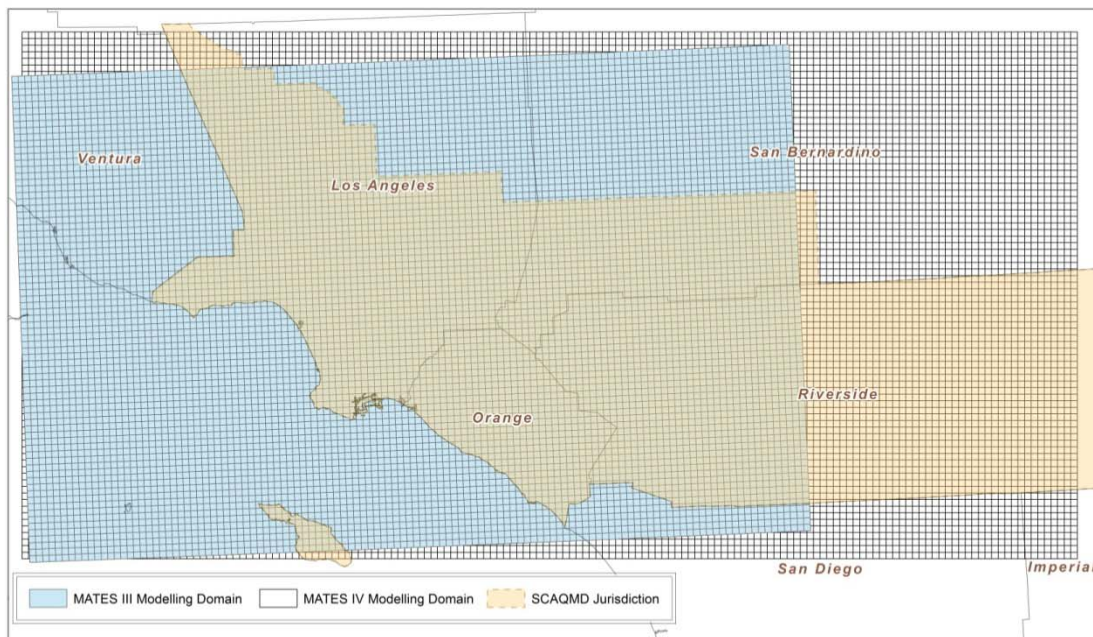
Figure IX-1
MATES IV Modeling Domain. Shaded area represents the MATES III modeling domain.

IX.4 Meteorological Summary for MATES IV Period

Most of the rainfall in Southern California occurs between late fall and early spring, with most rain typically in the months of January and February. Overall, the MATES IV time period from July 2012 through June 2013 had recorded precipitation well below normal (38% of normal), consistent with the developing drought conditions in Southern California. The total rainfall measured at the National Weather Service Downtown Los Angeles station, on the University of Southern California (USC) campus, measured a total of 5.67 inches of rain during the one-year MATES IV period, 38% of the 30-year normal value of 14.93 inches. The monthly precipitation and average temperatures are shown in Table 1. While the typically wet months of November and December 2012 had close to normal rainfall, the other typically wet months of October 2012 and January through April of 2013 all had very low rain amounts. For the calendar year of 2013, only 3.60 inches of precipitation were measured at Downtown Los Angeles, making it the driest calendar year measured in the downtown areas since records began in 1877. The drought-impacted low-rainfall conditions at Downtown Los Angeles were generally consistent with stations throughout southwestern California.

Table IX-1
Monthly Precipitation and Average Temperatures
at Downtown Los Angeles between July 2012 and June 2013

Month	Precipitation			Average Temperature		
	Measured (in.)	**30-Year Normal (in.)**	**Percent of Normal**	**Measured (°F)**	**30-Year Normal (°F)**	**Percent of Normal**
Jul-12	0.01	0.01	100	70.5	73.3	96.2
Aug-12	0.00	0.04	0	76.6	74.3	103.1
Sep-12	Trace	0.24	0	76.3	73.1	104.4
Oct-12	0.02	0.66	3	71.2	68.6	103.8
Nov-12	1.03	1.04	99	63.3	62.4	101.4
Dec-12	2.16	2.33	93	56.7	57.6	98.4
Jan-13	1.18	3.12	38	59.1	58.0	101.9
Feb-13	0.02	3.80	1	57.6	58.9	97.8
Mar-13	0.54	2.43	22	58.3	60.6	96.2
Apr-13	Trace	0.91	0	62.6	63.1	99.2
May-13	0.71	0.26	273	65.5	65.8	99.5
Jun-13	0.00	0.09	0	68.0	69.2	98.3
MATES-IV Period	**5.67**	**14.93**	**38**	**65.5**	**65.4**	**100.1**

The annual averaged temperature at Downtown Los Angeles for the entire MATES IV period was 0.1 degree F above the 30-year normal annual average temperature of 65.4. The months of August through November of 2012 were warmer than normal, along with January 2013. The months of July 2012, December 2012, and February through June of 2013 temperatures were slightly below normal.

Some notable weather events occurred in Southern California during the MATES IV period. A period of excessive heat occurred in the Inland Empire between August 5 through August 20, 2012, with temperatures between 96 and 110 degrees F. The southwestern monsoon was active between about July 21 and September 21, 2012, causing convection and thunderstorms in the desert and mountain areas, occasionally spilling into the South Coast Air Basin. Thunderstorms that occurred over the San Bernardino Mountains and the High Desert on August 9, 11, and 17 of 2012 led to some strong downburst winds and flooding. Thunderstorms that developed over Southern California on August 30, 2012, caused flash flooding in Moreno Valley and Redlands, as well as in the Coachella Valley. Between September 9 and 11, 2012, severe thunderstorms and flash flooding occurred in the desert and mountain areas, the Coachella Valley, and in vicinity of Temecula and Lake Elsinore.

Synoptic conditions were evaluated using 850 hPa temperature and dew point temperature measured via a rawinsonde launched at Miramar Marine Corps Air Station, the closest World Meteorological Organization's weather sounding station to the Basin. Average temperature and dew point temperature during the MATES IV period were 14.9 C and -4.6 C, respectively at 850

hPa height. These values are very close to those measured during the MATES III period: 14.1 C and -4.7 C. The difference in the ambient and dew point temperature confirms that the MATES IV period was drier than the MATES III period, confirming that drought conditions affected all of Southern California. Note that an ambient temperature close to dew point indicates that the atmosphere is near saturation. In other words, the closer the two temperatures are, the wetter the atmosphere is. When air is fully saturated, the relative humidity is 100 % and the ambient and dew point temperatures become identical.

IX.5 WRF Numerical Model Configuration

The WRF mesoscale model developed by National Center for Atmospheric Research (NCAR) was employed to produce meteorological fields for CAMx RTRAC simulations. The WRF simulations were comprised of four nested domains with horizontal grid distances of 36, 12, 4, and 2 km respectively. The first three domains were configured in a two-way nested approach, and the innermost domain was developed as one-way nesting from the 4 km domain. The relative sizes and locations of each domain are given in Figure IX-2. The innermost domain spans 334 km X 174 km in east-west and north-south directions, respectively, which overlaps the CAMx domain by three additional rows and columns in each lateral boundary. The initial guess field and lateral boundary values for the outermost domain were extracted from the operational National Center for Environmental Prediction North American Model (40 km grid resolution) grid analysis. The databases contain variables of air temperature, geopotential height, heat flux, humidity, precipitable water, sea level pressure, shortwave radiation, snow water equivalent, surface air temperature, surface winds, thermal infrared, upper level winds, vertical wind, and vorticity at each isobaric level of 1000, 975, 950, 925, 900, 875, 850, 800, 750, 700, 650, 600, 550, 500, 450, 400, 350, 300, 275, 250, 225, 200, 175, 150, 100, 50 hPa.   (Refer to http://dss.ucar.edu/datasets/ds609.2 for further dataset information).

Four dimensional data assimilation (FDDA) was conducted by utilizing the National Weather Service (NWS) twice-daily sounding data and hourly surface measurements. Each simulation was conducted for a four-day period with the first 24 hours used as a spin up period. The detailed configuration and physical options used in the WRF simulation are listed in Table IX-2.

WPS Domain Configuration
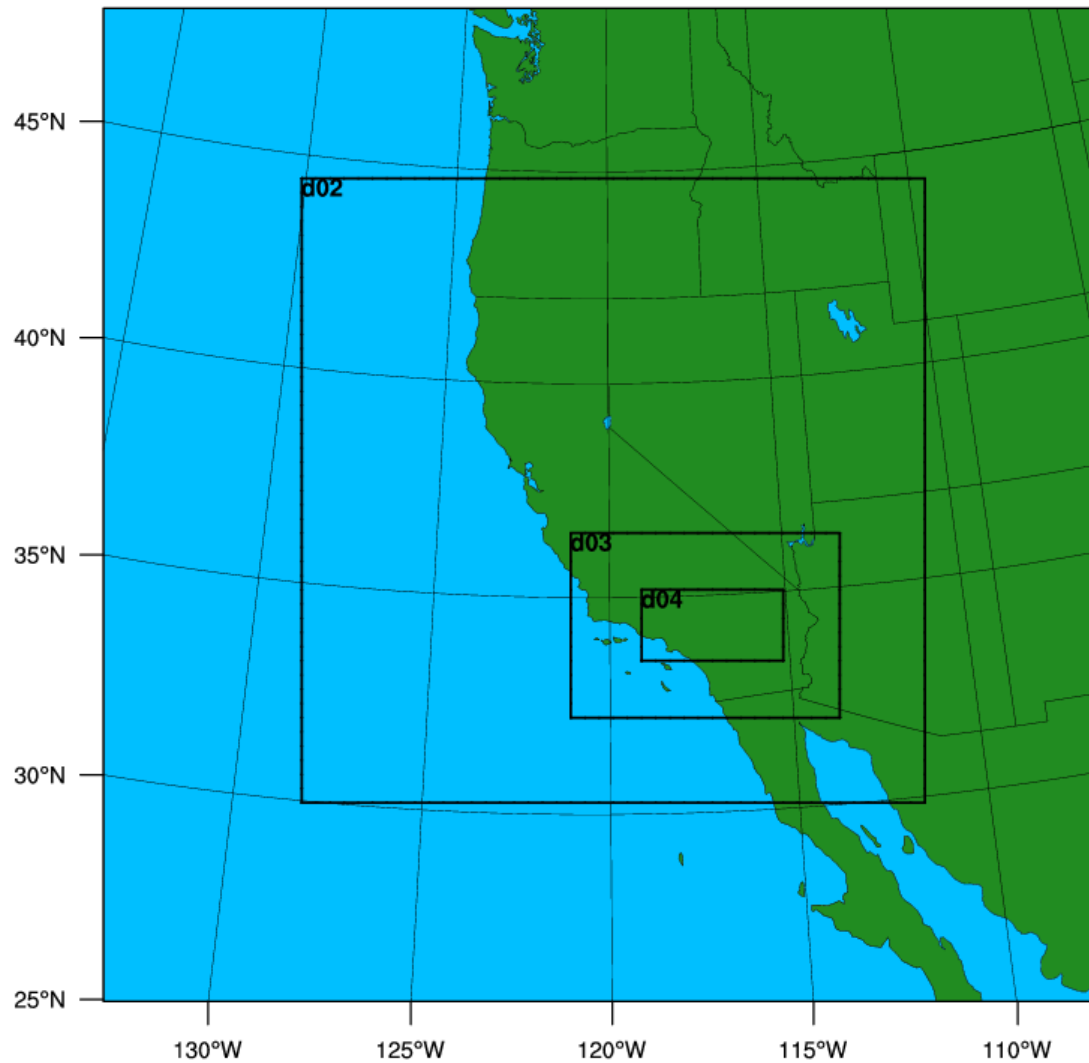
Figure IX-2.
The relative locations and sizes of the four WRF nested domains.

Table IX-2
WRF configuration and its comparison to MM5 used in the MATES III

Component	MATES IV (July 2012-June 2013)	MATES III (2005)
Numerical Platform	WRF version 3.4.1	MM5 version 3.7
Number of grids	(167 X 87) in east-west and north-south respectively	(127 X 82) in east-west and north-south respectively
Number of vertical layers	30 layers with the lowest layer being approximately at 20 m agl.	29 layers with the lowest layer being approximately at 20 m agl.
Initial and boundary values	NCEP NAM analysis field (40 km grid distance)	NCEP ETA 218 grid analysis field (12 km grid distance)
Boundary layer scheme	YSU	Blackadar
Soil model	Five-layer soil model	Five-layer soil model
Cumulus parameterization	Explicit	Explicit
Micro physics	Simple ice	Simple ice
Radiation	Cloud radiation	Cloud radiation
Four dimensional data analysis	Analysis nudging with NWS surface and upper air measurements	Analysis nudging with NWS surface and upper air measurements

IX.6 Meteorological Model Performance

The WRF performance was extensively evaluated using NWS surface measurements and Environ's METSTAT (ENVIRON, 2001) statistical software to compute mean, bias, gross error, root mean square error (RMSE), and index of agreement.

Figure IX-4 shows the time series of hourly observed and predicted temperature at 2 m above ground level (agl) for October 2012. The model successfully resolved overall cooling and warming trend induced by synoptic scale motions, while both daily minimum temperatures in the beginning of the month and daily maximum in the end of the month were slightly under-predicted. This can be partly attributed to inaccurate representation of surface characteristics such as soil moisture content and land use category.
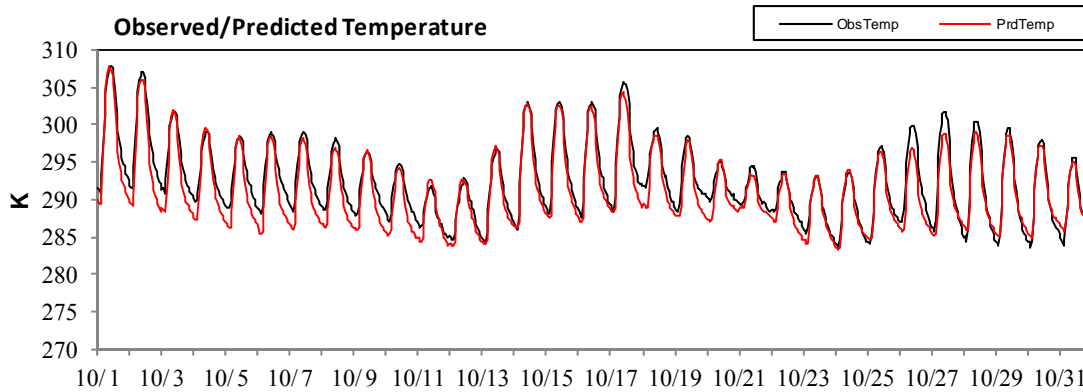
Figure IX-3

Time series of observed and predicted temperature at 2 m above ground level for October 2012. The data are hourly average observations of all available measurements within the domain and the corresponding predictions.

In all, the model has less than 4 degrees of bias and gross error and approximately 4 degrees of RMSE, which are approximately equivalent to WRF performance for 2012 Air Quality Management Plan (AQMP) modeling case. Wind speed turned out to be underpredicted by less than 1.7 m s^{-1}. In general, all conventional surface parameters including wind speed, direction, temperature and water vapor mixing ratio showed good agreement with the observations (Figures IX-4 through IX-6).
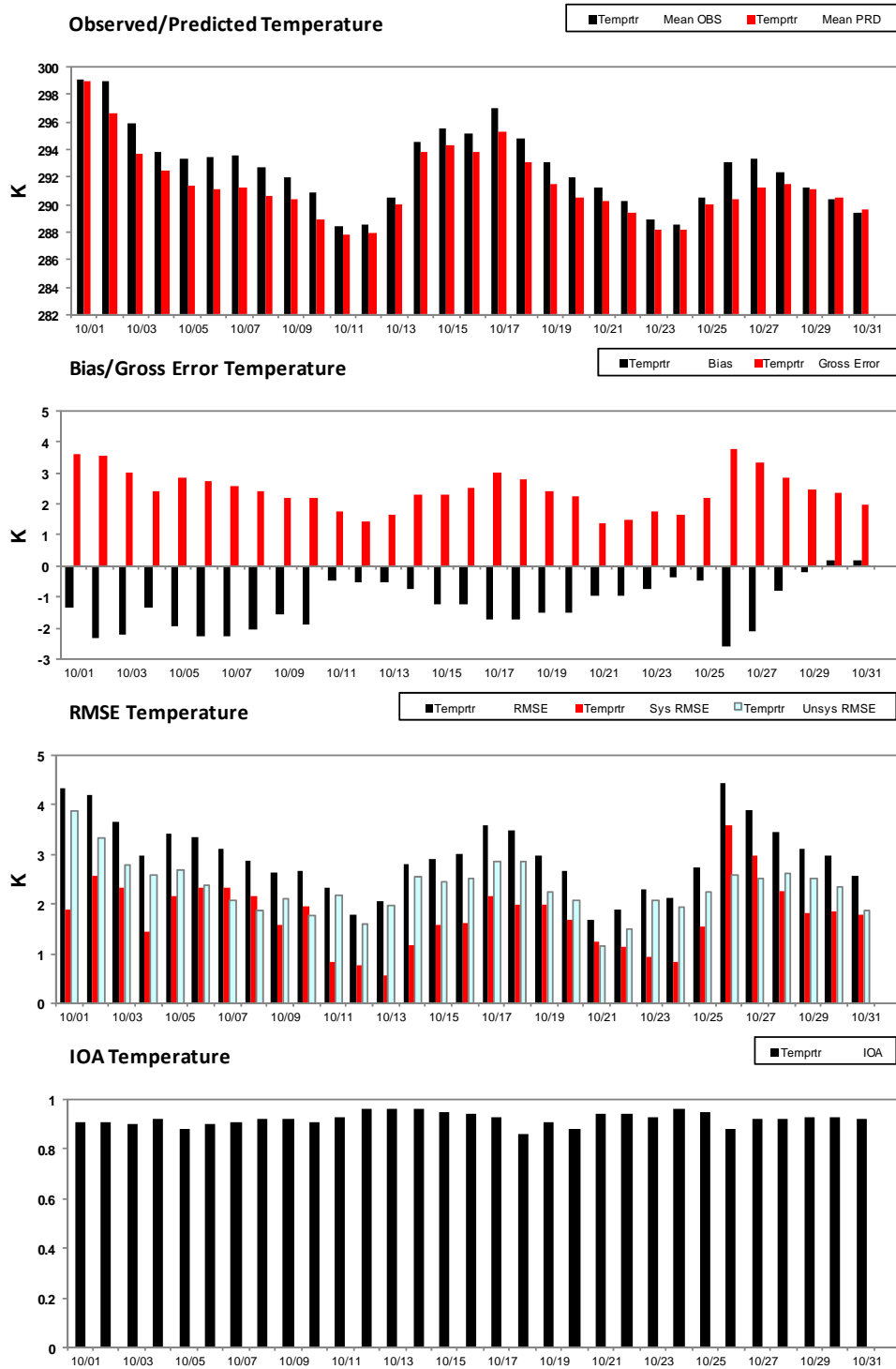
Figure IX-4

Daily averaged (a) mean, (b) bias and gross error, (c) root mean square error, and (d) index of agreement for observed and predicted temperature at 2 m agl.
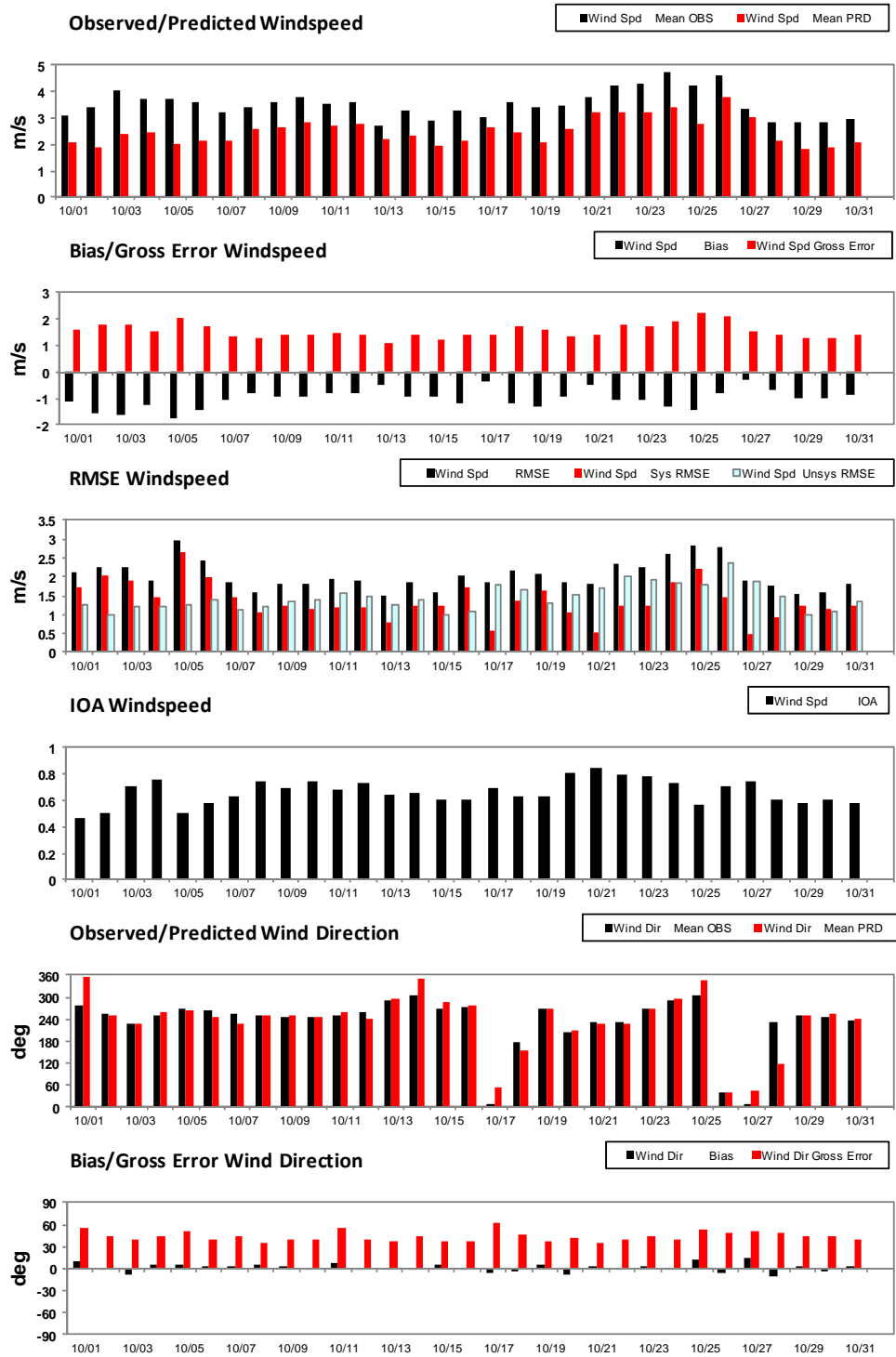
Figure IX-5

Daily averaged (a) mean, (b) bias and gross error, (c) root mean square error, and (d) index of agreement for observed and predicted wind speed. (e) Mean and (f) bias and gross error of wind direction are presented as well.
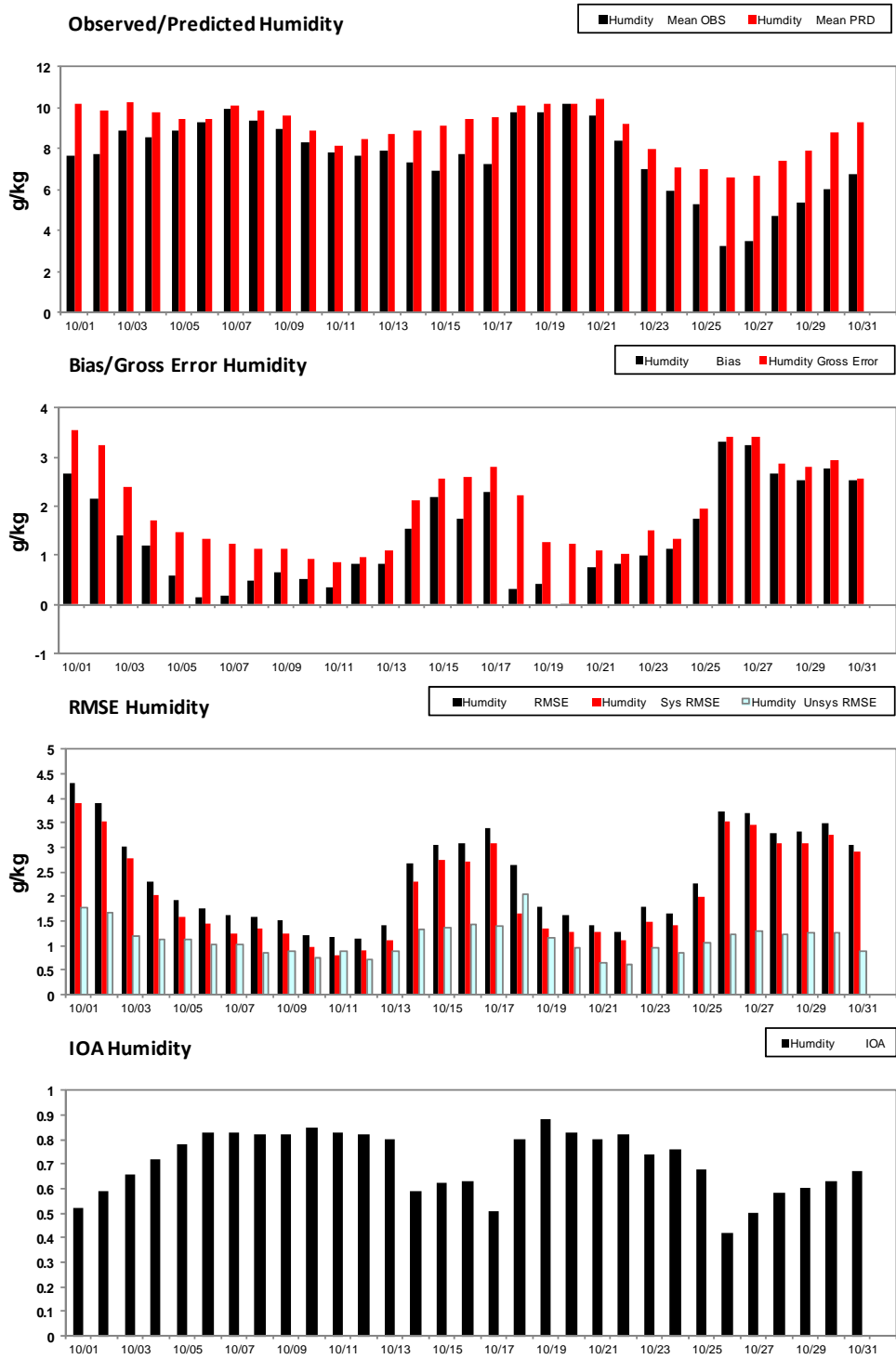
Figure IX-6

Daily averaged (a) mean, (b) bias and gross error, (c) root mean square error, and (d) index of agreement for observed and predicted humidity at 2 m agl.

IX.7 Wind Rose Comparison

While the METSTAT evaluation is a useful tool to assess the performance of the regional WRF simulations, it is important to examine the capability to recreate observed annual local scale wind patterns. To assess the local scale prevailing flow, wind roses were generated from the hourly WRF model output for the 2 km by 2 km grid cell and measurements from NWS stations. The WRF winds were retrieved from a grid in which a NWS station is located. An exact replication of the measured winds was not expected in the analysis. However, comparison of the modeled and measured annual average wind roses offers a visual comparison of the fit of the simulation to the local scale and assists in the evaluation of chemical transport model performances.

Figures IX-7a through IX-7f depict the wind roses for Fullerton, Burbank, San Bernardino, Long Beach, Santa Monica, and Riverside during the MATES IV sampling period from July 2012, to June 2013. Subtle nuances between the simulated and observed winds are observed at all stations.   In general, wind speeds are slightly lower for the WRF simulation. The directional frequencies are reasonably well-captured at most sites, with an offset in the primary wind vector of less than one sector (22.5 degrees). It is important to note that the local emissions sources (particularly ground level) directly upwind of the monitoring site have a significant impact to the measured concentration profile. As such, a minor one-sector difference in the simulated wind direction may impact the CAMx RTRAC performance.
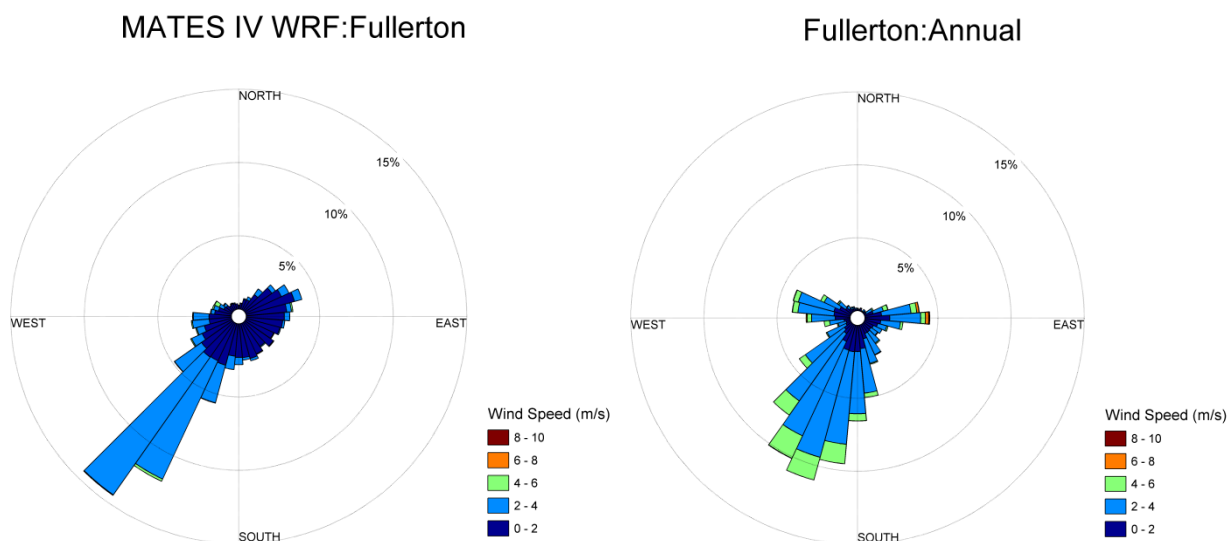
Figure IX-7a.
WRF Simulated and Observed Annual Wind Roses at Fullerton.

MATES IV WRF:Burbank   Burbank:Annual
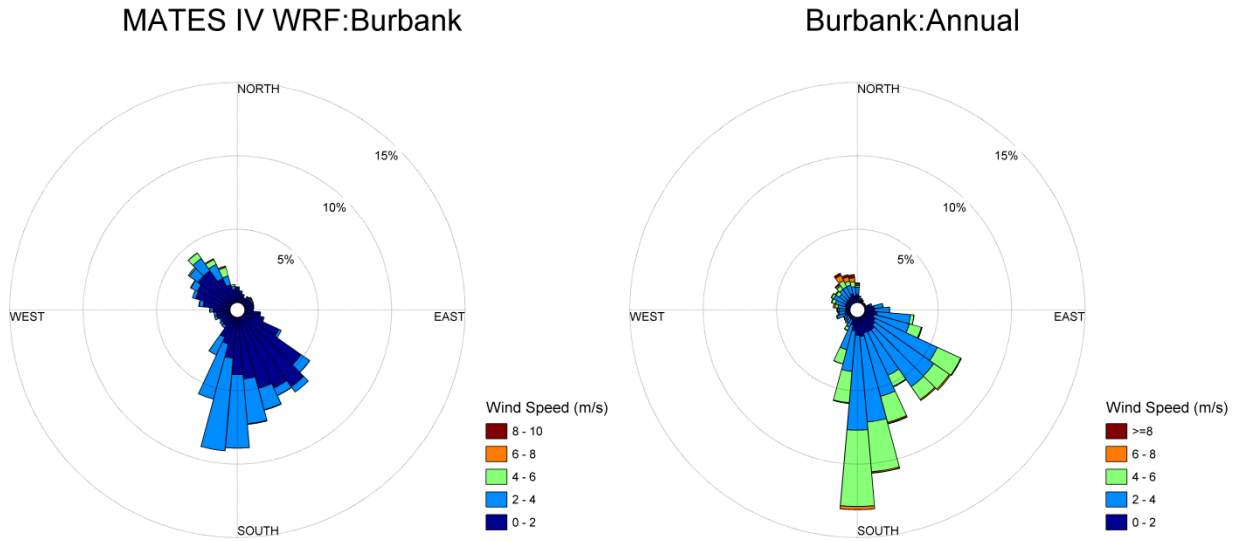
Figure IX-7b.
WRF Simulated and Observed Annual Wind Roses at Burbank.

MATES IV WRF:San Bernardino   San Bernardino:Annual
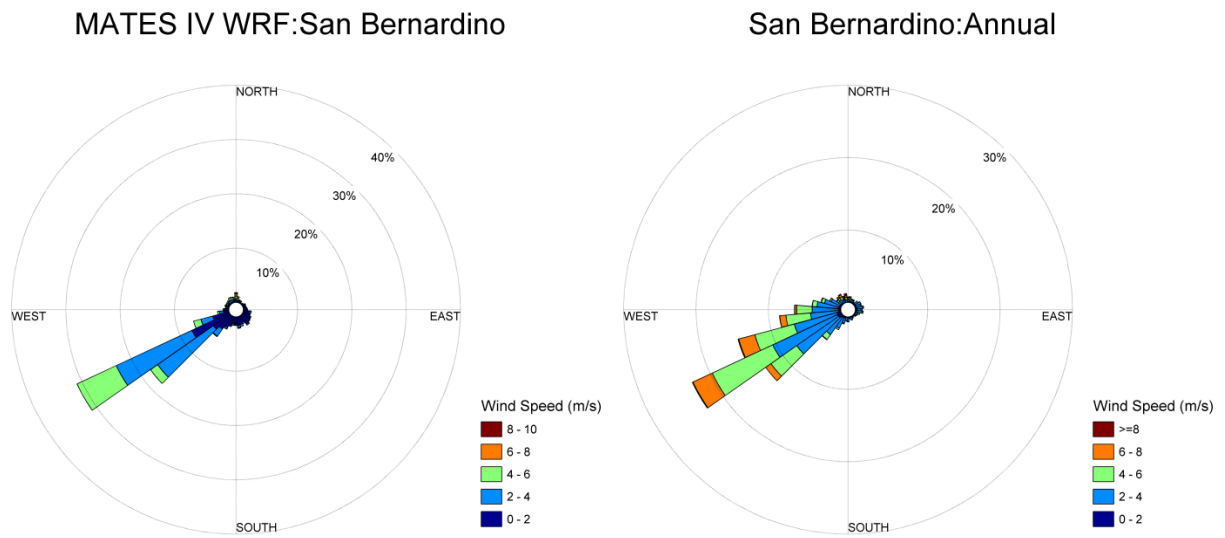
Figure IX-7c.
WRF Simulated and Observed Annual Wind Roses at San Bernardino.

MATES IV WRF:Long Beach
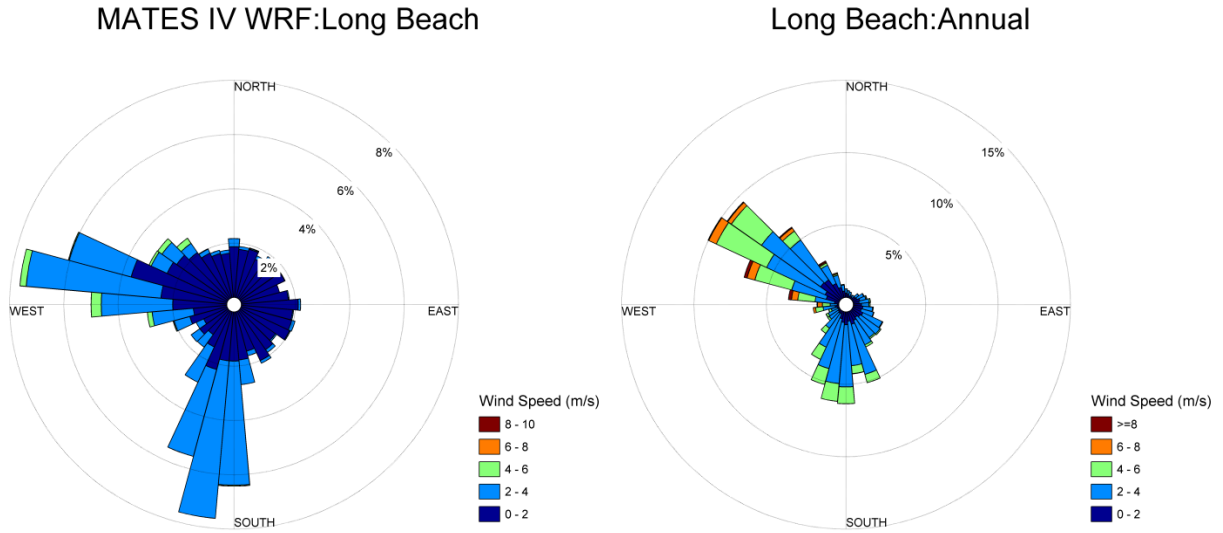
Long Beach:Annual

Figure IX-7d.
WRF Simulated and Observed Annual Wind Roses at Long Beach.

MATES IV WRF:Santa Monica

Santa Monica:Annual
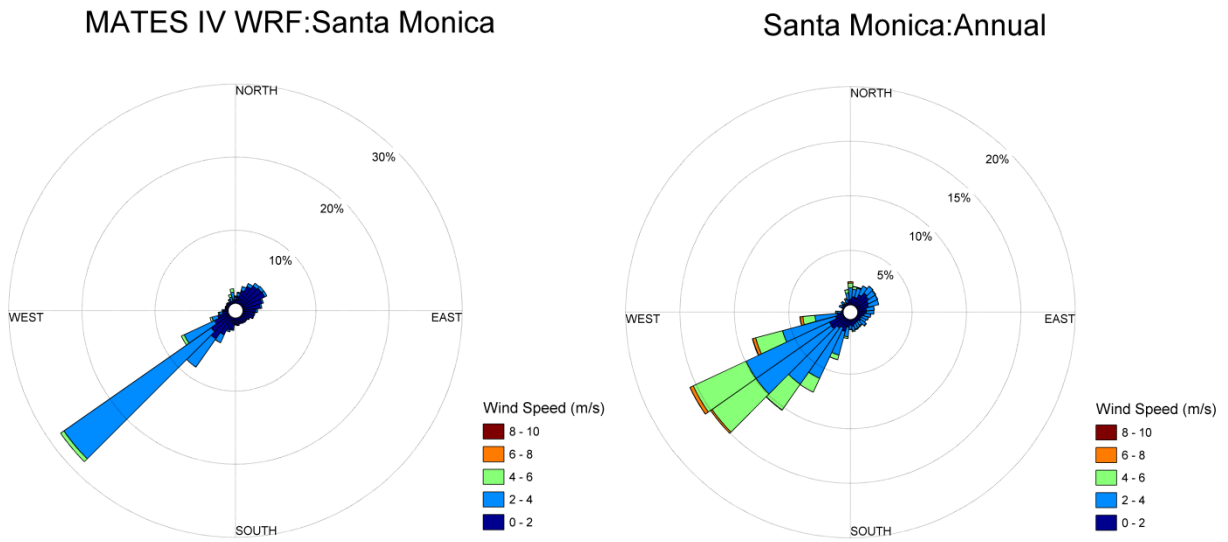
Figure IX-7e.
WRF Simulated and Observed Annual Wind Roses at Santa Monica.
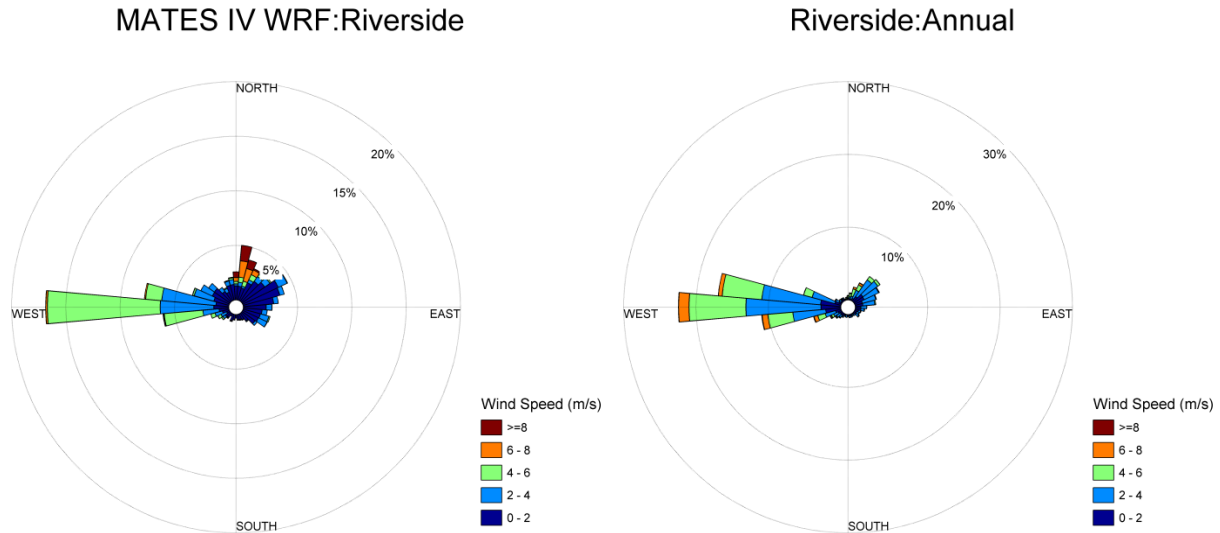
Figure IX-7f.
WRF Simulated and Observed Annual Hourly Averaged Wind Roses at Riverside.

IX.8 Vertical Dispersion

The WRF output was converted to the CAMx RTRAC format using 'wrfcamx_v3.2' software. Vertical diffusivity (Kv), which is critical in vertical dispersion, was computed using CMAQ vertical diffusivity scheme with a minimum value of 1.0 m^2/sec. The number of vertical layers was reduced to 18 layers from the 30 layer configuration used in the WRF. The layers of which height was below 2 km from the ground level were not modified. The layers above 2 km were collapsed to four layers in order to reduce computation cost. Note that the vertical structure was chosen carefully to optimize computational efficiency and numerical accuracy after an extensive sensitivity study to evaluate the impact of vertical layer structure using various numbers of computational layers.

During the development phase of the meteorological data sets, WRF was tested using a variety of mixing scheme including CMAQ (Byun and Ching, 1999) and the O'Brien 70 [OB70] (O'Brien, 1970), with various values of default minimum vertical diffusivity, ranging from 0.1 to 1.0 m^2/sec.

Based on peer review comments from MATES III and experiences from previous MATES and AQMP attainment demonstrations, the Kv patch algorithm (Environ, 2006) was applied in the dispersion calculation. The Kv patch algorithm imposes minimum Kv values that are pre-assigned for each land use category, regardless of the diffusivity estimated from the WRF simulated meteorological condition. In the current study, the first and second computational layers, which are centered approximately 80 m and 140 m above ground level, respectively, were subject to the direct modification of the Kv through the Kv patch.

$EC_{2.5}$ concentration from CAMx RTRAC revealed that that the *OB70* scheme predicted higher concentrations at key sites. This overprediction occurred in the CMAQ scheme with 0.1 m²/sec minimum diffusivity, as well. All of the combinations, regardless of layer structure or minimum *Kv*, resulted in overprediction at Long Beach and West Long Beach and underprediction to varying degrees at Rubidoux and Inland Valley San Bernardino. The use of *Kv* patch modestly improved the bias. This nominal impact was attributed to the fact that 1.0 m²/sec chosen as default minimum *Kv* was relatively large so that the *Kv* patch did not introduce significant changes in tracer dispersion.

In all, after careful evaluation of various sensitivity analyses, the vertical dispersion profile used in the final MATES IV CAMx RTRAC simulations relied on a 16-layer structure using the CMAQ diffusivity scheme overlaid with the *Kv*-patch option set at 1.0 m²/sec value of *Kv*.

IX.9 MATES IV Modeling Emissions

An updated version of the 2012 AQMP emissions inventory for the year 2012 provided mobile and stationary source input for the MATES IV CAMx RTRAC simulations. Mobile source emissions were adjusted for time-of-day and day-of-week travel patterns based on CalTrans weigh-in-motion data profiles. Table IX-3 lists the annual average day emissions projected for 2012. (A comprehensive breakdown of the planning VOC, NOx, CO, SO2 and particulate emissions for 2012 used in the MATES IV simulation is provided in Chapter 3 and Appendix XIII). Table IX-3 also includes the MATES III TSP and $PM_{2.5}$ diesel emissions for 2005 for comparison.

A comparison of the MATES IV (2012 AQMP) 2012 projection of the $PM_{2.5}$ diesel emissions shows a 66% reduction in emissions from the 2005 emissions used in MATES III. The most significant area of diesel particulate matter emissions reduction occurs in the off-road categories. While most of those emissions reductions are real, reflecting control efforts and fleet turnover in the past several years, some of the changes are due to methodological changes in emissions inventories employed in the two AQMPs.

Figures IX-8a through IX-8x provide the grid-based weekday modeling emissions for selected toxic pollutant and precursor emissions categories.

IX.10 MATES IV vs. MATES III: Key Emissions Modeling Assumptions

Since the regional modeling effort in MATES II, the basic approach in preparing modeling emissions remained the same, i.e., based on the corresponding AQMP inventories and speciation profiles. Three relatively minor changes to emissions data preparation were implemented in the MATES IV modeling. First, emissions from ocean-going vessels in the shipping lanes and ports were assumed emitted into the stacks with stack parameters based on Mason, *et al.* (2008) while emissions from harbor craft and commercial boats were released at sea level. In MATES III, the combined shipping emissions were assumed to be 70% released through stacks while the rest at sea level.

Table IX-3
Annual Average Diesel/EC Emissions in the SCAB (TPD)

Compound	MATES IV 2012		MATES III 2005	
	PM$_{2.5}$	TSP	PM$_{2.5}$	TSP
EC	11.58	14.74	14.38	19.44
Total Diesel Particulate Matter (DPM)	9.43	10.24	27.99	30.34
DPM per Major Source Category				
On-road	4.97	5.40	10.20	11.08
Off-road	2.94	3.20	11.23	12.21
Ships	0.74	0.78	5.18	5.55
Trains	0.56	0.61	0.86	0.94
Stationary	0.22	0.25	0.52	0.55
Total DPM	9.43	10.24	27.99	30.34

Diesel Emissions (PM2.5)
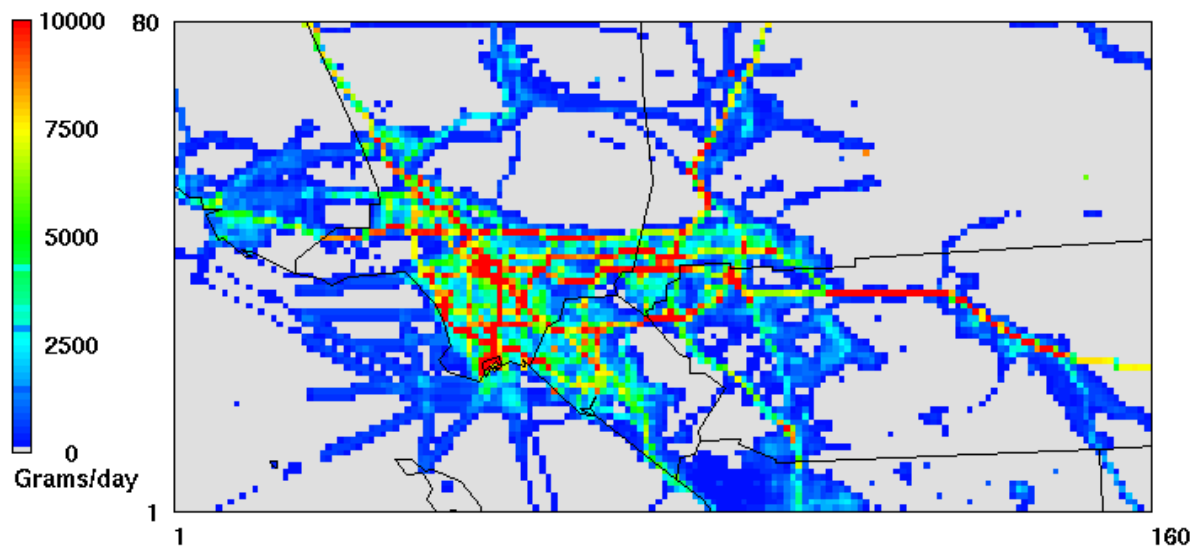
Figure IX-8a
Weekday average emissions pattern for Total Diesel PM$_{2.5.}$

Elemental Carbon Emissions (PM2.5)
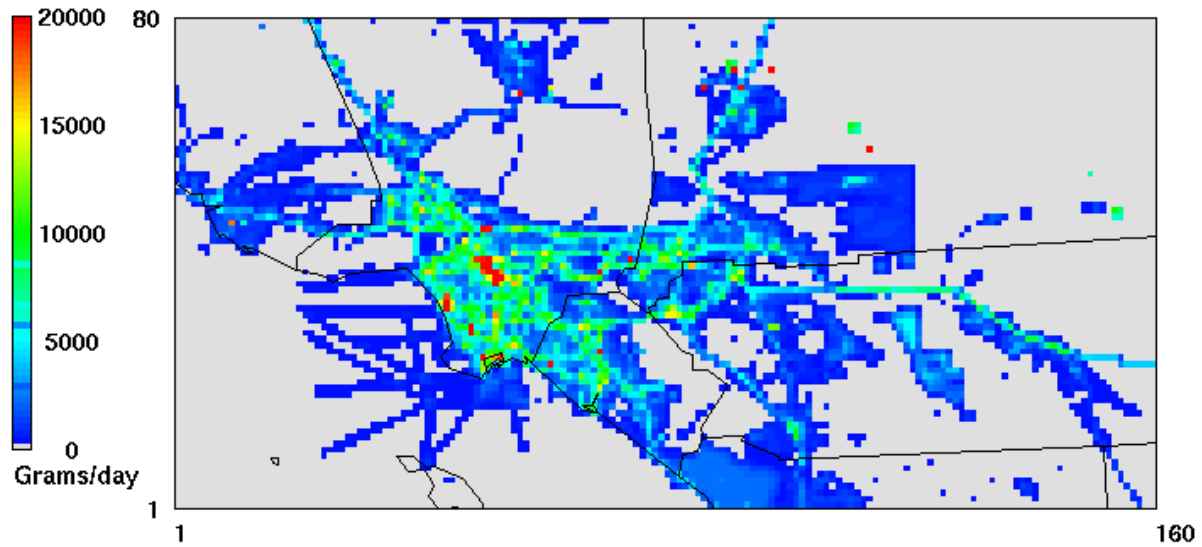
Figure IX-8b
Weekday average emissions pattern for Elemental Carbon.

On-Road Diesel Emissions (PM2.5)
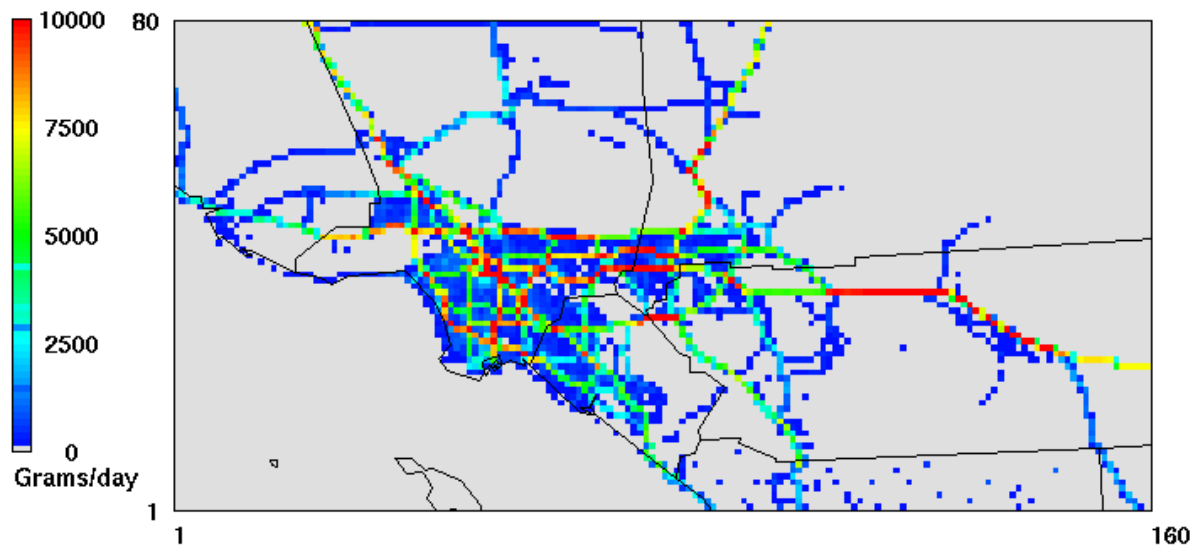
Figure IX-8c
Weekday average emissions pattern for On-Road Diesel PM$_{2.5.}$

Off-Road Diesel Emissions (PM2.5)
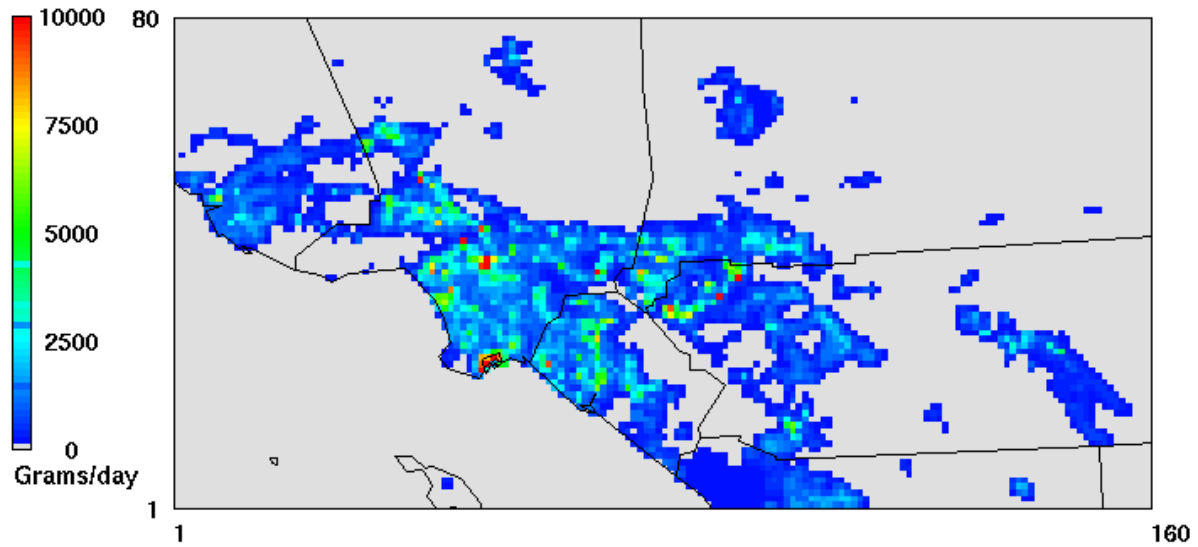
Figure IX-8d
Weekday average emissions pattern for Off-Road Diesel PM$_{2.5}$.

Pattern of Diesel Emissions (PM2.5) from Ships
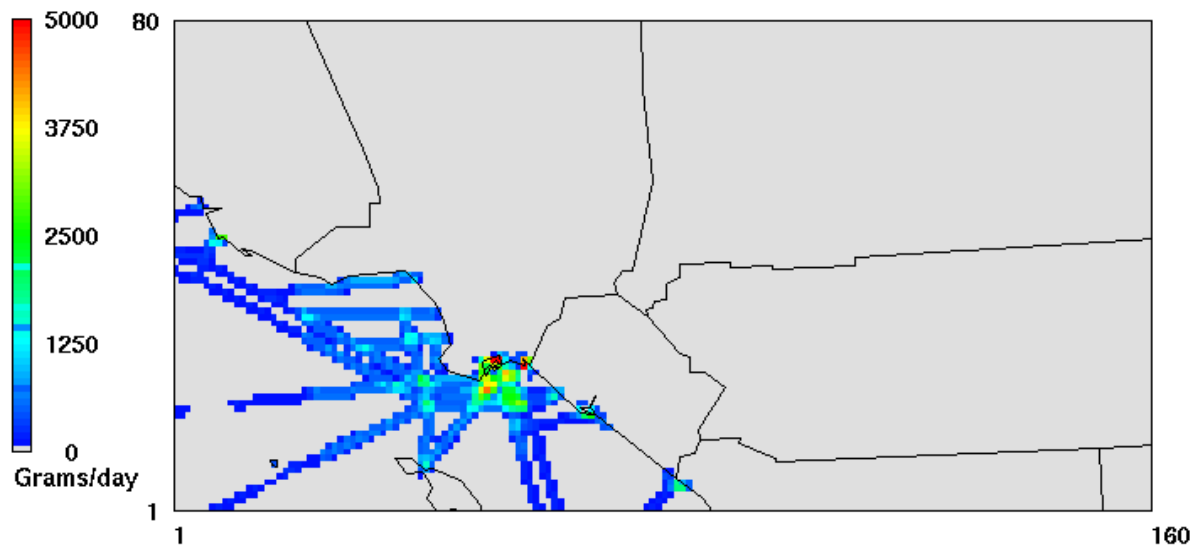
Figure IX-8e
Weekday average emissions pattern Diesel PM$_{2.5}$ from Ships.

Diesel Emissions (PM2.5) from Trains
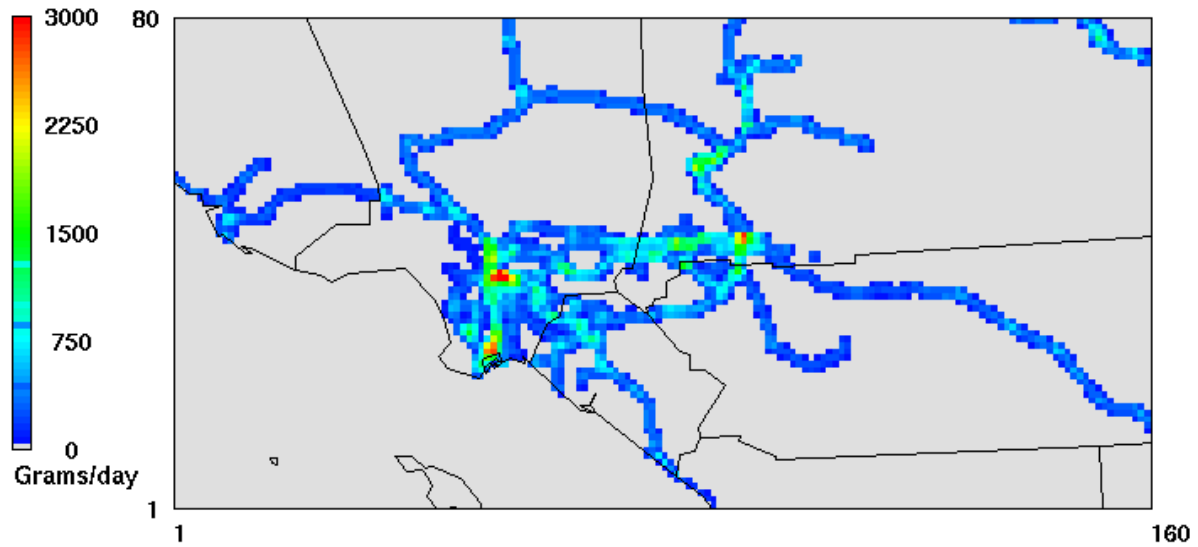
Figure IX-8f
Weekday average emissions pattern Diesel PM$_{2.5}$ from Trains.

Stationary Diesel Emissions (PM2.5)
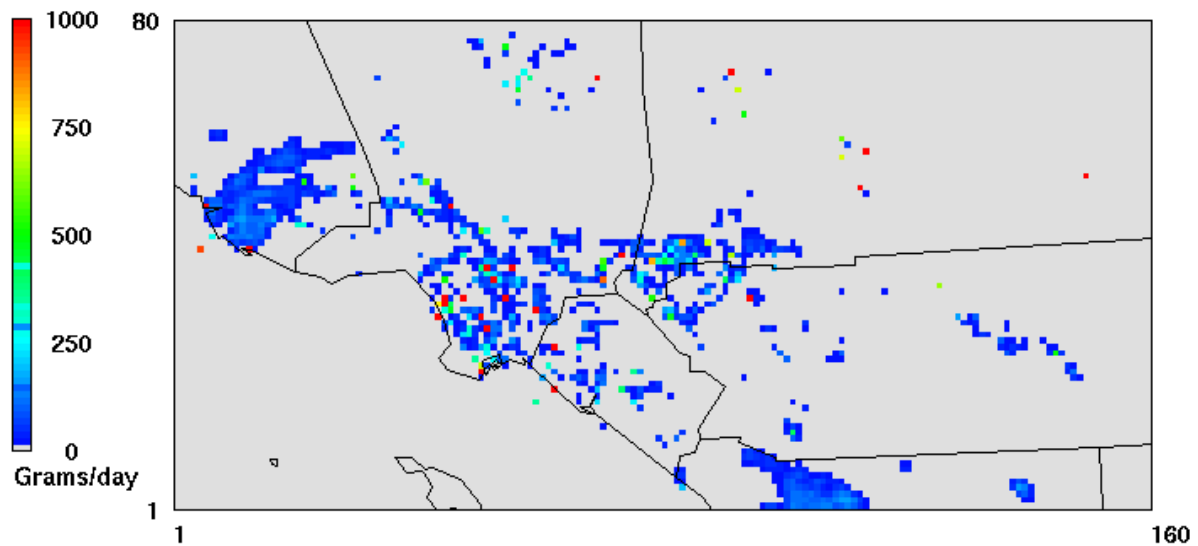
Figure IX-8g
Weekday average emissions pattern Diesel PM$_{2.5}$ from Stationary Sources.

Distributions of VOC Emissions

as represented by ALK4 emissions
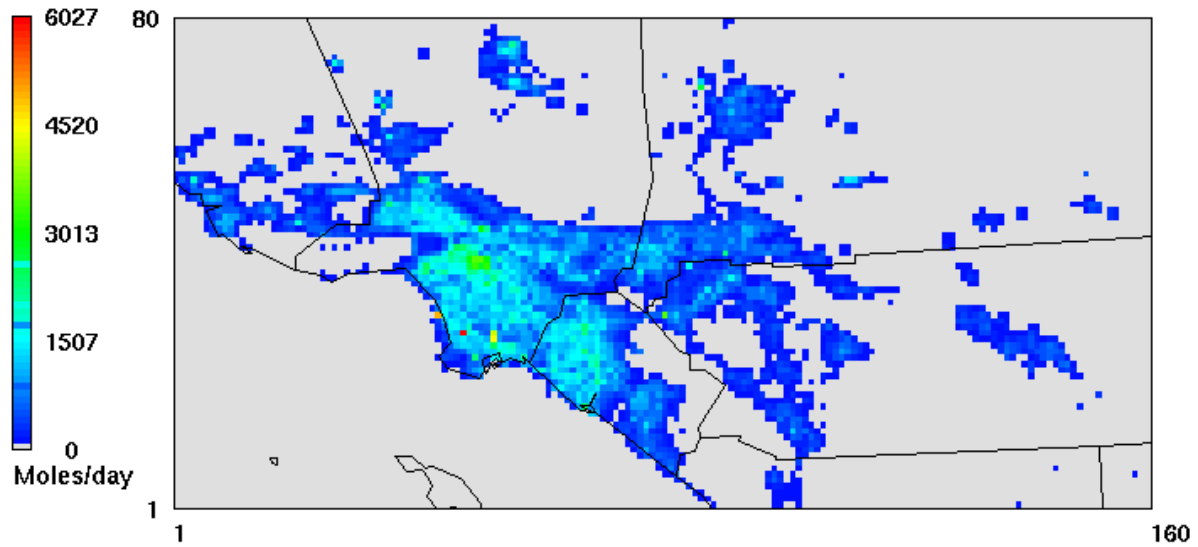
Figure IX-8h
Weekday average VOC emissions pattern.

NOx Emissions
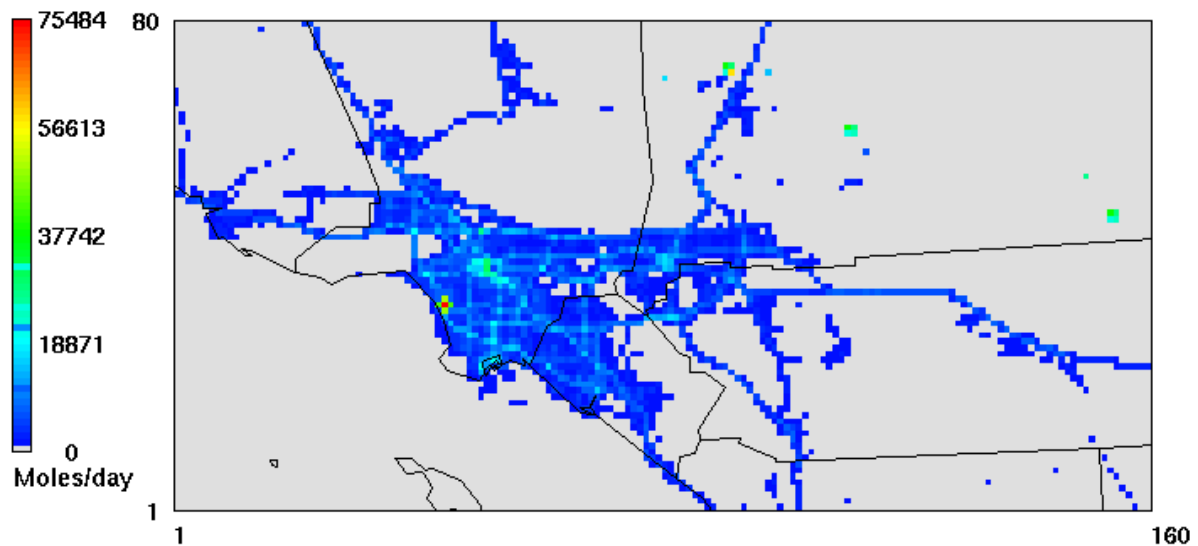
Figure IX-8i
Weekday average NOx emissions pattern.

CO Emissions
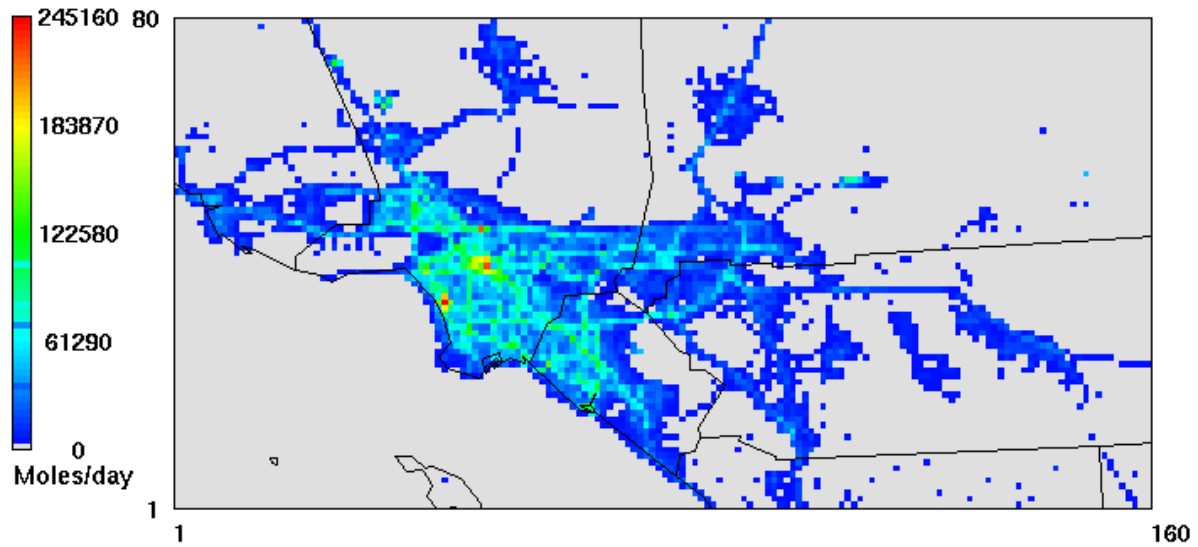
Figure IX-8j
Weekday average CO emissions pattern.

Acetaldehyde Emissions
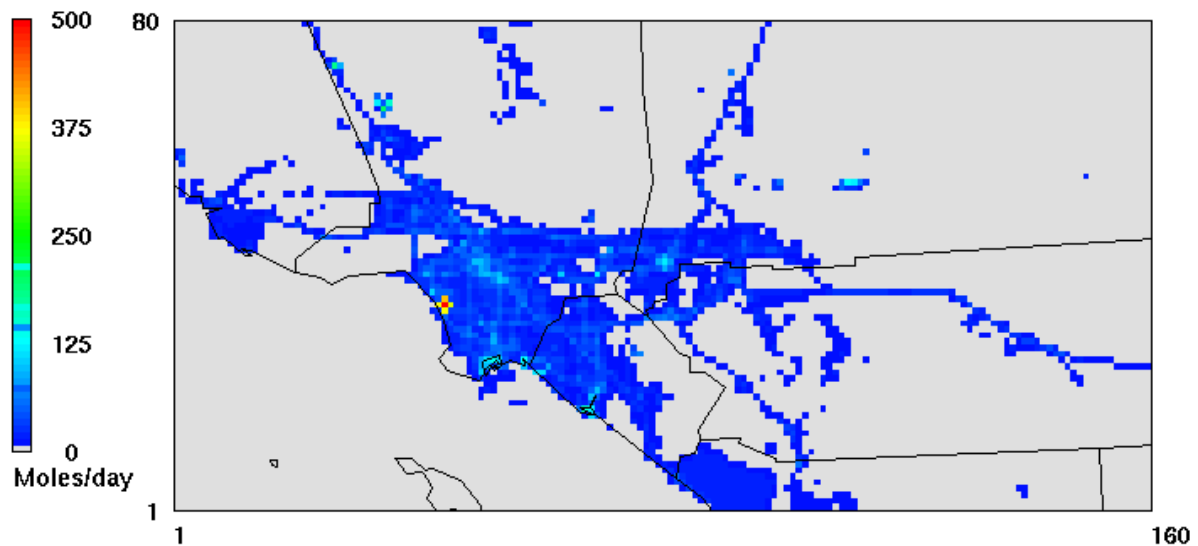
Figure IX-8k
Weekday average emissions pattern for Acetaldehyde.

Arsenic Emissions (PM2.5)
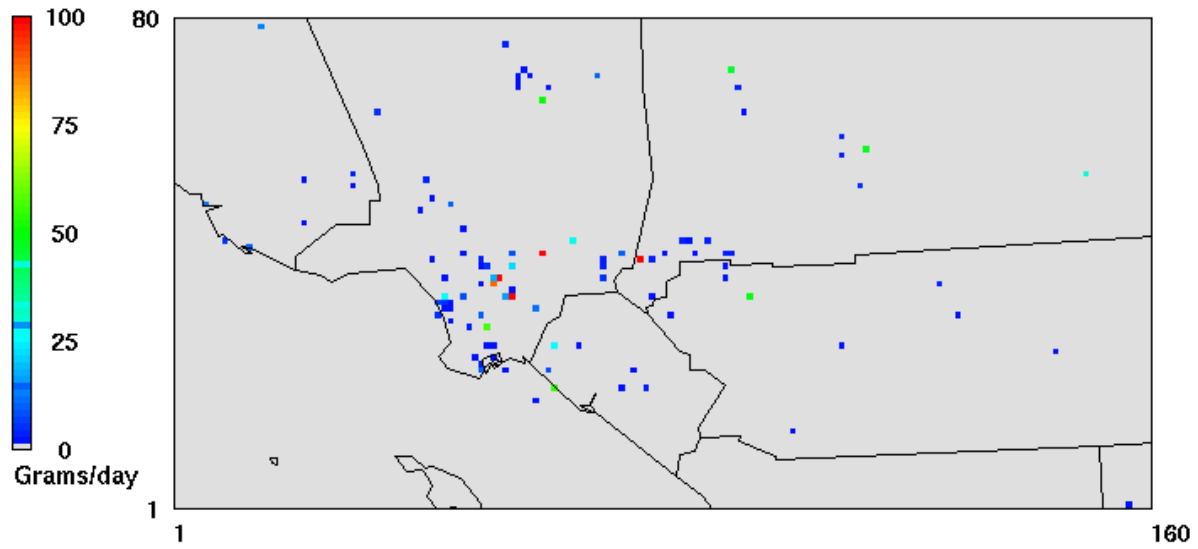
Figure IX-8l
Weekday average Arsenic emissions pattern.

Benzene Emissions
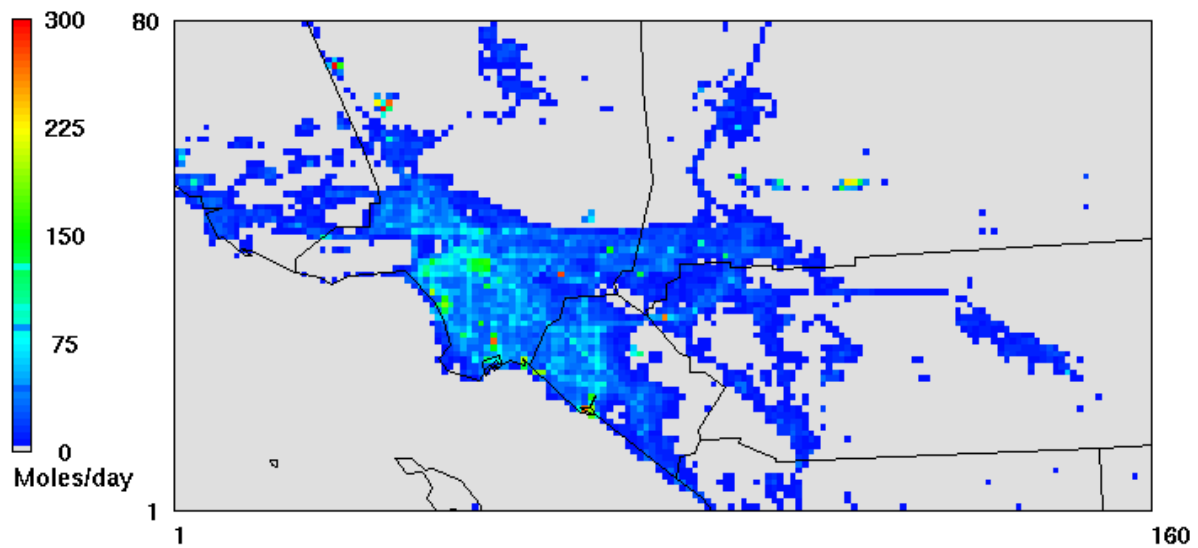
Figure IX-8m
Weekday average Benzene emissions pattern.

1,3Butadiene Emissions
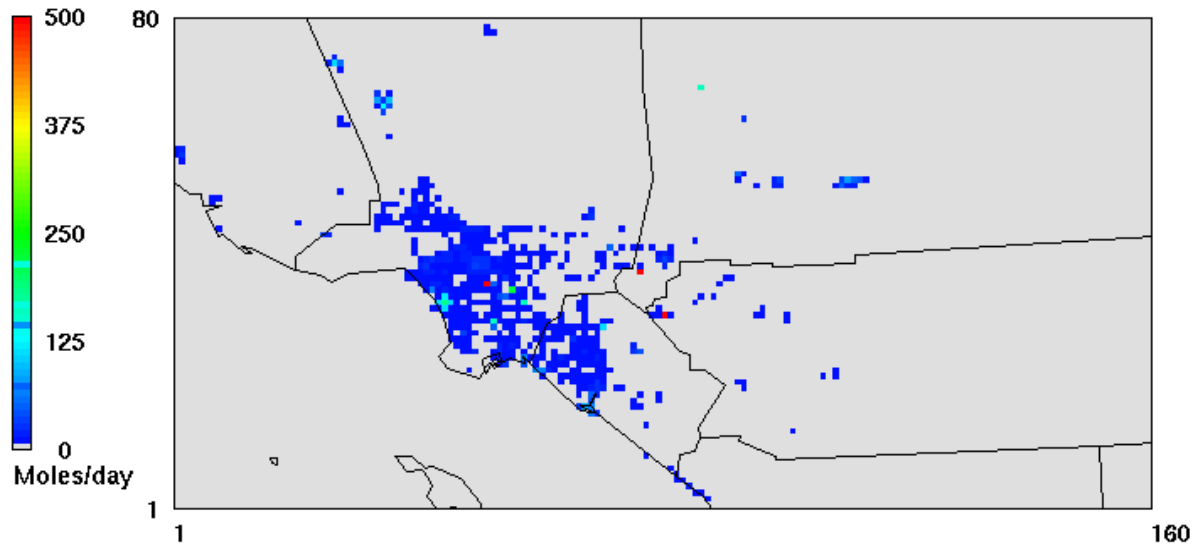
Figure IX-8n
Weekday average 1,3-Butadiene emissions pattern.

Cadmium Emissions (PM2.5)
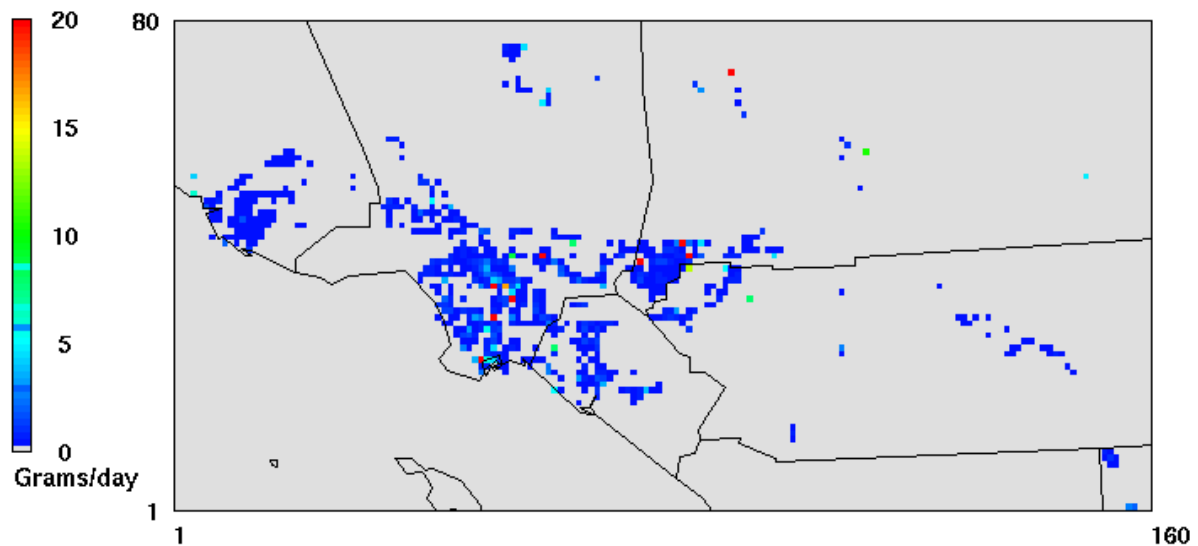
Figure IX-8o
Weekday average Cadmium $PM_{2.5}$ emissions pattern.

Chromium Emissions (PM2.5)
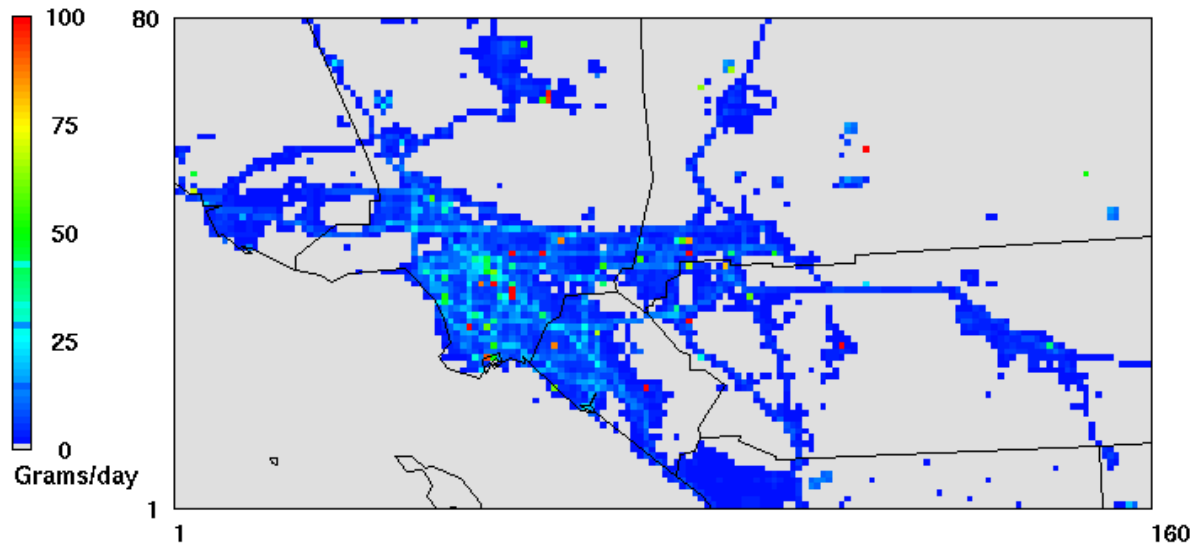
Figure IX-8p
Weekday average Chromium PM$_{2.5}$ emissions pattern.

Hexavalent Chromium Emissions (PM2.5)
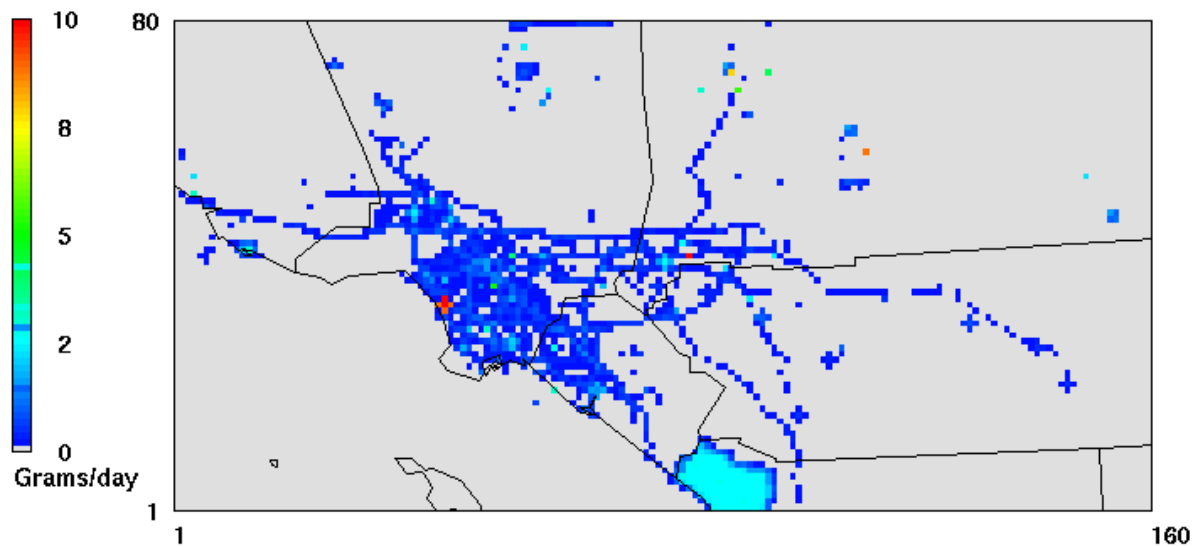
Figure IX-8q
Weekday average Hexavalent Chromium PM$_{2.5}$ emissions pattern.

Lead Emissions (PM2.5)
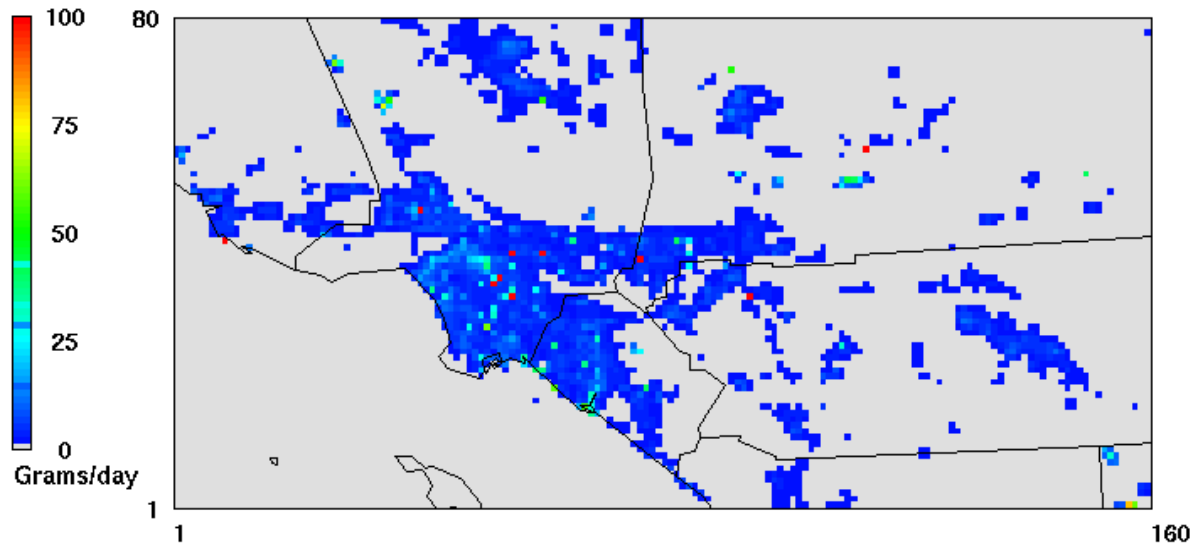
Figure IX-8r
Weekday average Lead $PM_{2.5}$ emissions pattern.

Methylene Chloride Emissions
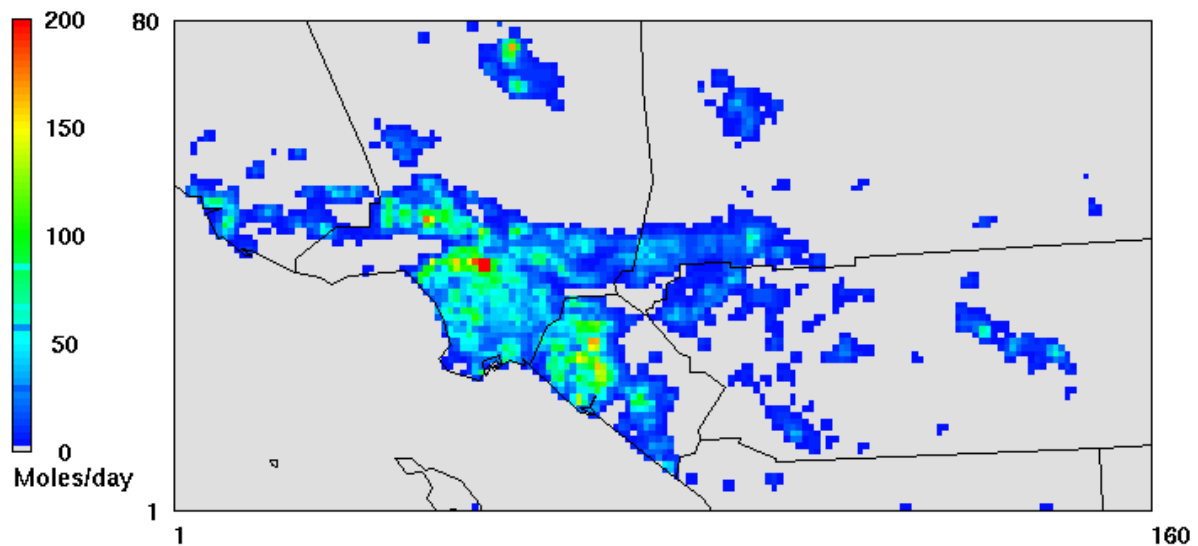
Figure IX-8s
Weekday average Methylene Chloride emissions pattern.

Naphthalene Emissions
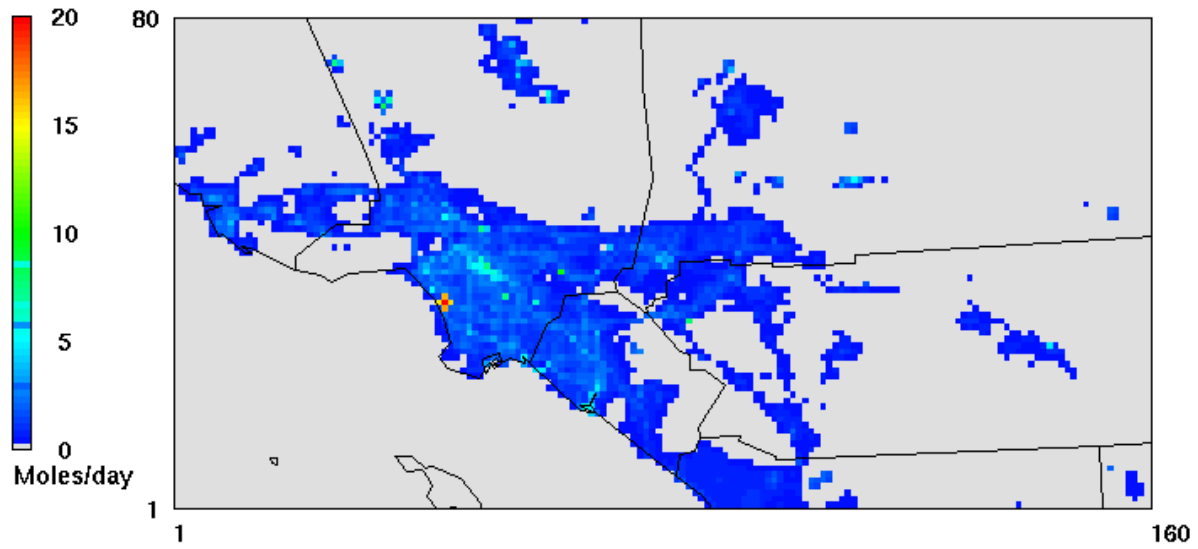
Figure IX-8t
Weekday average Naphthalene emissions pattern.

Nickel Emissions (PM2.5)
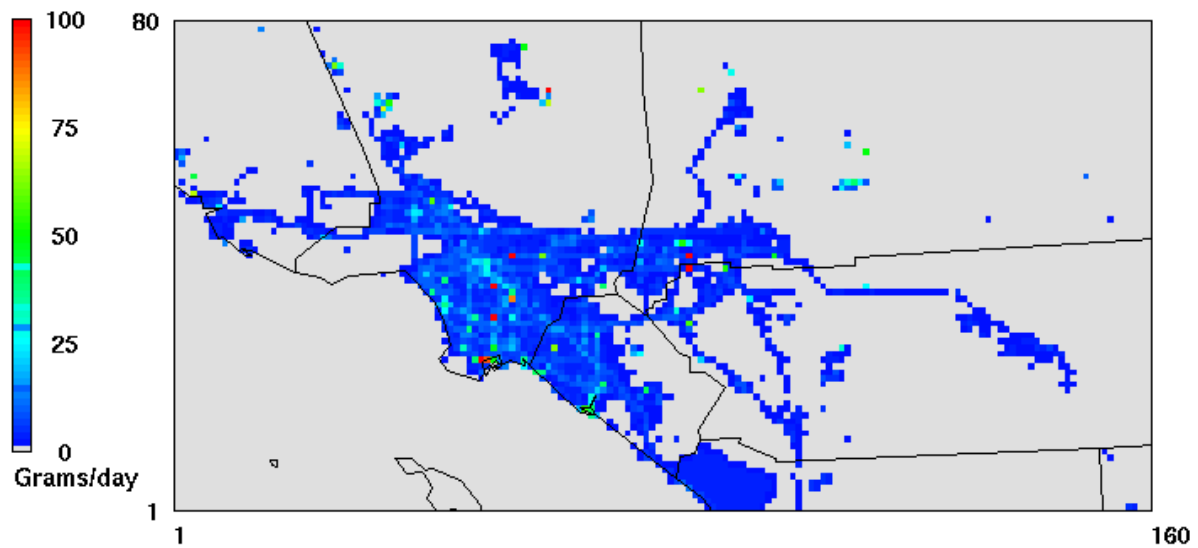
Figure IX-8u
Weekday average Nickel PM$_{2.5}$ emissions pattern.

p-Dichlorobenzene Emissions
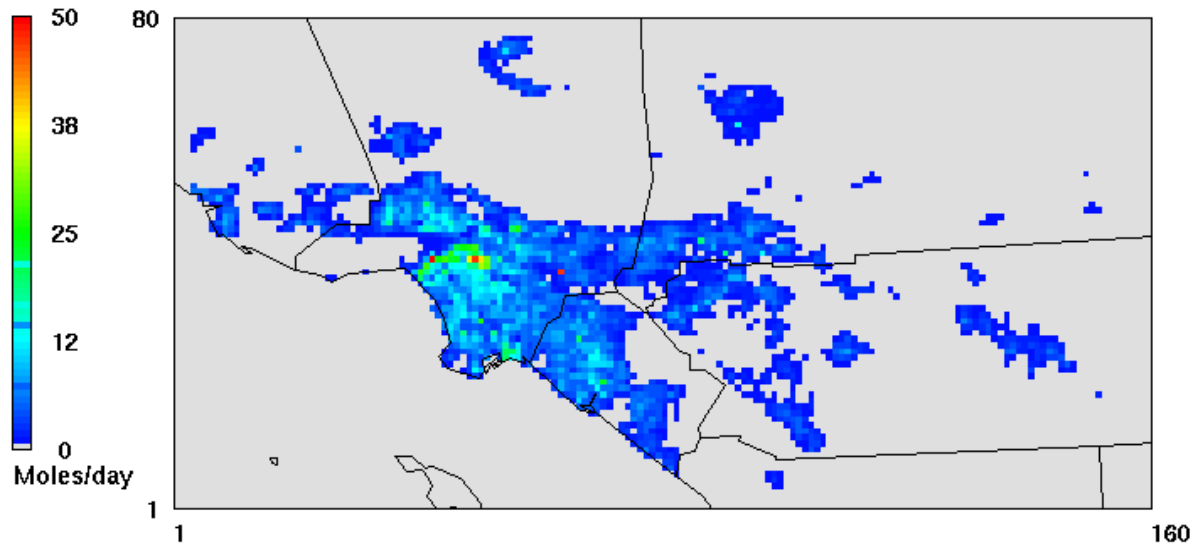
Figure IX-8v
Weekday average p-Dichlorobenzene emissions pattern.

Perchloroethylene Emissions
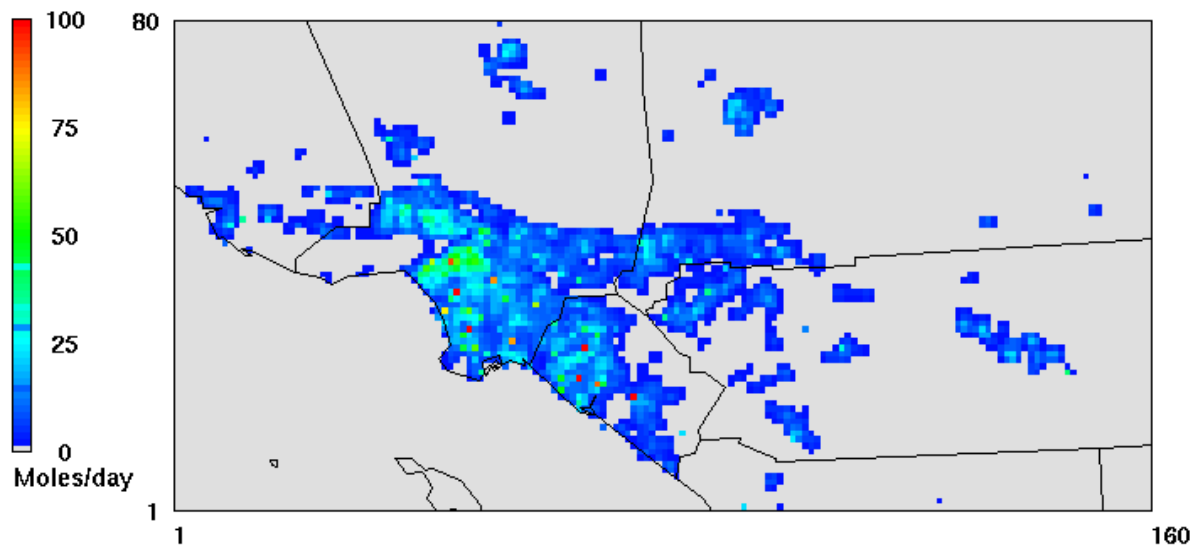
Figure IX-8w
Weekday average Perchloroethylene emissions pattern.

Trichloroethylene Emissions
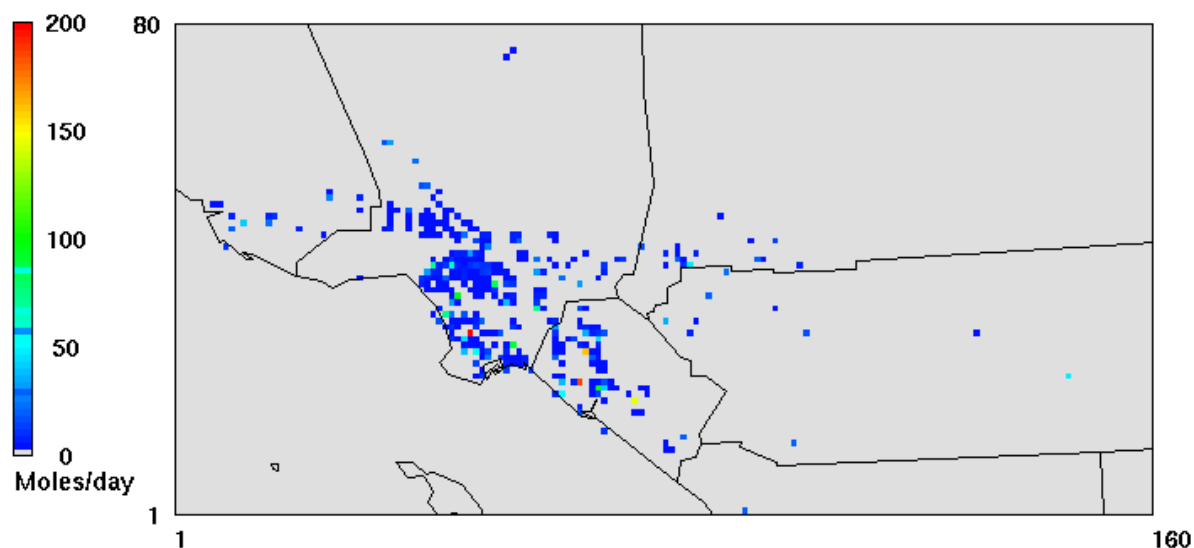
Figure IX-8x
Weekday average Trichloroethylene emissions pattern.

The California Air Resources Board (CARB) maintains the speciation profile library for the California emissions and provides periodic updates. Compared to the MATES III, there are some significant changes in the speciation profiles. In particular, elemental carbon content in diesel emissions increased substantially. In addition, the preparation of on-road emissions was modified. For MATES IV, on-road emissions were prepared based on day-specific temperature and relative humidity with vehicular activities for Monday, Friday, Saturday, Sunday and a single profile representing Tuesday through Thursday, while the MATES III on-road inventories were made with monthly averages of Weekday, Saturday, and Sunday emissions.

IX.11 Boundary and Initial Conditions

The initial and boundary condition files were prepared using the *icbcprep* utility included in the CAMx standard package. The utility prepares uniform boundary and initial conditions with prescribed values. Those values were presented in the Table IX-4. However, the initial values turn out to be not significant in the annual modeling, since the footprint of the initial values typically disappear in approximately seven to 10 days of time integration, depending on grid size and chemical mechanism.

Table IX-4
Boundary Condition Values

Gas (ppm)				Particle (ug/m^3)			
Compound	Value	Compound	Value	Compound	Values	Compound	Value
NO	0.000	ARO1	0.00021	DSL	0.05	DSLC	0.003
NO2	0.0001	ARO2	0.00007	EC	0.05	ECC	0.003
O3	0.03	OLE1	0.00018	OC	0.10	OCC	0.01
HCHO	0.00093	PHCHO	0.0001	CR	0.00001	CRC	0.00001
CCHO	0.00053	PACET	0.0001	CR6	0.00	CR6C	0.00
RCHO	0.00025	SFORM	0.00083	AR	0.00001	ARC	0.00001
ISOP	0.00002	SACET	0.00043	CD	0.00001	CDC	0.00001
MEOH	0.0001	BENZ	0.0001	NI	0.00001	NIC	0.00001
COOH	0.00005	BUTA	0.00001	PB	0.00001	PBC	0.00001
CO	0.2	PDIC	0.00001	DPMa	0.045	DPMaC	0.0001
ETHE	0.00018	MCHL	0.00001	DPMb	0.020	DPMbC	0.0001
ALK1	0.0025	PERC	0.00001	DPMc	0.010	DPMcC	0.0001
ALK2	0.0023	TCE	0.00001	DPMd	0.010	DPMdC	0.0001
ALK3	0.00093	NAPH	0.00001	DPMe	0.001	DPMeC	0.0001

IX.12 Modeling Results

The performance of the CAMx regional modeling simulation is summarized through statistical and graphical analysis, including time series of key pollutant concentrations. Summarized in Table IX-5 are the measurements and model predictions of toxic components during the sampling period. Prediction Accuracy (PA), defined as the percentage difference between the mean observed and simulated concentrations, is given as an indicator for the model performance.

For 2012-2013 period, the model simulated concentrations of particulate matter species, such as $EC_{2.5}$, $EC_{10,}$ and TSP metals, were biased high; this bias was the result, to a large extent, of uncertainties in emission inventory as well as the model's inability to accurately predict extremely low concentrations of PM species present during spring and summer. The model performed better for gaseous species. Concentrations of perchloroethylene, p-dichloroebenzene, trichloroethylene, 1,3-butadiene and naphthalene have become low enough that model performances for those pollutants are immaterial. Benzene, formaldehyde, and acetaldehyde were relatively well-simulated. Modeled and observed concentrations of methylene chloride compared well except at the Rudidoux site. Monitors at this site have experienced a dramatic increase in methylene chloride concentrations since 2009. The source(s) of this increase have not been determined.

Simulated annual average $EC_{2.5}$ and EC_{10} were used to assess overall model performance for the 2012-2013 MATES IV period. Tables IX-6a and IX-6b summarize the 2012-2013 MATES IV $EC_{2.5}$ and EC_{10} model performance, respectively.

EPA guidance (U.S. EPA, 2006) recommends evaluating gaseous and particulate modeling performance using measures of prediction bias and error. PA goals of ±20% for ozone and ±30% for individual components of $PM_{2.5}$ or PM_{10} have been used to assess simulation performance in previous modeling attainment demonstrations.

As shown in the Tables IX-6a and IX-6b, five of the 10 MATES IV sites meet the $PM_{2.5}$ PA goal. The model performed significantly better with predictions of PM_{10} concentrations, with only the Long Beach site exhibiting a large degree (34%) of overprediction of the annual average concentrations. In general, the model underpredicts annual average concentrations in places like Burbank, Inland Valley San Bernardino and Rubidoux, consistent with what was observed in our past modeling effort. On the contrary, concentrations in locations such as Long Beach, Compton, and Los Angeles are overpredicted.

For $EC_{2.5,}$ overprediction was more pronounced than underprediction. Five of the 10 sites did not meet the performance goal due to overprediction. The greatest tendency for overprediction is at the West Long Beach site, with a PA of 67%. The mean error of the simulated versus measured concentrations ranges from 0.40 μg/m³ to 1.00 μg/m³. For $EC_{10,}$ the model performance is markedly better. PA at nine of the10 MATES IV sites meets the particulate goal with only Long Beach exhibiting a large degree (34%) of overprediction of the annual average concentration. Of the remaining sites, Compton, Los Angeles and West Long Beach are overpredicted by 21, 30 and 21%, respectively. For the remaining sites, PA falls within ±20% of observations. The mean error of the simulated versus measured concentrations ranges from 0.44 μg/m³ to 0.86 μg/m³.

Table IX-7 provides the CAMx RTRAC performance for benzene at the 10 MATES IV monitoring sites. Benzene model performance is included in the evaluation because of the confidence in the benzene measurement data based on the long-term monitoring conducted in the Basin and throughout California. With the exception of West Long Beach (15% over), the annual average benzene concentrations are underpredicted with Compton showing the largest low bias (43 %). This underprediction, can be mostly attributed to lower boundary values than used in the MATES III. Benzene emissions have been reduced by 47% since MATES III. Consequently, a boundary value of 0.15 ppb was used in MATES IV compared to 0.2 ppb in MATES III. In hindsight, since benzene has a long atmospheric residence time, its background value is influenced more by the global emissions. Reduction in the boundary value due to local emissions reductions is probably not warranted. Even with the negative bias, the overall model performance for benzene is reasonable.

The time series fit of the simulated $EC_{2.5}$ and EC_{10} concentrations to measurements for each station is depicted in Figures IX-9a through IX-9j. As evident in the plots, for the four sites (Burbank, Inland Valley San Bernardino, Pico Rivera, and Rubidoux) with moderate under-predictions, the negative bias is mostly due to uncertainties associated with emissions inventory as well as meteorological conditions inductive for high concentrations occurred during winter. In contrast, at the sites where the model overpredicts, low concentrations measured during spring and summer were not simulated accurately, indicating a limitation that a current numerical model has for an exceptionally low concentration case.

IX.13 Comparison with MATES III Simulation

Tables IX-8 and IX-9 provide a comparison of the 2012-2013 MATES IV and 2005 MATES III model performance for $EC_{2.5}$ and benzene, respectively. Listed in each table are PA, bias, and mean error.

As presented in Table IX-9, compared to MATES III modeling, where only one site (Burbank) exhibited substantial underprediction, MATES IV modeling exhibited an overall tendency to overpredict $EC_{2.5}$. The overall characteristics of the two sets of modeling are similar: i.e. the sites with under or overpredictions are consistent. The two sets of modeling results for benzene behaved similarly. The model underpredicted concentrations in places like Burbank and Compton and overpredicted concentrations in West Long Beach.

IX.14 Simulation Evaluation Averaged Over the Monitoring Network

For this comparison, the monitored data for six stations are combined to provide an estimate of average Basin-wide conditions for the two sampling periods: 2012-2013 and 2005. Table IX-10 summarizes the network average measured and predicted pollutant concentrations over the eight sites. Two stations in 2005, Huntington Park and Pico Rivera, did not have complete measurement records for the full 12 months and were excluded from the analysis. CAMx RTRAC simulated pollutant concentrations for the eight stations that have complete data for the two measurement periods were calculated from the grid data using the distance weighted nine-cell average. Measured concentrations of naphthalene were available for Long Beach, Central

Los Angeles, and Rubidoux. Each of the four counties is represented by at least one station. The eight stations' average measured and simulated concentrations provide an estimate of the regional profile but with a bias towards impacts to the coastal communities in the heavily transited areas of the Basin. Moreover, the assessment provides a direct comparison for model performance evaluation.

For 2012-2013, the model simulated concentrations of particulate matter species, such as $EC_{2.5}$, EC_{10}, and TSP metals were biased high. The model performed better for gaseous species. Concentrations of perchloroethylene, p-dichloroebenzene, trichloroethylene, 1,3-butadiene and naphthalene have become low enough that model performances for those pollutants are immaterial. Benzene, formaldehyde and acetaldehyde were well-simulated. Modeled and observed concentrations of methylene chloride compared exceptionally well except at the Rubidoux site. Monitors at this site have experienced a dramatic increase in methylene chloride concentrations since 2009. The source(s) of this increase have not been determined.

In general, 2005 model simulated particulate $EC_{2.5}$, EC_{10}, hexavalent chromium and $PM_{2.5}$ nickel average annual toxic compound concentrations compared well with the measured annual average values. The majority of gaseous components were well-simulated with the sole exception of acetaldehyde, which was underpredicted. Arsenic and TSP lead exhibit the greatest tendency for overprediction. Cadmium and $PM_{2.5}$ lead concentrations tend to be underpredicted. In general, the concentrations of the gaseous compounds are closely recreated.

IX.15 Simulation Estimated Spatial Concentration Fields

Figures IX-10a through IX-10u depict the CAMx projected annual average concentration distributions of selected toxic compounds as well as the impacts of five emissions categories of diesel particulates in the Basin. In general, the distribution of diesel particulates follows the major arterials. The highest concentration (2.9 $\mu g/m^3$) was simulated to occur around the Ports of Los Angeles and Long Beach. The peak diesel concentration is much lower than the previous MATES studies, due, in a large part, to emission reductions from ocean-going vessels at near coastal waters and at ports. Figures IX-10h and IX-10i provide the distributions of benzene and 1,3-butadiene, respectively, whereby the toxic compounds are almost uniformly distributed throughout the Basin (reflecting patterns of gasoline fuel consumption). The ambient concentrations of formaldehyde in the SCAB are made up from direct emissions, primarily from combustion sources, secondary formation from the oxidation of anthropogenic and biogenic VOCs. The formaldehyde profile, shown in Figure IX-10j, depicts this characteristic of its origins, with measurable concentrations in the heavily traveled western and central Basin and additional elevated levels in the downwind areas of the Basin that are impacted by higher levels of ozone formation. Due to continued reduction of combustion source emissions, the formaldehyde concentrations are dominated by secondary formation. The peak formaldehyde concentrations are now in the areas with elevated biogenic emissions.

Table IX-5
2012-2013 Station Observed and CAMx Simulated MATES IV Annual Average Concentrations

Compound	Units	Anaheim			Burbank			Compton			Inland Valley San Bernardino		
		Obs	Model	PA	Obs	Model	PA	Obs	Model	PA	Obs	Model	PA
1,3-Butadiene	ppb	0.09	0.04	-57	0.12	0.04	-71	0.14	0.05	-62	0.07	0.02	-65
Acetaldehyde	ppb	0.59	0.90	53	1.08	0.98	-9	0.84	0.87	3	1.03	0.99	4
As (2.5)	$\eta g/m^3$	N/A	0.40	N/A	N/A	0.37	N/A	N/A	0.62	N/A	N/A	0.36	N/A
As (TSP)	$\eta g/m^3$	0.24	0.53	121	0.46	0.58	27	0.52	1.42	175	0.91	0.87	-5
Benzene	ppb	0.33	0.28	-14	0.46	0.28	-38	0.50	0.28	-43	0.29	0.22	-24
Cd (2.5)	$\eta g/m^3$	N/A	0.15	N/A	N/A	0.12	N/A	N/A	0.54	N/A	N/A	0.35	N/A
Cd (TSP)	$\eta g/m^3$	N/A	0.25	N/A	N/A	0.23	N/A	N/A	0.69	N/A	N/A	0.70	N/A
Cr6 (TSP)	$\eta g/m^3$	0.03	0.15	470	0.04	0.16	575	0.12	0.19	60	0.05	0.18	296
EC_{10}	$\mu g/m^3$	1.17	1.39	18	1.74	1.43	-18	1.50	1.81	21	1.74	1.42	-18
$EC_{2.5}$	$\mu g/m^3$	0.90	1.10	22	1.32	1.19	-9	1.06	1.48	39	1.38	1.13	-18
Formaldehyde	ppb	1.19	1.67	40	2.58	1.89	-27	2.08	1.66	-20	2.63	1.89	-28
Methylene Chloride	ppb	0.37	0.30	-20	0.24	0.28	18	0.17	0.26	50	0.28	0.13	-53
Naphthalene	ppb												
Ni (2.5)	$\eta g/m^3$	N/A	2.87	N/A	N/A	1.85	N/A	N/A	6.98	N/A	N/A	3.07	N/A
Ni (TSP)	$\eta g/m^3$	1.74	4.72	171	3.90	3.02	-22	4.06	8.31	105	4.05	4.57	13
Pb (2.5)	$\eta g/m^3$	N/A	1.25	N/A	N/A	1.27	N/A	N/A	1.96	N/A	N/A	3.69	N/A
Pb (TSP)	$\eta g/m^3$	2.14	3.37	57	5.27	3.82	-28	6.24	4.83	-23	9.80	9.67	-1
p-Dichlorobenzene	ppb	0.02	0.06	273	0.02	0.06	146	0.02	0.06	233	0.01	0.04	282
Perchloroethylene	ppb	0.04	0.09	118	0.05	0.08	83	0.04	0.09	113	0.05	0.05	6
Trichloroethylene	ppb	0.01	0.04	266	0.02	0.04	112	0.01	0.05	342	0.01	0.03	108

Table IX-5 (Continued)
2012-2013 Station Observed and CAMx Simulated MATES IV Annual Average Concentrations

Compound	Units	Huntington Park			North Long Beach			Central Los Angeles			Pico Rivera		
		Obs	Model	PA	Obs	Model	PA	Obs	Model	PA	Obs	Model	PA
1,3-Butadiene	ppb	0.15	0.18	21	0.09	0.05	-48	0.11	0.05	-52	0.09	0.04	-57
Acetaldehyde	ppb	1.04	0.97	-7	0.67	0.85	27	0.94	1.05	11	1.25	1.00	-20
As (2.5)	$\eta g/m^3$	N/A	5.21	N/A	N/A	0.98	N/A	N/A	0.64	N/A	N/A	1.14	N/A
As (TSP)	$\eta g/m^3$	0.56	6.11	997	0.41	1.45	256	0.64	1.45	72	0.57	1.77	209
Benzene	ppb	0.53	0.33	-38	0.33	0.30	-10	0.40	0.37	-8	0.35	0.27	-21
Cd (2.5)	$\eta g/m^3$	N/A	0.40	N/A	N/A	0.49	N/A	N/A	0.22	N/A	N/A	0.27	N/A
Cd (TSP)	$\eta g/m^3$	N/A	0.62	N/A	N/A	0.64	N/A	N/A	0.40	N/A	N/A	0.46	N/A
Cr6 (TSP)	$\eta g/m^3$	0.07	0.28	289	0.04	0.19	334	0.07	0.24	247	0.05	0.17	251
EC_{10}	$\mu g/m^3$	1.65	1.98	20	1.29	1.72	34	1.67	2.17	30	1.87	1.69	-10
$EC_{2.5}$	$\mu g/m^3$	1.30	1.70	31	0.91	1.45	59	1.23	1.81	47	1.39	1.30	-6
Formaldehyde	ppb	2.73	1.92	-30	1.86	1.76	-6	2.93	2.11	-28	2.81	1.81	-36
Methylene Chloride	ppb	0.24	0.33	37	0.24	0.23	-1	0.32	0.42	0.32	0.17	0.23	38
Naphthalene	ppb				0.015	0.011	-27	0.029	0.014	-51			
Ni (2.5)	$\eta g/m^3$	N/A	4.03	N/A	N/A	6.92	N/A	N/A	2.76	N/A	N/A	2.77	N/A
Ni (TSP)	$\eta g/m^3$	5.40	5.68	5	3.65	8.59	136	3.37	4.57	36	4.48	4.11	-8
Pb (2.5)	$\eta g/m^3$	N/A	3.75	N/A	N/A	2.26	N/A	N/A	2.14	N/A	N/A	1.80	N/A
Pb (TSP)	$\eta g/m^3$	9.46	7.66	-19	4.47	4.99	12	7.34	6.17	-16	5.89	4.69	-20
p-Dichlorobenzene	ppb	0.03	0.07	180	0.01	0.06	321	0.03	0.09	203	0.01	0.06	293
Perchloroethylene	ppb	0.04	0.11	165	0.02	0.10	390	0.03	0.09	203	0.03	0.08	192
Trichloroethylene	ppb	0.02	0.06	300	0.01	0.07	550	0.03	0.04	35	0.02	0.03	120

Table IX-5 (Continued)
2012-2013 Station Observed and CAMx Simulated MATES IV Annual Average Concentrations

Compound	Units	Rubidoux			West Long Beach		
		Obs	Model	PA	Obs	Model	PA
1,3-Butadiene	ppb	0.08	0.02	-77	0.11	0.05	-55
Acetaldehyde	ppb	0.84	0.97	16	0.75	0.87	16
As (2.5)	$\eta g/m^3$	N/A	0.38	N/A	N/A	0.57	N/A
As (TSP)	$\eta g/m^3$	0.76	0.62	-18	0.50	2.15	333
Benzene	ppb	0.28	0.21	-24	0.36	0.41	15
Cd (2.5)	$\eta g/m^3$	N/A	0.15	N/A	N/A	1.04	N/A
Cd (TSP)	$\eta g/m^3$	N/A	0.44	N/A	N/A	1.24	N/A
Cr6 (TSP)	$\eta g/m^3$	0.04	0.12	180	0.03	0.19	471
EC_{10}	$\mu g/m^3$	1.48	1.26	-14	1.78	2.15	21
$EC_{2.5}$	$\mu g/m^3$	1.11	0.98	-12	1.13	1.88	67
Formaldehyde	ppb	2.00	1.76	-12	1.55	2.12	37
Methylene Chloride	ppb	2.11	0.13	-94	0.24	0.22	-10
Naphthalene	ppb	0.017	0.011	-35			
Ni (2.5))	$\eta g/m^3$	N/A	2.18	N/A	N/A	13.29	N/A
Ni (TSP)	$\eta g/m^3$	3.35	3.17	-5	3.73	15.42	313
Pb (2.5)	$\eta g/m^3$	N/A	1.16	N/A	N/A	3.04	N/A
Pb (TSP)	$\eta g/m^3$	6.21	3.70	-41	5.83	5.74	-1
p-Dichlorobenzene	ppb	0.02	0.04	123	0.01	0.06	417
Perchloroethylene	ppb	0.02	0.05	179	0.02	0.09	355
Trichloroethylene	ppb	0.01	0.03	133	0.03	0.07	127

Table IX-6a
MATES IV 2012-2013 EC$_{2.5}$ Model Performance

Location	EC$_{2.5}$ Observed (μg/m^3)	Samples	Modeled Sampling Days (μg/m^3)	Prediction Accuracy	Mean Bias (μg/m^3)	Mean Error (μg/m^3)	Normalized Mean Bias	Normalized Mean Error
Anaheim	0.90	59	1.10	22	0.20	0.56	1.08	1.24
Burbank	1.32	58	1.19	-9	-0.12	0.64	0.43	0.73
Compton	1.06	61	1.48	39	0.42	0.76	1.52	1.64
Inland Valley San Bernardino.	1.38	59	1.13	-18	-0.25	0.46	-0.03	0.31
Huntington Park	1.30	58	1.70	31	0.40	0.67	0.85	0.93
Long Beach	0.91	60	1.45	59	0.53	0.80	2.18	2.27
Central L.A.	1.23	60	1.81	47	0.58	0.70	0.91	0.96
Pico Rivera	1.39	60	1.30	-6	-0.09	0.48	0.26	0.52
Rubidoux	1.11	61	0.98	-12	-0.13	0.40	0.12	0.44
West Long Beach	1.13	61	1.88	67	0.75	1.00	2.10	2.17
All Stations	1.17	597	1.40	20	0.23	0.65	0.95	1.13

Table IX-6b
MATES IV 2012-2013 EC_{10} Model Performance

Location	$EC_{2.5}$ Observed ($\mu g/m^3$)	Samples	Modeled Sampling Days ($\mu g/m^3$)	Prediction Accuracy	Mean Bias ($\mu g/m^3$)	Mean Error ($\mu g/m^3$)	Normalized Mean Bias	Normalized Mean Error
Anaheim	1.17	61	1.39	18	0.22	0.49	0.44	0.54
Burbank	1.74	57	1.43	-18	-0.31	0.60	-0.03	0.34
Compton	1.50	57	1.81	21	0.32	0.66	0.58	0.68
Inland Valley San Bernardino.	1.74	61	1.42	-18	-0.32	0.47	-0.08	0.27
Huntington Park	1.65	52	1.98	20	0.33	0.54	0.36	0.43
Long Beach	1.29	58	1.72	34	0.44	0.59	0.61	0.68
Central L.A.	1.67	60	2.17	30	0.50	0.61	0.46	0.51
Pico Rivera	1.87	50	1.69	-10	-0.18	0.44	-0.02	0.24
Rubidoux	1.48	59	1.26	-14	-0.22	0.44	-0.06	0.29
West Long Beach	1.78	51	2.15	21	0.37	0.86	0.53	0.69
All Stations	1.58	566	1.69	7	0.11	0.57	0.28	0.47

Table IX-7
2012-2013 Simulation Performance Statistics for Benzene

Location	Observed (ppb)	Samples	Predicted (ppb)	PA	Mean Bias (ppb)	Mean Error (ppb)	Normalized Mean Bias	Normalized Mean Error
Anaheim	0.33	51	0.28	-14	-0.05	0.16	0.24	0.58
Burbank	0.46	55	0.28	-38	-0.17	0.22	-0.18	0.39
Compton	0.50	57	0.28	-43	-0.21	0.26	-0.09	0.40
Inland Valley San Bernardino	0.29	53	0.22	-24	-0.07	0.09	-0.13	0.28
Huntington Park	0.53	52	0.33	-38	-0.20	0.22	-0.21	0.30
North Long Beach	0.33	54	0.30	-10	-0.03	0.10	0.07	0.31
Central L.A.	0.40	51	0.37	-8	-0.03	0.12	0.05	0.30
Pico Rivera	0.35	57	0.27	-21	-0.07	0.12	-0.03	0.33
Rubidoux	0.28	51	0.21	-24	-0.07	0.10	-0.10	0.32
West Long Beach	0.36	57	0.41	15	0.05	0.20	0.77	0.95

Table IX-8
Comparative Simulation Performance Statistics for $EC_{2.5}$

Location	MATES IV (2012-2013)					MATES III (2005)				
	Observed Days ($\mu g/m^3$)	Modeled Sampling Days ($\mu g/m^3$)	PA	Bias ($\mu g/m^3$)	Mean Error ($\mu g/m^3$)	Observed Days ($\mu g/m^3$)	Modeled Sampling Days ($\mu g/m^3$)	PA	Bias ($\mu g/m^3$)	Mean Error ($\mu g/m^3$)
Anaheim	0.90	1.10	22	0.20	0.56	1.41	1.35	-4	-0.06	0.54
Burbank	1.32	1.19	-9	-0.12	0.64	2.04	1.03	-50	-1.02	1.11
Compton	1.06	1.48	39	0.42	0.76	1.76	1.88	7	0.12	0.61
Inland Valley San Bernardino	1.38	1.13	-18	-0.25	0.46	2.18	1.77	-19	-0.41	0.91
Huntington Park	1.30	1.70	31	0.40	0.67	-	-	-	-	-
North Long Beach	0.91	1.45	59	0.53	0.80	1.40	1.71	21	0.30	0.61
Central L.A.	1.23	1.81	47	0.58	0.70	1.93	2.04	6	0.11	0.76
Pico Rivera	1.39	1.30	-6	-0.09	0.48	-	-	-	-	-
Rubidoux	1.11	0.98	-12	-0.13	0.40	1.69	1.32	-22	-0.38	0.74
West Long Beach	1.13	1.88	67	0.75	1.00	2.07	2.14	3	0.07	0.79

Table IX-9
Comparative Simulation Performance Statistics for Benzene

Location	MATES IV (2012-2013)					MATES III (2005)				
	Observed Days (ppb)	Modeled Sampling Days (ppb)	PA	Bias (ppb)	Mean Error (ppb)	Observed Days (ppb)	Modeled Sampling Days (ppb)	PA	Bias (ppb)	Mean Error (ppb)
Anaheim	0.33	0.28	-14	-0.05	0.16	0.44	0.50	15	0.06	0.22
Burbank	0.46	0.28	-38	-0.17	0.22	0.71	0.47	-34	-0.24	0.34
Compton	0.50	0.28	-43	-0.21	0.26	0.80	0.57	-29	-0.23	0.39
Inland Valley San Bernardino.	0.29	0.22	-24	-0.07	0.09	0.49	0.44	-11	-0.05	0.17
Huntington Park	0.53	0.33	-38	-0.20	0.22					
North Long Beach	0.33	0.30	-10	-0.03	0.10	0.50	0.57	13	0.07	0.21
Central L.A.	0.40	0.37	-8	-0.03	0.12	0.59	0.69	16	0.10	0.25
Pico Rivera	0.35	0.27	-21	-0.07	0.12					
Rubidoux	0.28	0.21	-24	-0.07	0.10	0.44	0.44	2	0.01	0.16
West Long Beach	0.36	0.41	15	0.05	0.20	0.53	0.60	14	0.07	0.21
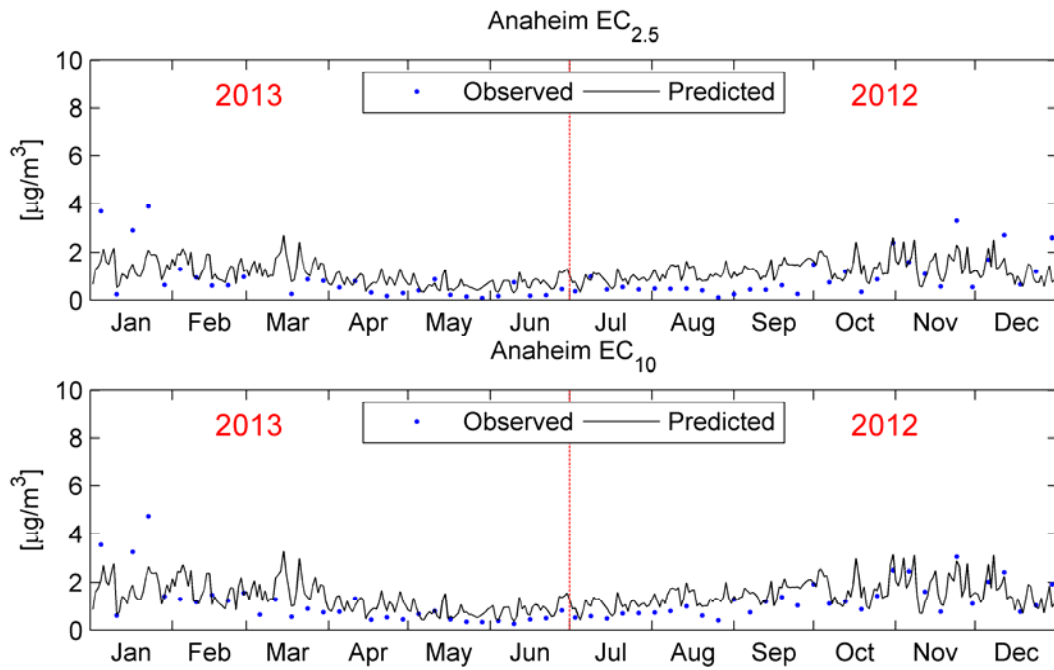
Figure IX-9a
EC$_{2.5}$ and EC$_{10}$ Time Series: Simulated vs. Measured at Anaheim.
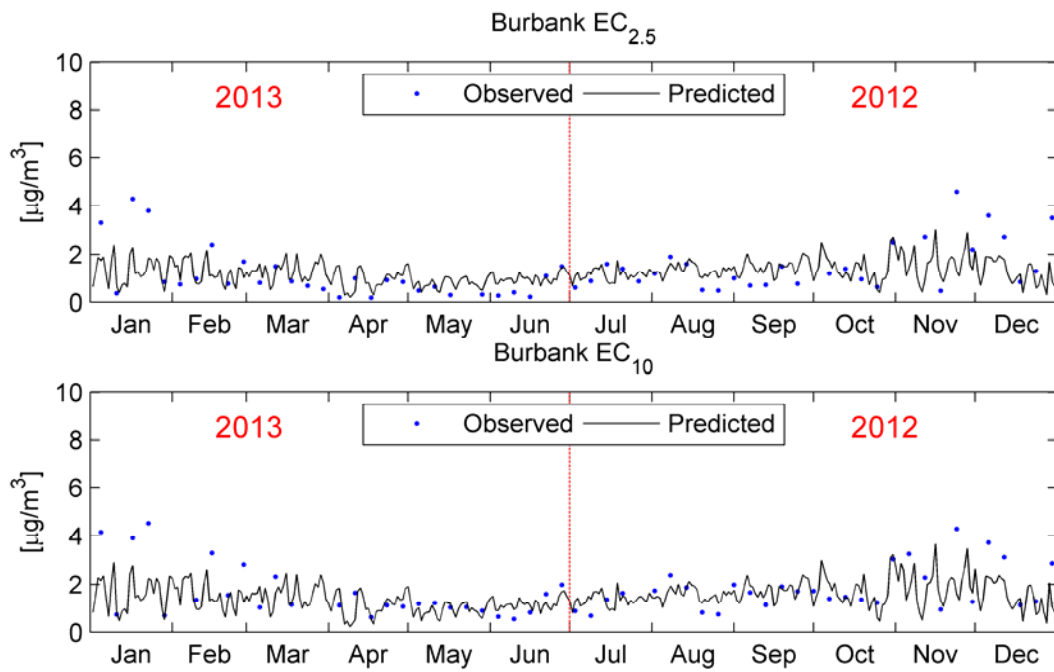
Figure IX-9b
Same as Figure IX-9a except Burbank.
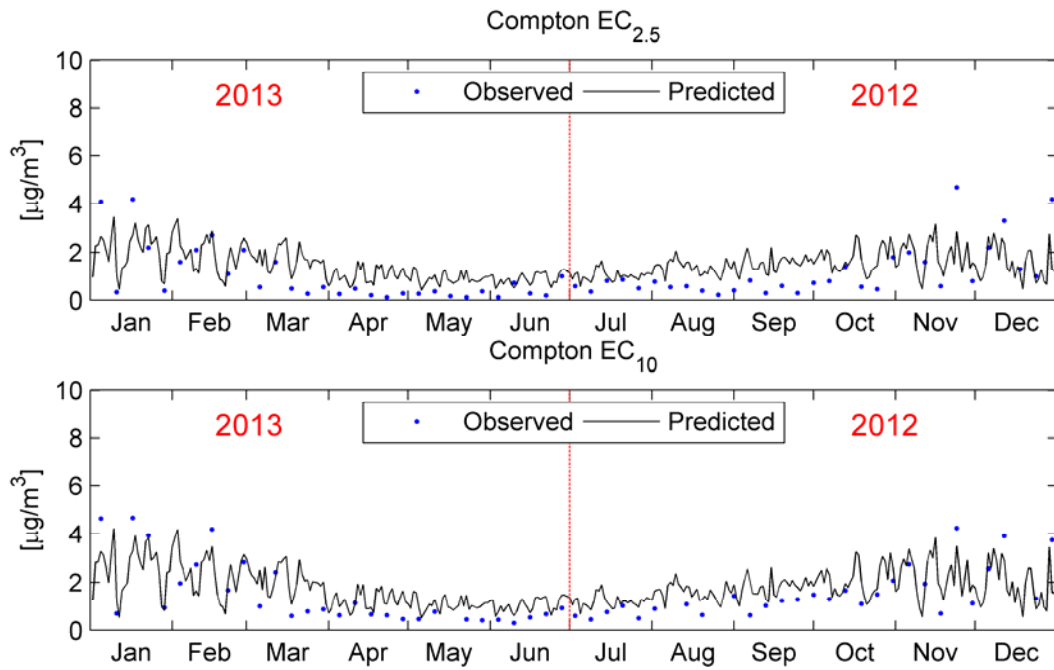
Figure IX-9c
Same as Figure IX-9a except Compton.
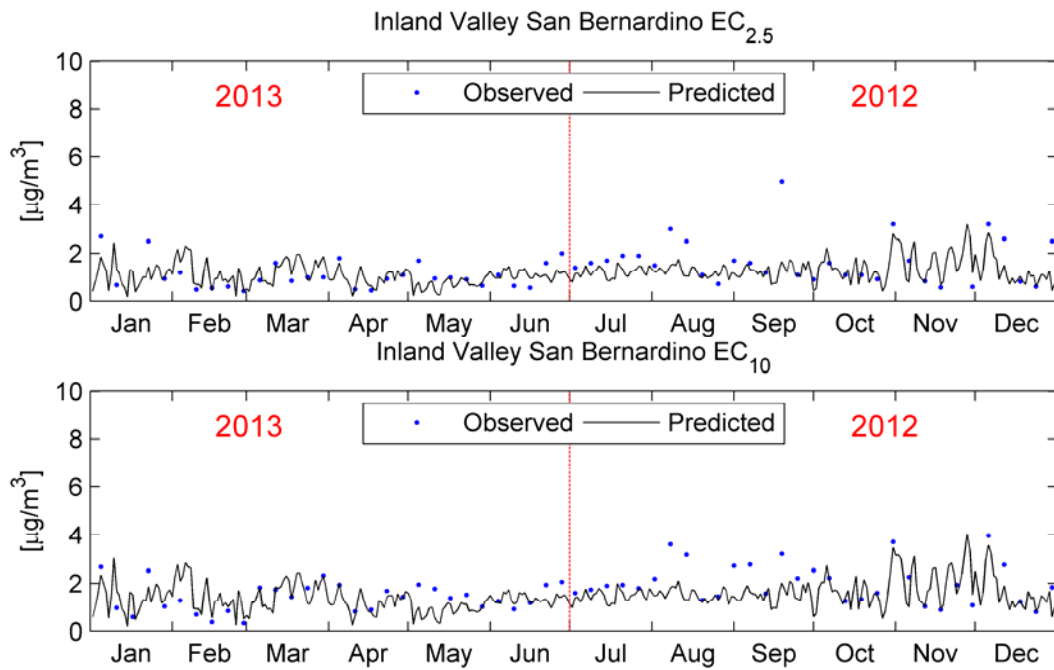
Figure IX-9d
Same as Figure IX-9a except Inland Valley San Bernardino.
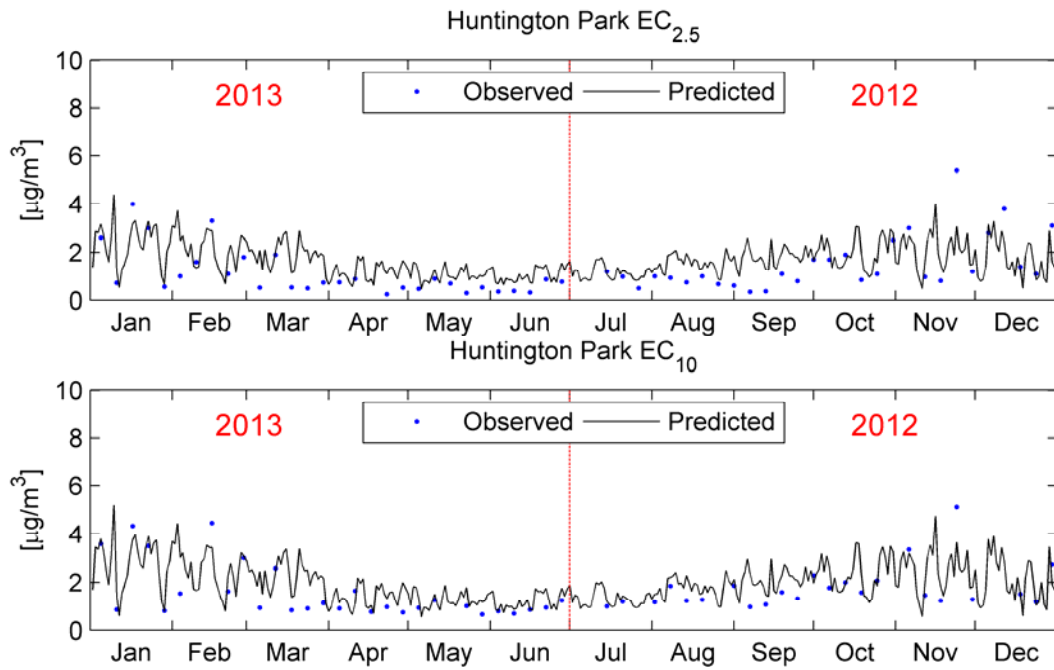
Figure IX-9e
Same as Figure IX-9a except Huntington Park
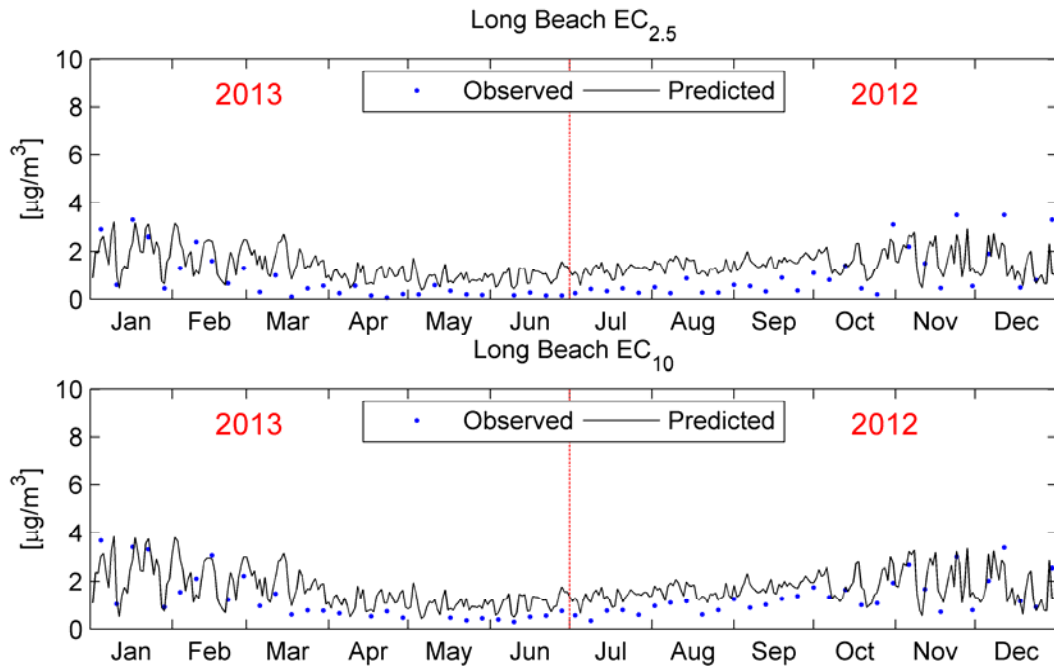
Figure IX-9f
Same as Figure IX-9a except North Long Beach.
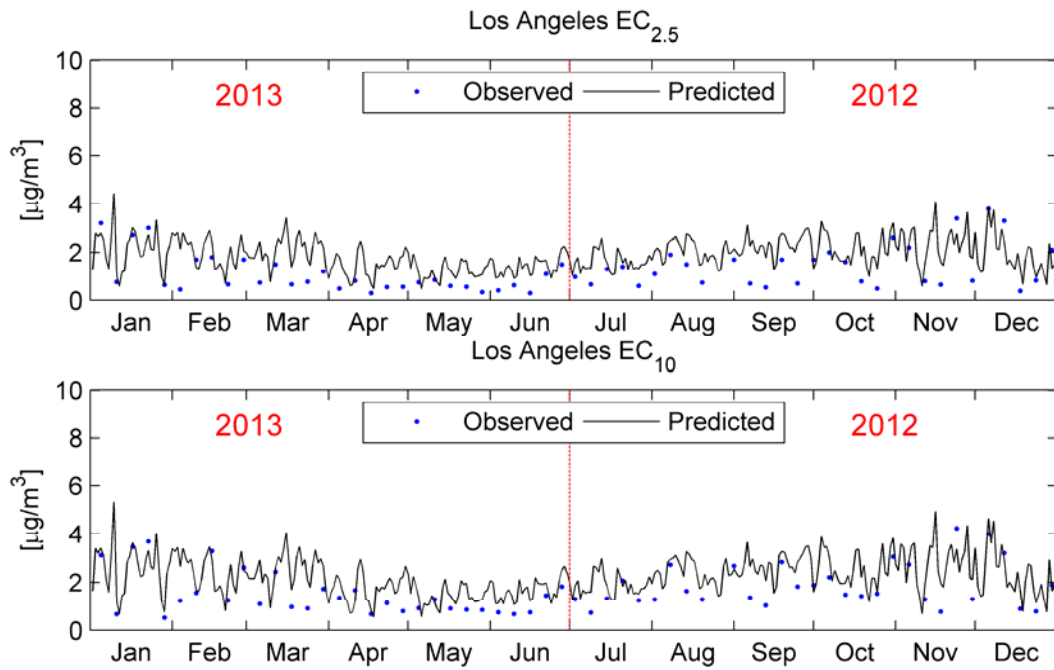
Figure IX-9g
Same as Figure IX-9a except Central Los Angeles.
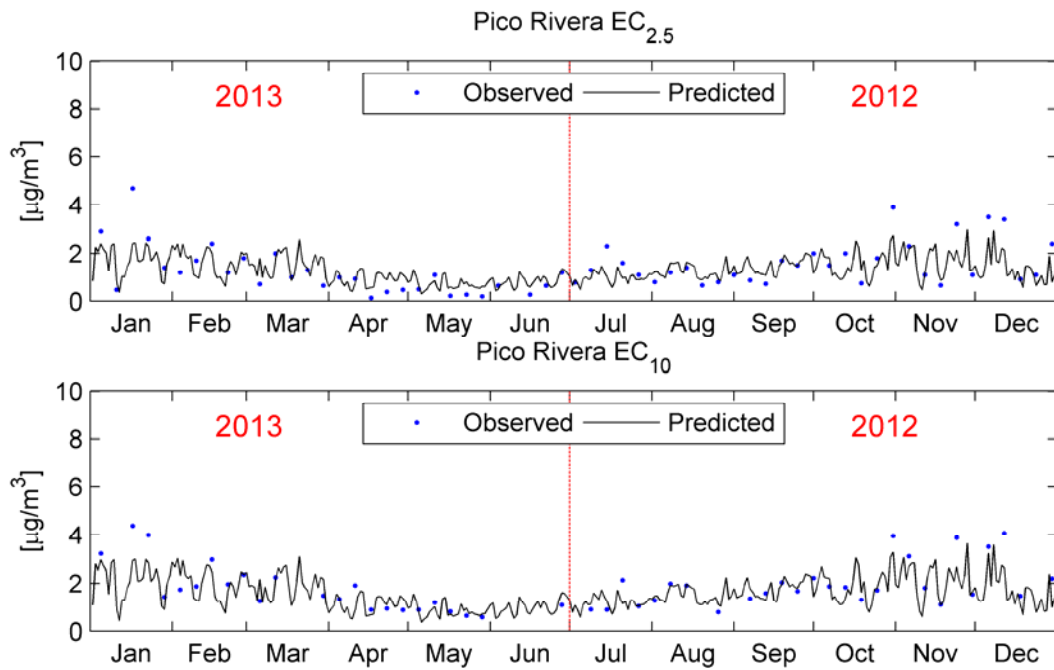
Figure IX-9h
Same as Figure IX-9a except Pico Rivera.
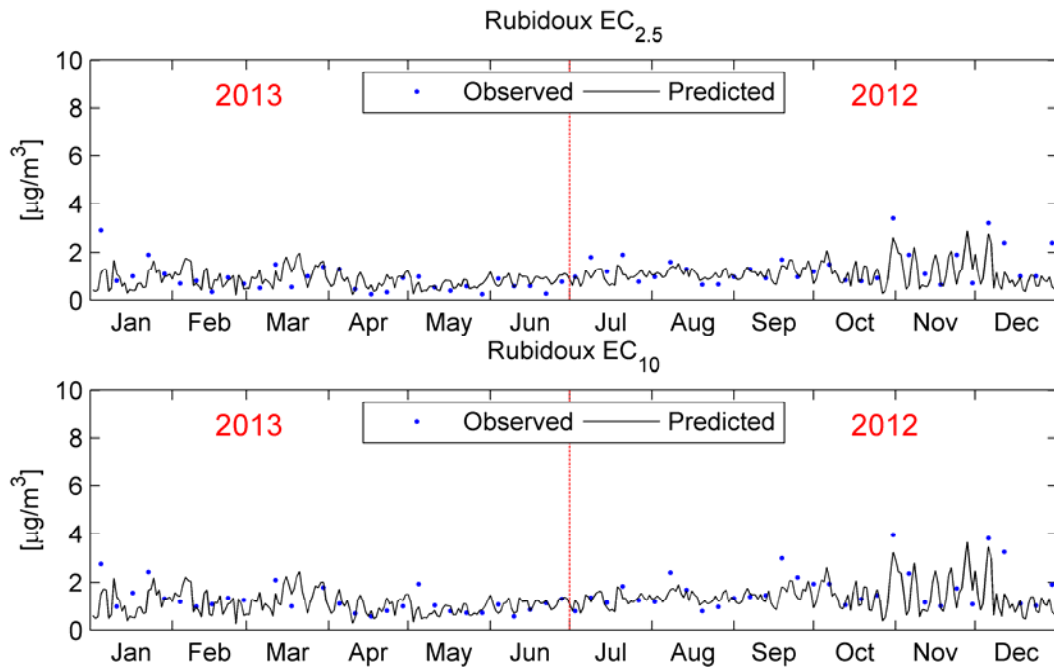
Figure IX-9i
Same as Figure IX-9a except Rubidoux.
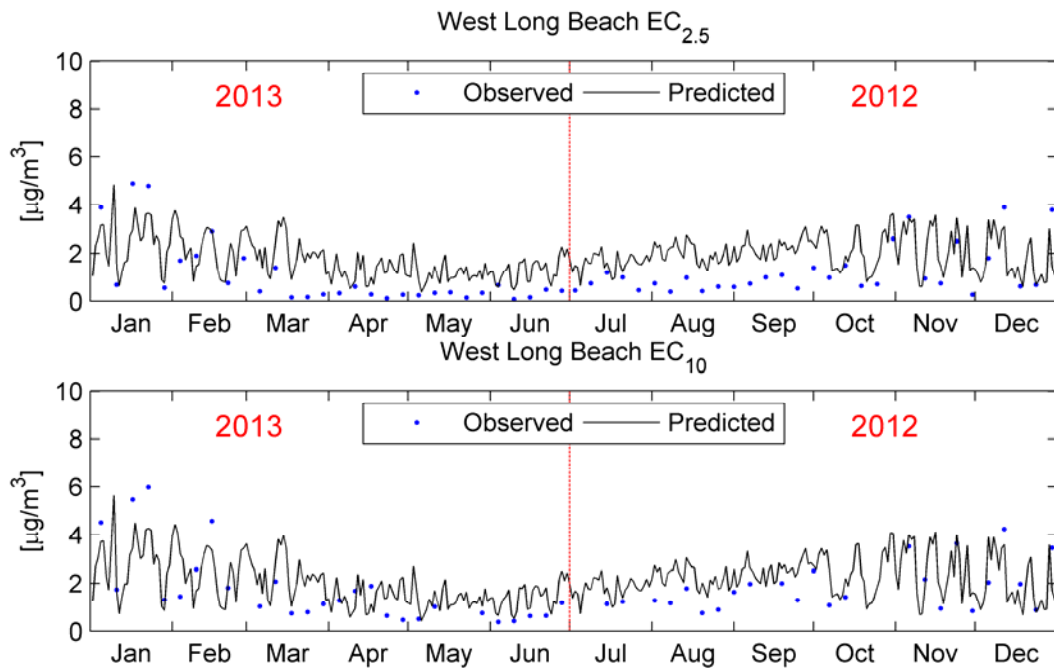
Figure IX-9j
Same as Figure IX-9a except West Long Beach.

Table IX-10
Toxic Compounds Simulated and Measured Eight-Station Annual Average Concentrations
For 2012-2013 MATES IV and 2005MATES III periods using CAMX RTRAC

Compound	Units	2012-2013MATES IV		2005 MATES III	
		Measured Annual Average	Simulated Annual Average	Measured Annual Average	Simulated Annual Average
$EC_{2.5}$	$\mu g/m^3$	0.96	1.39	1.81	1.69
EC_{10}	$\mu g/m^3$	1.33	1.68	2.05	2.15
Cr 6 (TSP)	$\eta g/m^3$	0.05	0.18	0.23	0.21
As (2.5)	$\eta g/m^3$	N/A	0.66	0.49	1.07
As (TSP)	$\eta g/m^3$	0.44	1.07	0.68	2.57
Cd (2.5)	$\eta g/m^3$	N/A	0.38	1.49	0.59
Cd (TSP)	$\eta g/m^3$	0.13	0.56	1.53	0.88
Ni (2.5))	$\eta g/m^3$	N/A	4.58	4.44	4.88
Ni (TSP)	$\eta g/m^3$	2.98	6.64	5.40	7.55
Pb (2.5)	$\eta g/m^3$	N/A	2.10	5.32	2.53
Pb (TSP)	$\eta g/m^3$	4.69	5.26	10.64	8.68
Benzene	ppb	0.33	0.29	0.56	0.54
Perchloroethylene	ppb	0.03	0.08	0.06	0.10
p-Dichlorobenzene	ppb	0.02	0.04	0.04	0.08
Methylene Chloride	ppb	0.46	0.24	0.32	0.33
Trichloroethylene	ppb	0.02	0.04	0.03	0.03
1,3-Butadiene	ppb	0.09	0.04	0.11	0.09
Formaldehyde	ppb	1.78	1.91	3.52	3.26
Acetaldehyde	ppb	0.71	0.95	1.60	1.11
Naphthalene	ppb	0.02*	0.01	0.02*	0.01

* Three station average

Diesel (PM2.5)

2012/13 Annual Average Concentrations

June 1,2003 0:00:00
Min= 0.00 at (1,1), Max= 2.94 at (53,25)
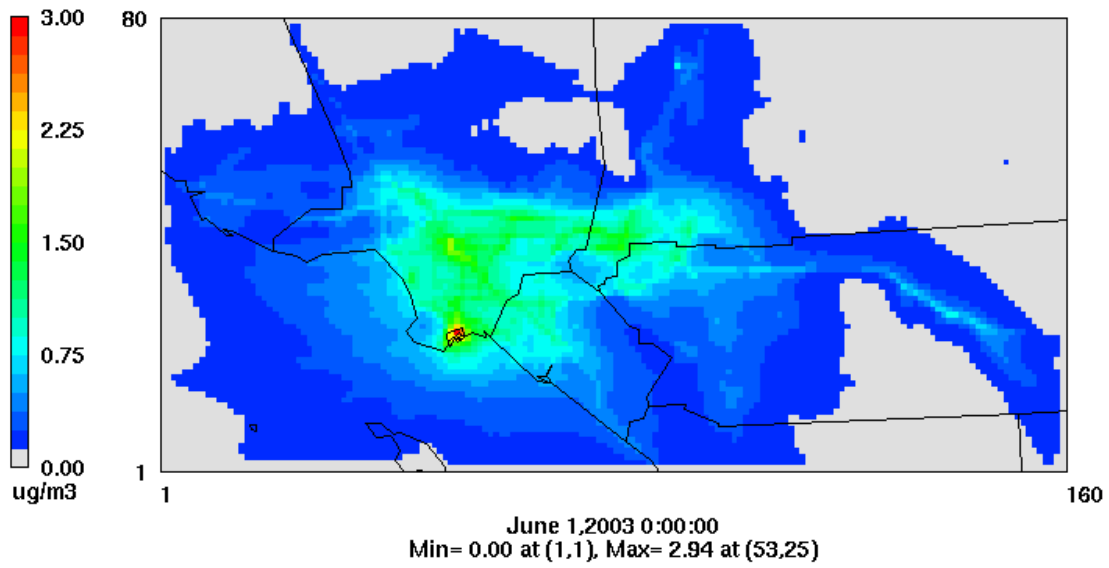
Figure IX-10a
CAMx simulated 2012 annual average Diesel PM$_{2.5}$.

Elemental Carbon (PM2.5)

2012/13 Annual Average Concentrations

June 1,2003 0:00:00
Min= 0.00 at (1,1), Max= 2.98 at (93,69)
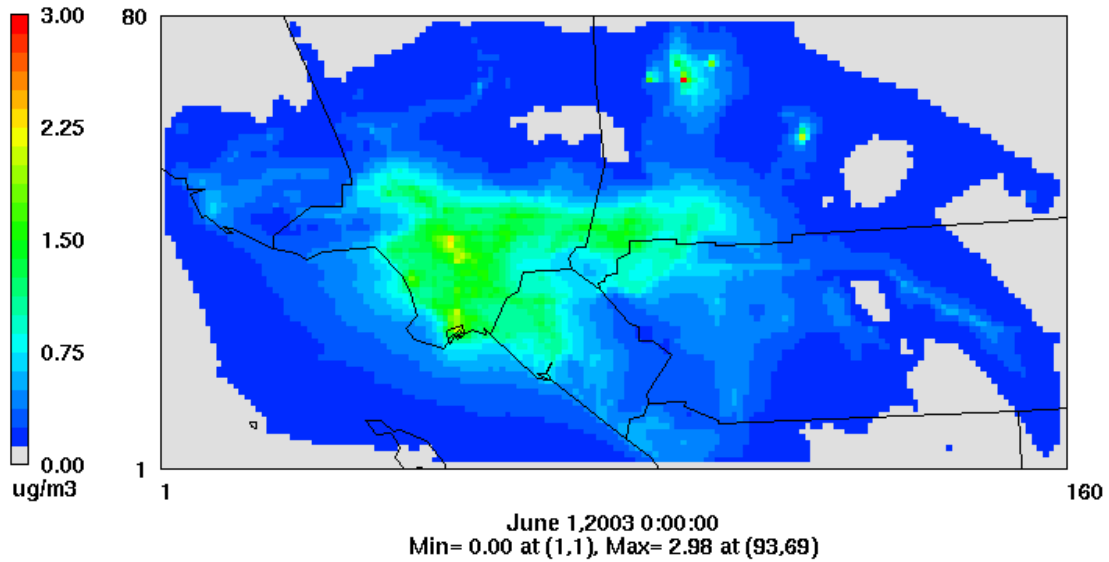
Figure IX-10b
CAMx simulated 2012 annual average Elemental Carbon PM$_{2.5}$.

On-Road Diesel (PM2.5)

2012/13 Annual Average Concentrations
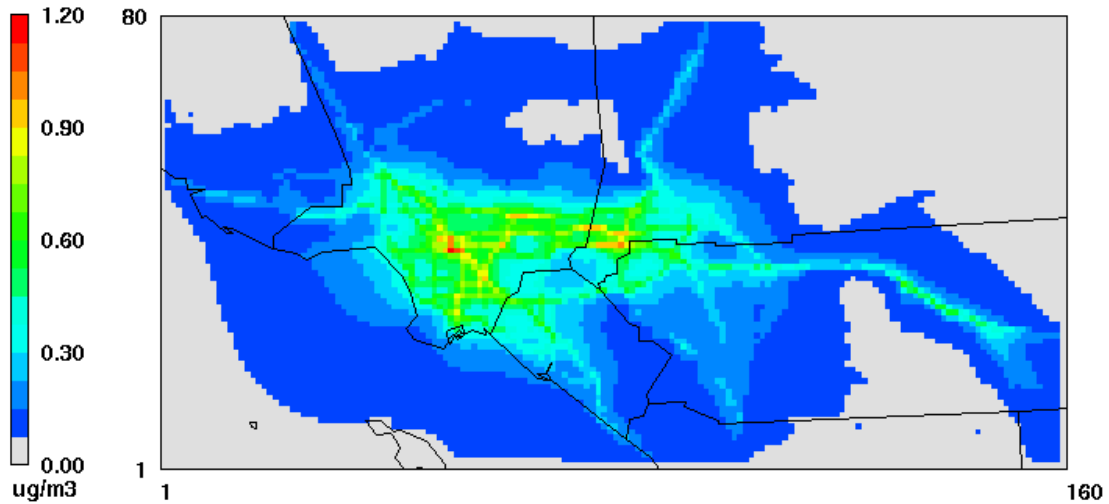
Figure IX-10c
CAMx simulated 2012 annual average On-Road Diesel PM$_{2.5}$.

Off-Road Diesel (PM2.5)

2012/13 Annual Average Concentrations
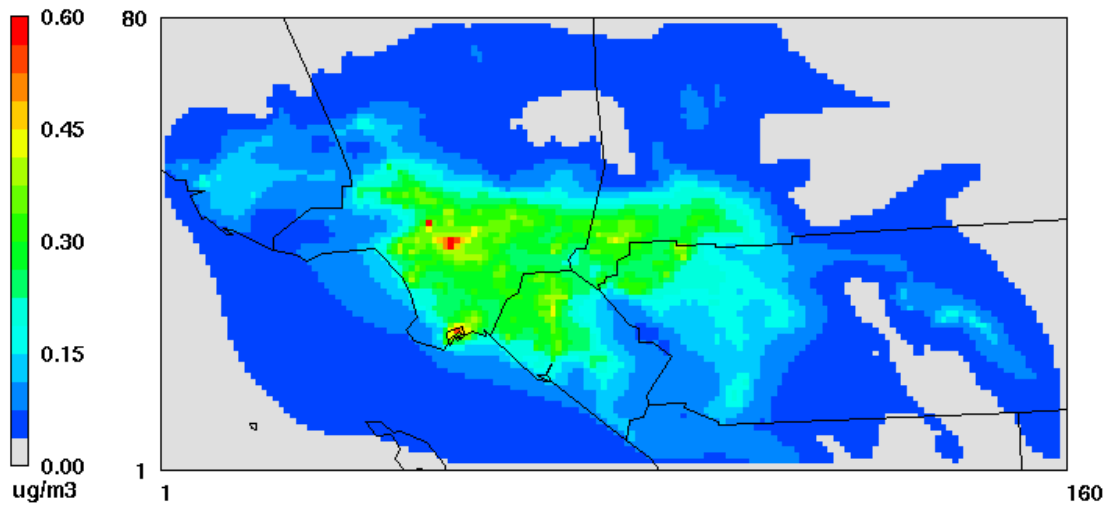
Figure IX-10d
CAMx simulated 2012 annual average Off-Road Diesel PM$_{2.5}$.

Diesel from OGV and Commercial Boats (PM2.5)

2012 Annual Average Concentrations
v=average.draft.plot
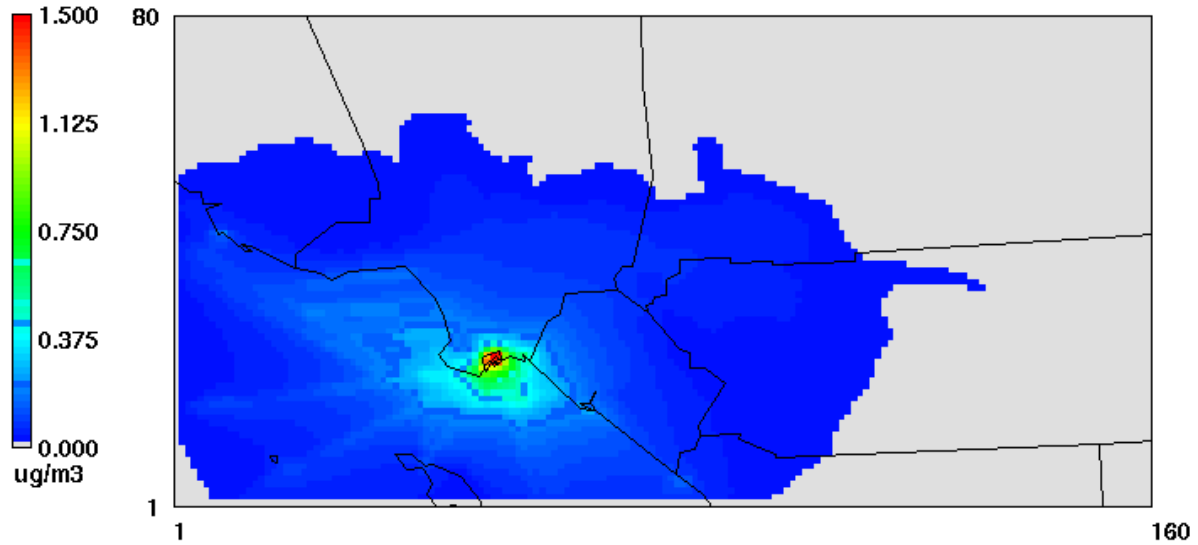
Figure IX-10e
CAMx simulated 2012 annual average Diesel from Ships PM$_{2.5}$.

Diesel from Trains (PM2.5)

2012/13 Annual Average Concentrations
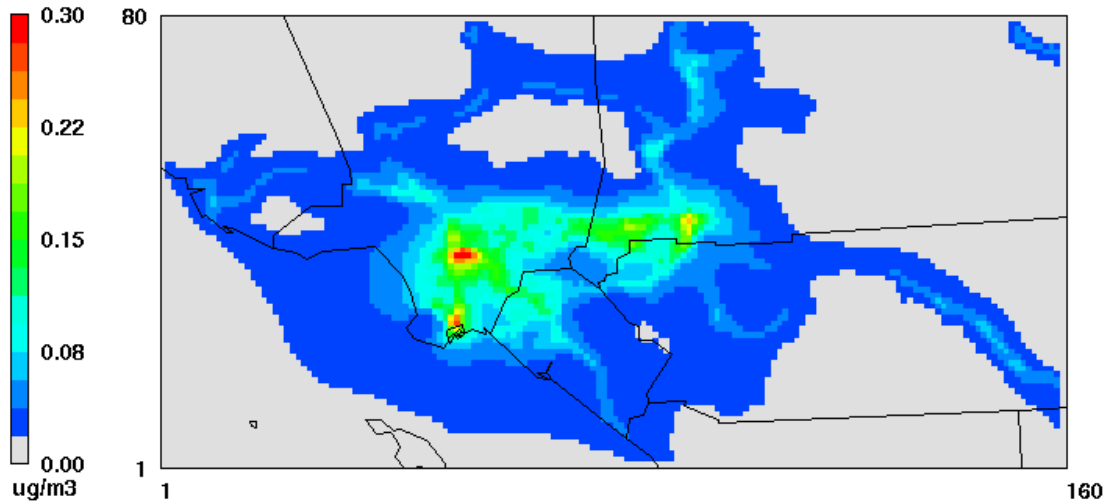
Figure IX-10f
CAMx simulated 2012 annual average Diesel from Trains PM$_{2.5}$.

Stationary Diesel (PM2.5)

2012/13 Annual Average Concentrations
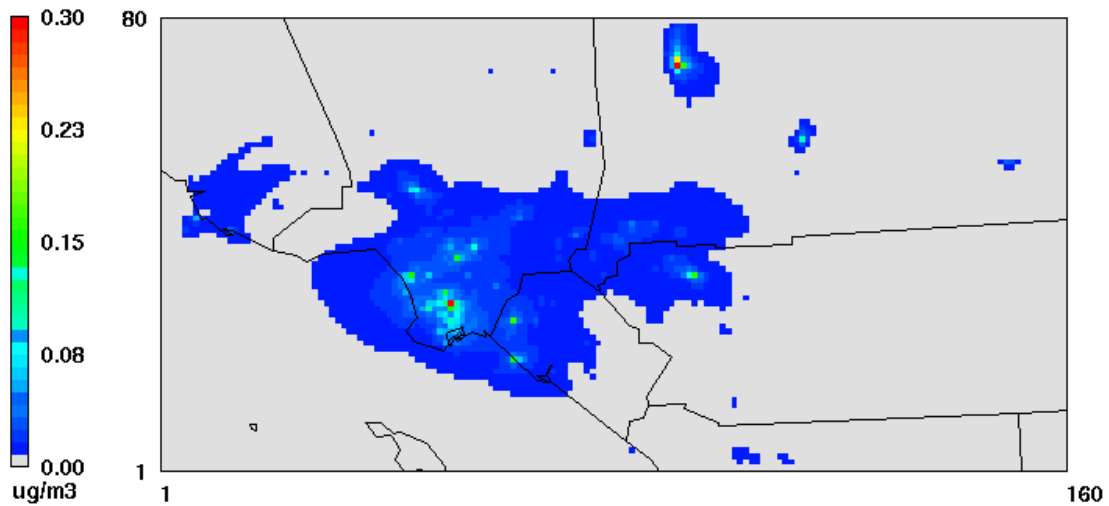
Figure IX-10g
CAMx simulated 2012 annual average Diesel from Stationary Sources PM$_{2.5}$.

Benzene

2012 Annaul Average Concentrations
w=average.dgas_CMAQ.plot
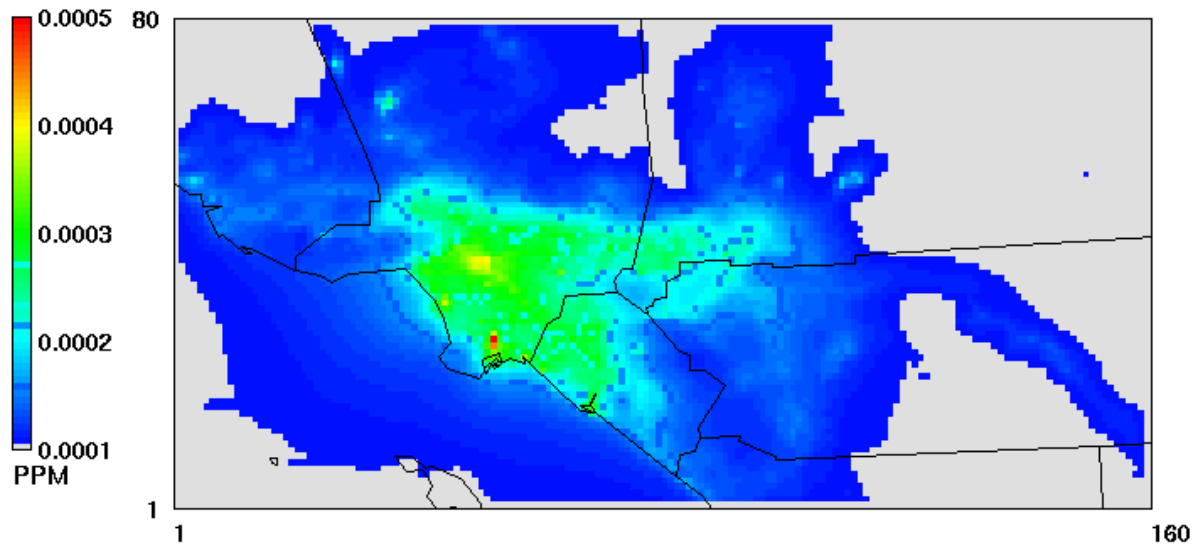
Figure IX-10h
CAMx simulated 2012 annual average Benzene.

1,3Butadiene

2012 Annaul Average Concentrations
w=average.dgas_CMAQ.plot
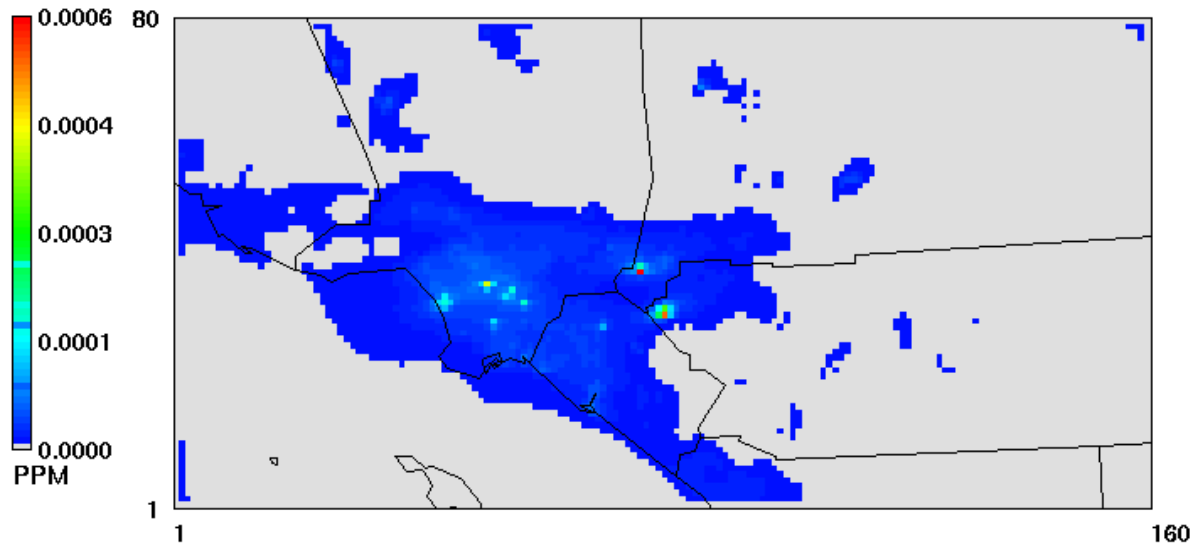
Figure IX-10i
CAMx simulated 2012 annual average 1,3-Butadiene.

Total Formaldehyde

2012 Annaul Average Concentrations
w=average.dgas_CMAQ.plot
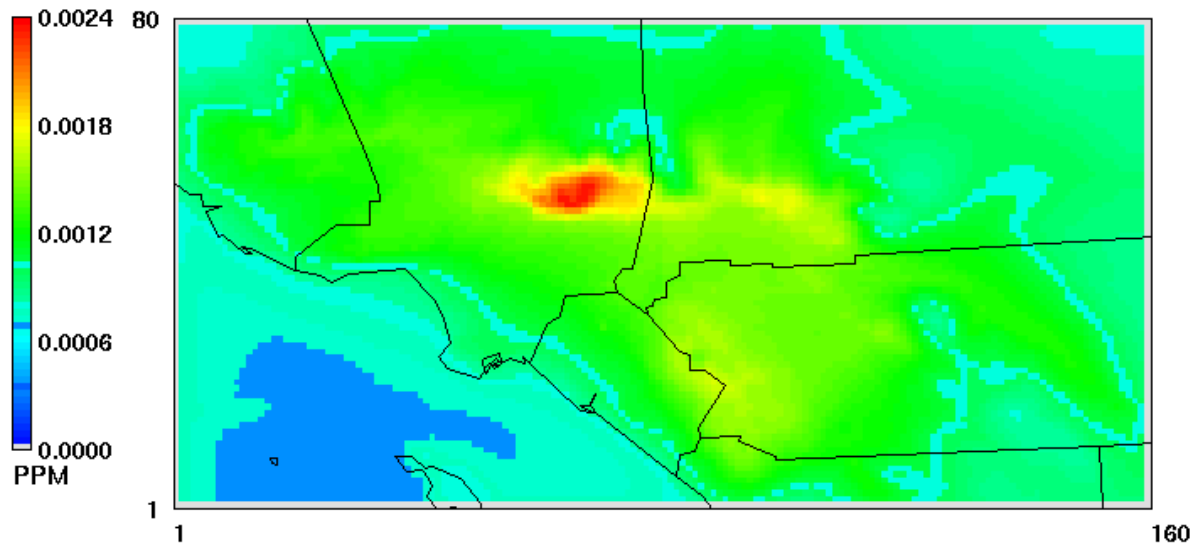
Figure IX-10j
CAMx simulated 2012 annual average for Total Formaldehyde.

Total Acetaldehyde

2012 Annaul Average Concentrations
w=average.dgas_CMAQ.plot
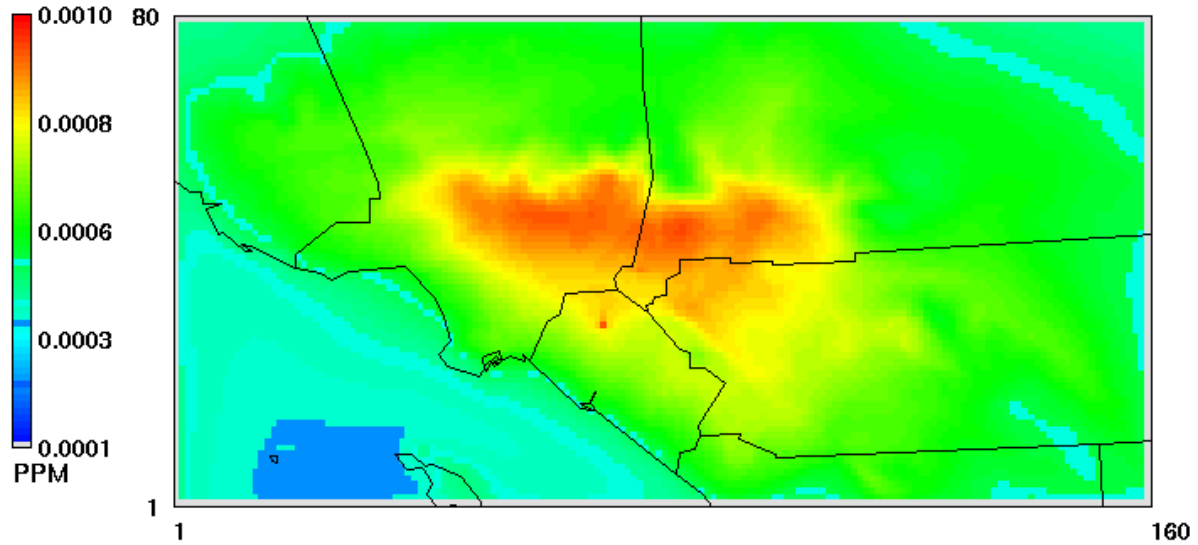
Figure IX-10k
CAMx simulated 2012 annual average Acetaldehyde.

Arsenic (PM2.5)

2012 Annual Average Concentrations
v=average.draft.plot
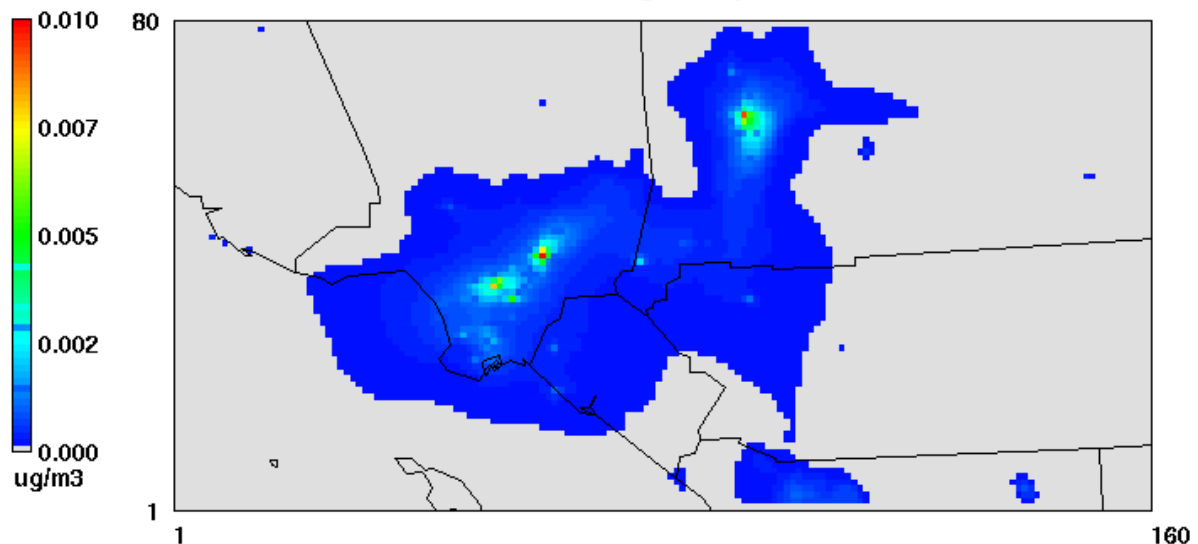
Figure IX-10l
CAMx simulated 2012 annual average Arsenic PM$_{2.5}$.

Cadmium (PM2.5)

2012 Annual Average Concentrations
v=average.draft.plot
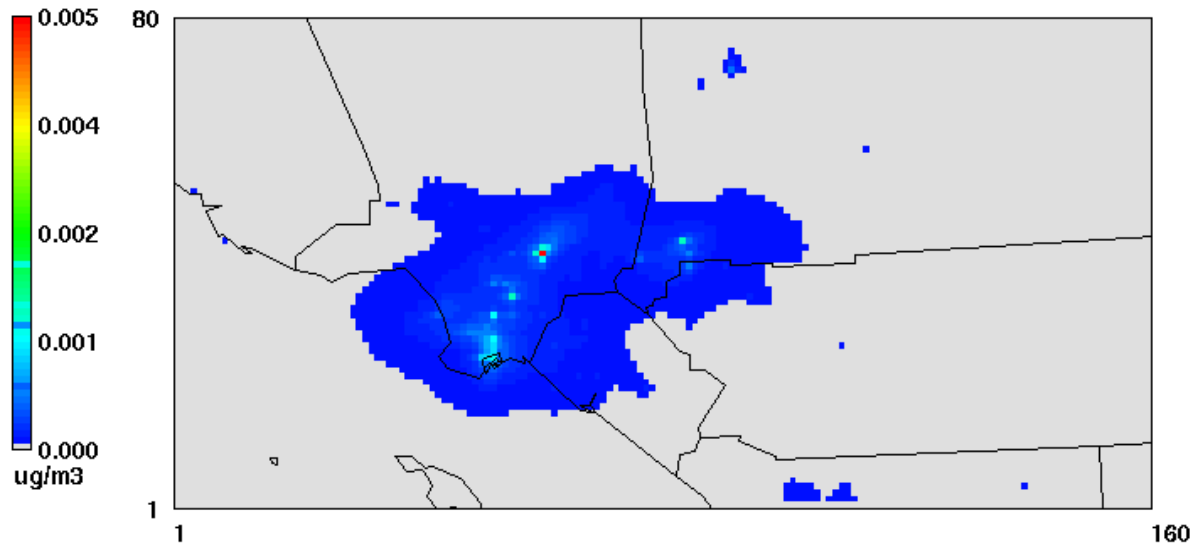
Figure IX-10m
CAMx simulated 2012 annual average Cadmium PM$_{2.5}$.

Hexavalent Chromium (PM2.5)

2012 Annual Average Concentrations
v=average.draft.plot
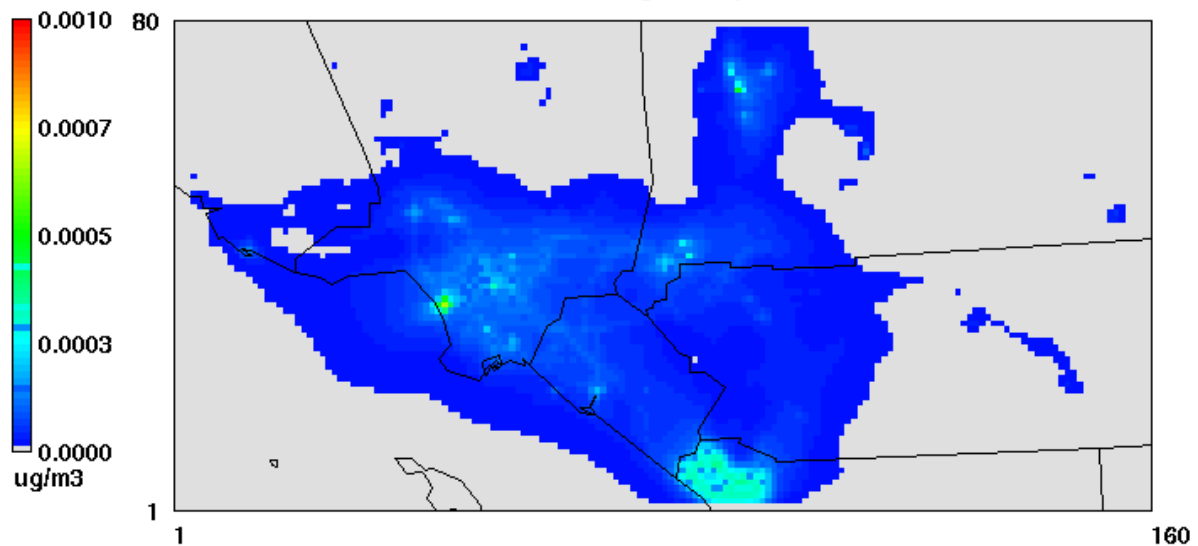
Figure IX-10n
CAMx simulated 2012 annual average Chromium PM$_{2.5}$.

Lead (PM2.5)

2012 Annual Average Concentrations
v=average.draft.plot
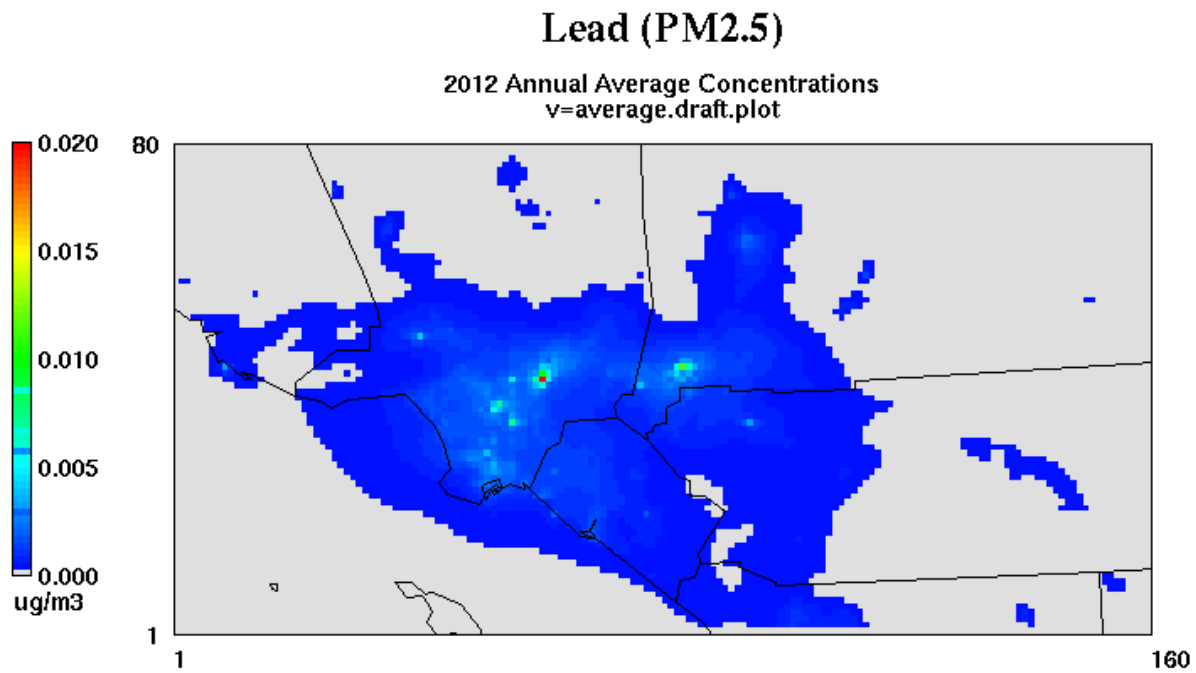
Figure IX-10o
CAMx simulated 2012 annual average Lead PM$_{2.5}$.

Methylene Chloride

2012 Annaul Average Concentrations
w=average.dgas_CMAQ.plot
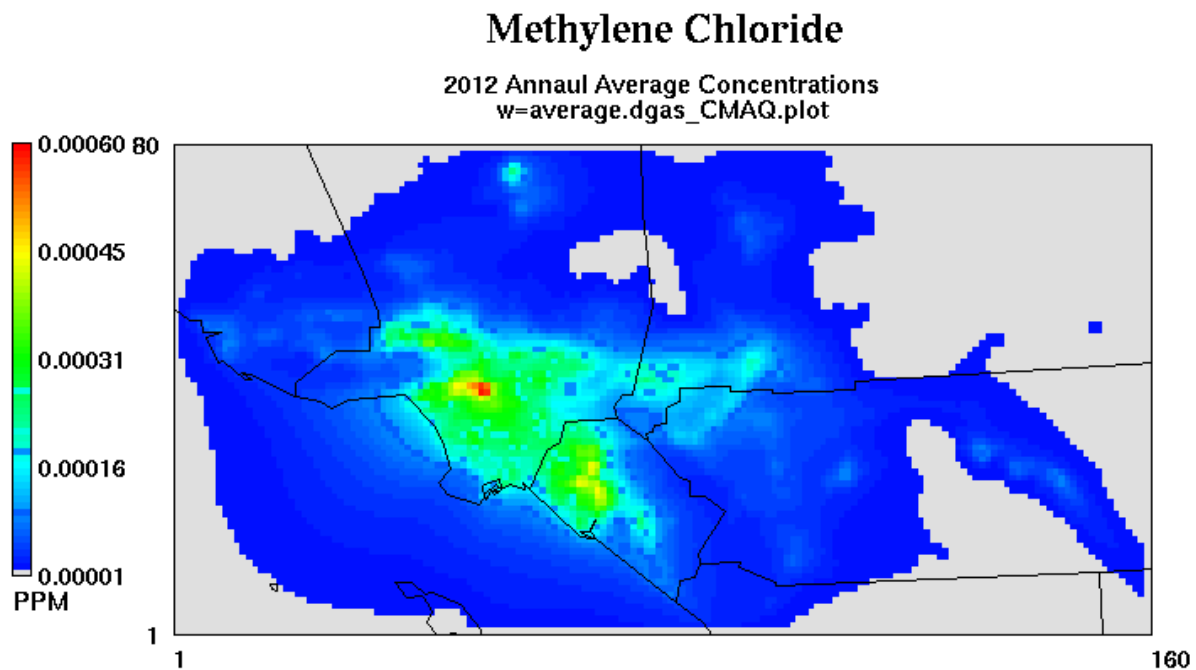
Figure IX-10p
CAMx simulated 2012 annual average Methylene Chloride.

Naphthalene

2012 Annaul Average Concentrations
w=average.dgas_CMAQ.plot
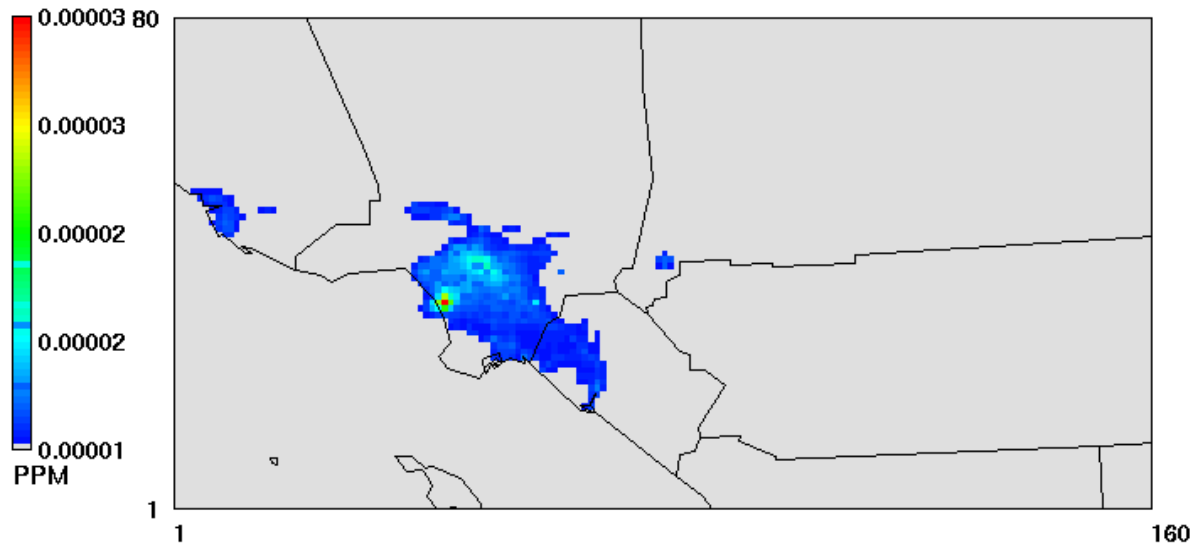
Figure IX-10q
CAMx simulated 2012 annual average Naphthalene.

NIckel (PM2.5)

2012 Annual Average Concentrations
v=average.draft.plot
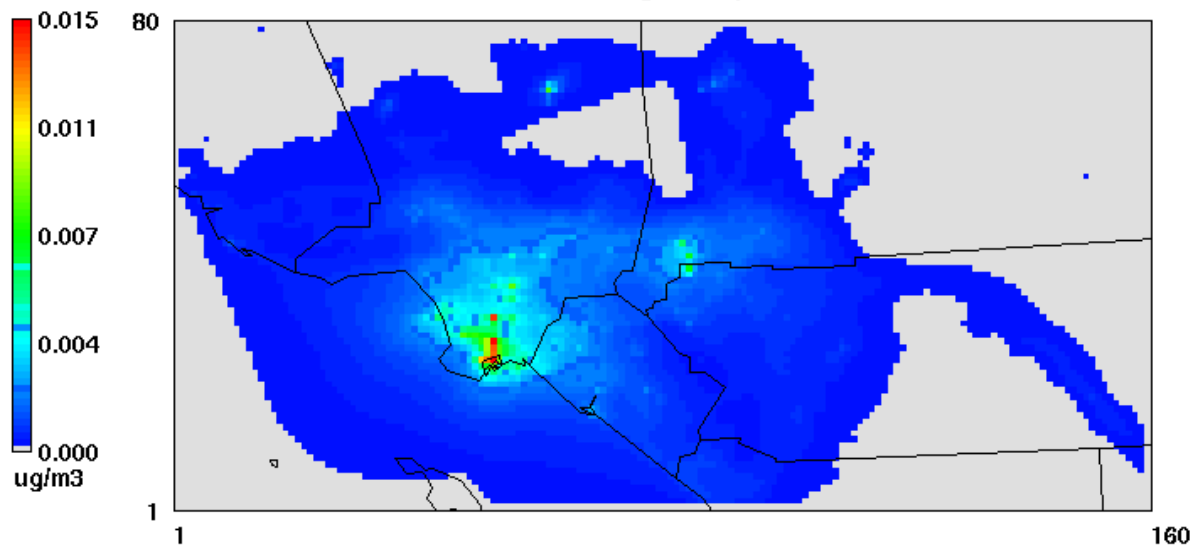
Figure IX-10r
CAMx simulated 2012 annual average Nickel PM$_{2.5}$.
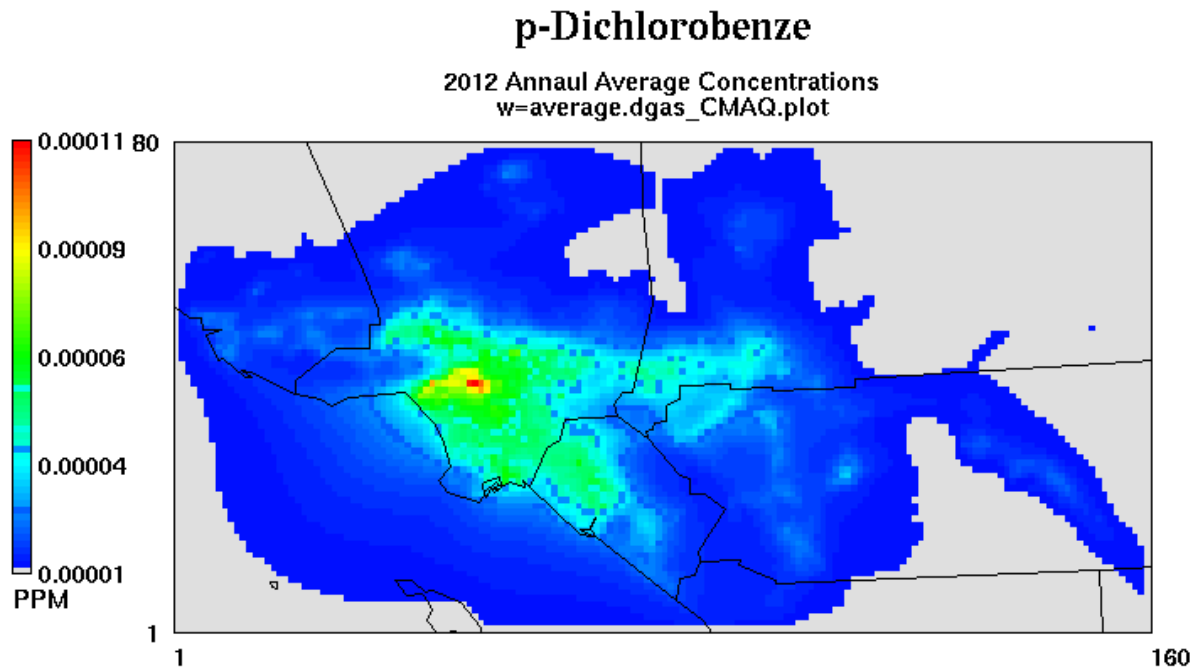
p-Dichlorobenze

Figure IX-10s
CAMx simulated 2012 annual average p-Dichlorobenzene.

Perchloroethylene
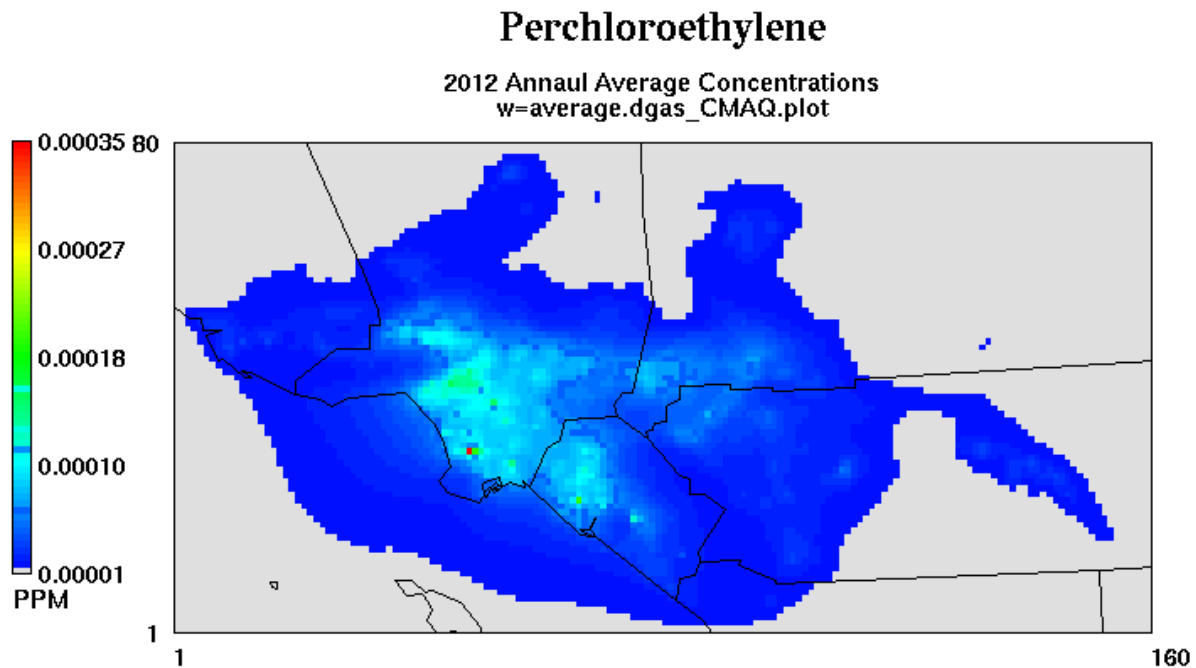
Figure IX-10t
CAMx simulated 2012 annual average Perchloroethylene.
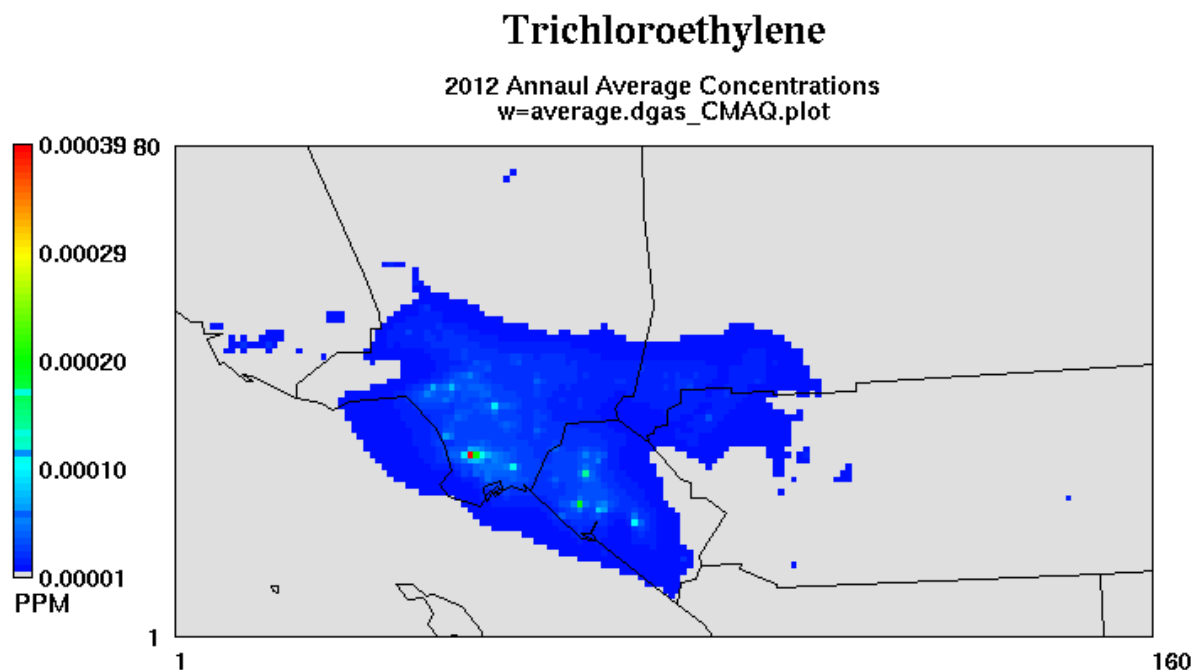
Figure IX-10u
CAMx simulated 2012 annual average Trichloroethylene.

IX.17 Estimation of Risk

Figure IX-11 depicts the distribution of risk estimated from the predicted annual average concentrations of the key toxic compounds. Risk is calculated for each grid cell as follows:

$$\text{Risk}_{i,j} = \Sigma \text{ Concentration}_{i,j,k} \text{ X Risk Factor}_{i,j,k},$$

where i,j is the grid cell (easting, northing) and k is the toxic compound.

The grid cell having the maximum simulated risk of 1,057 was located in the Ports of Los Angeles and Long Beach. In addition to the cluster of cells around the port area with high risk, a second cluster of high risk area is centered on the railyard in Los Angeles. In general, as in the past studies, the higher risk areas tend to be along transportation corridors.

Figure IX-12 provides the CAMx RTRAC simulated air toxics risk for the 2005 MATES III period. Figure IX-13 depicts the changes in risk from 2005 to 2012-2013 estimated from the CAMx RTRAC simulations. The greatest decrease in risk occurred in the port area, reflecting the emission reductions from shipping and port operations. Overall, air toxics risk improves significantly, consistent with air toxic emissions reductions that occurred over the period.

The 2012-2013 Basin average population-weighted risk summed for all the toxic components yielded a cancer risk of 367 in a million. The average risk included all populated over-land cells that reside within the Basin portion of the modeling domain. The MATES III Basin average risk was 853 per million. From the MATES III to the MATES IV period, the simulated risk decreased by 57%. This reduction in Basin risk can be attributed to several factors, most notably changes in diesel emissions between 2005 and 2012. While weather profiles between the two monitoring periods varied, no appreciable difference was observed in the meteorological dispersion potential.

Figures IX-14a through IX-14f depict risk associated with diesel and its specific emissions categories. Figure IX-15 provides the Basin risk excluding the contribution of diesel particulates. On and off-road diesel impacts are spread throughout the Basin following the transportation corridors and off-road facilities such as the intermodal transfer sites. The shipping impacts are concentrated in the vicinity of the Ports of Los Angeles and Long Beach and the adjacent downwind communities.

Regional risk from nondiesel sources (Figure IX-15) is also uniformly distributed throughout the Basin with values typically around 100 in one million, with only a few selected cells showing values in excess of 200.
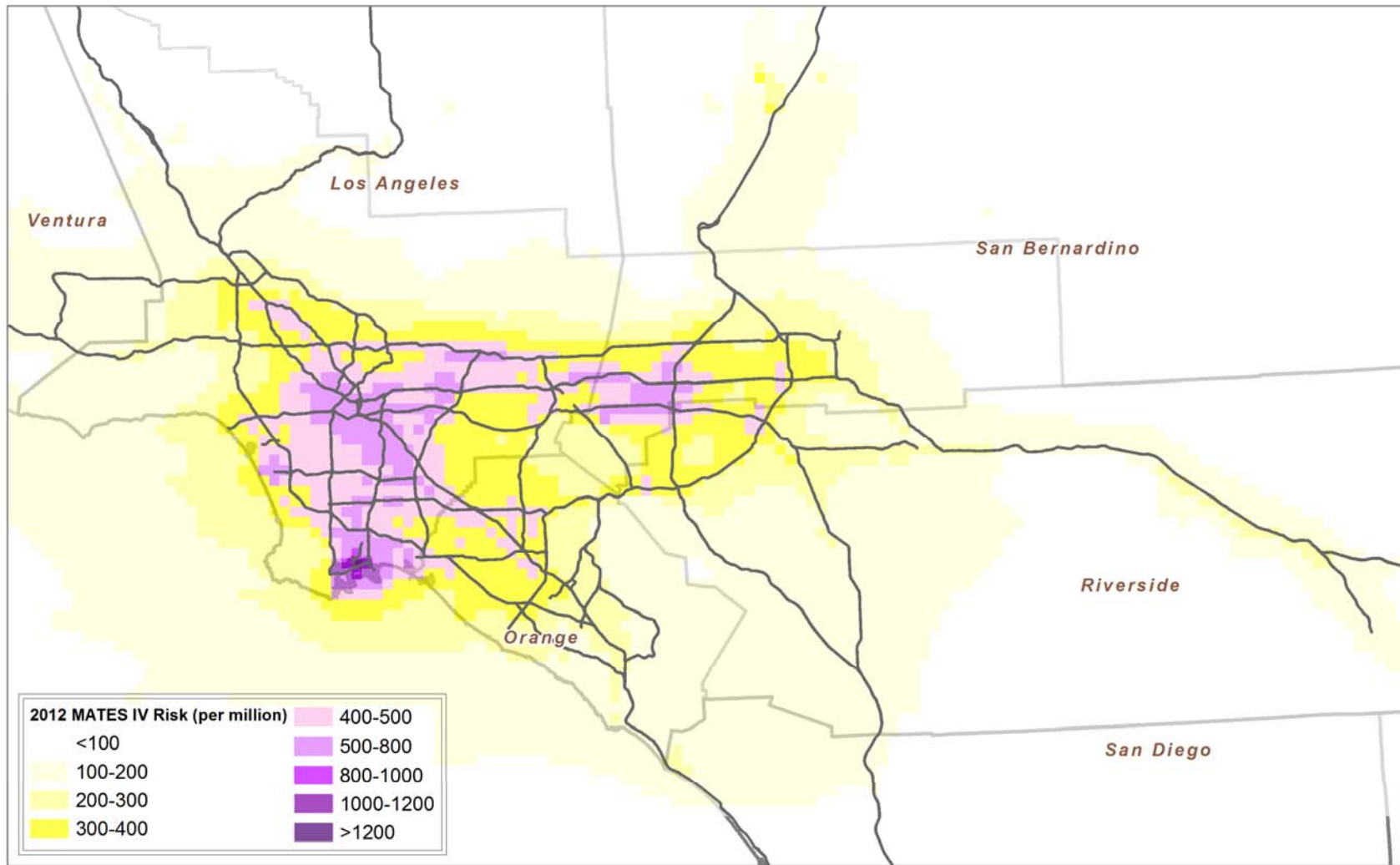
Figure IX-11
2012 MATES IV CAMx RTRAC Simulated Air Toxic Risk.
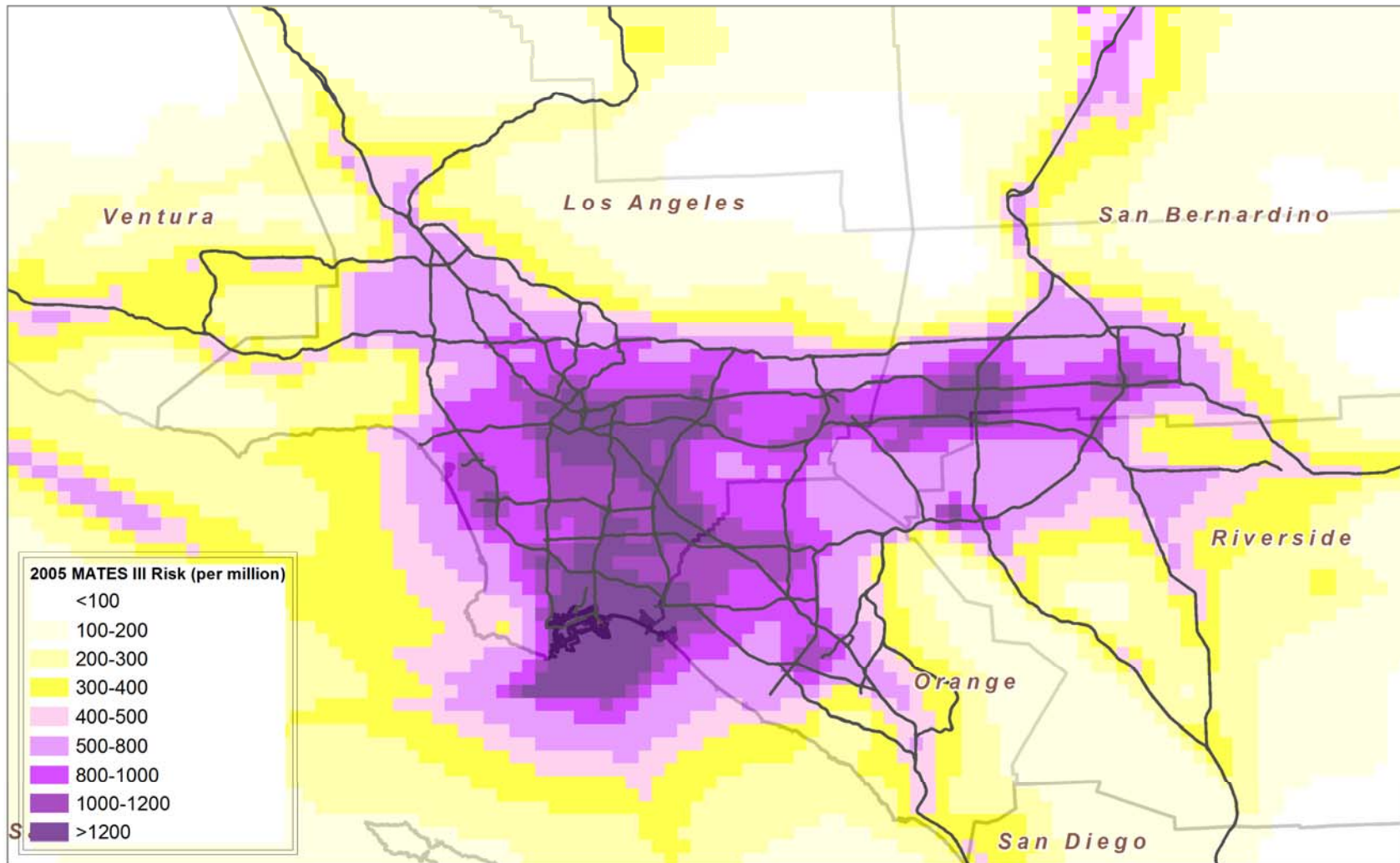
Figure IX-12
2005 CAMx RTRAC Simulated Air Toxic Risk.
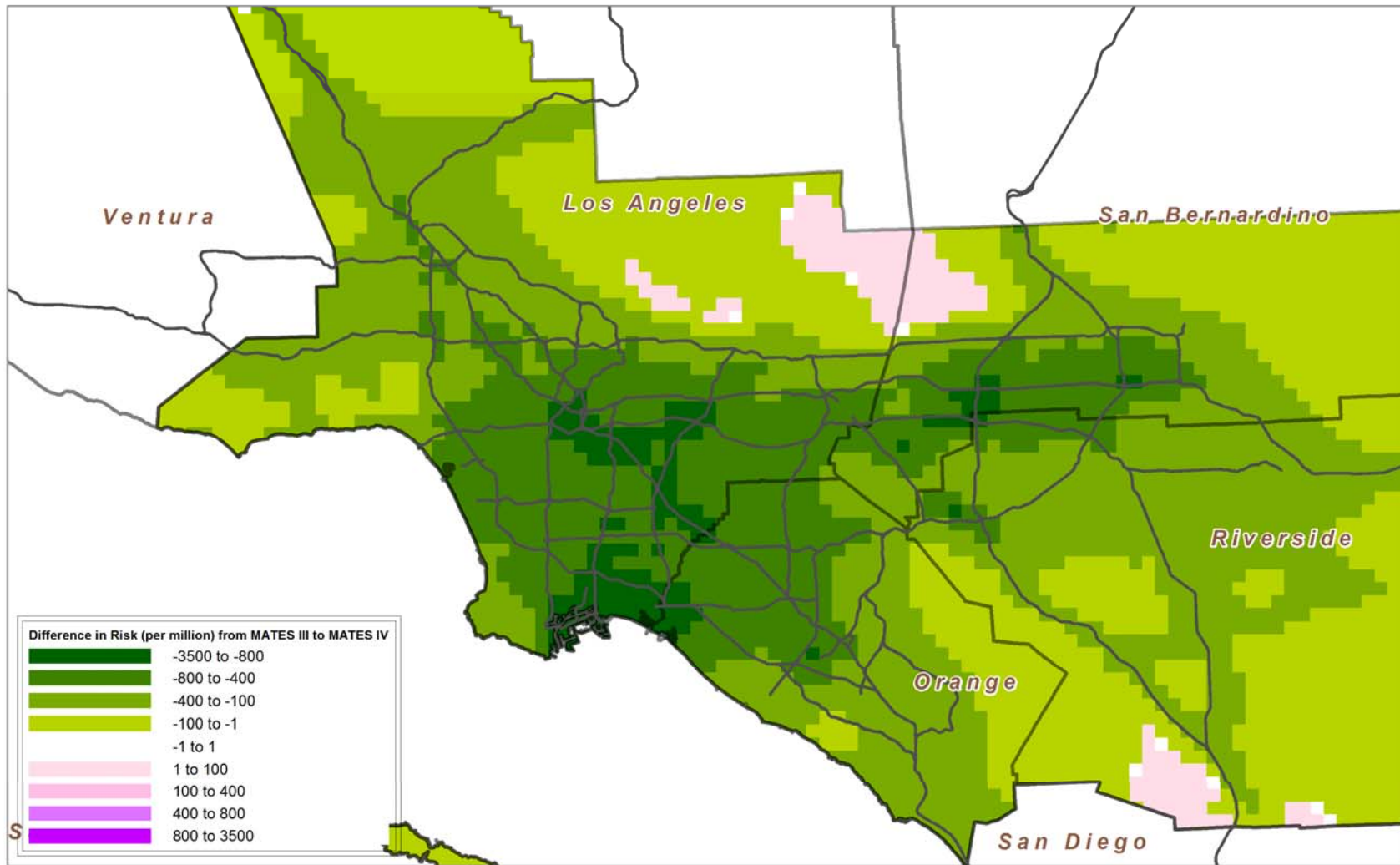
Figure IX-13
Change in CAMx RTRAC simulated risk from the 2005 to 2012
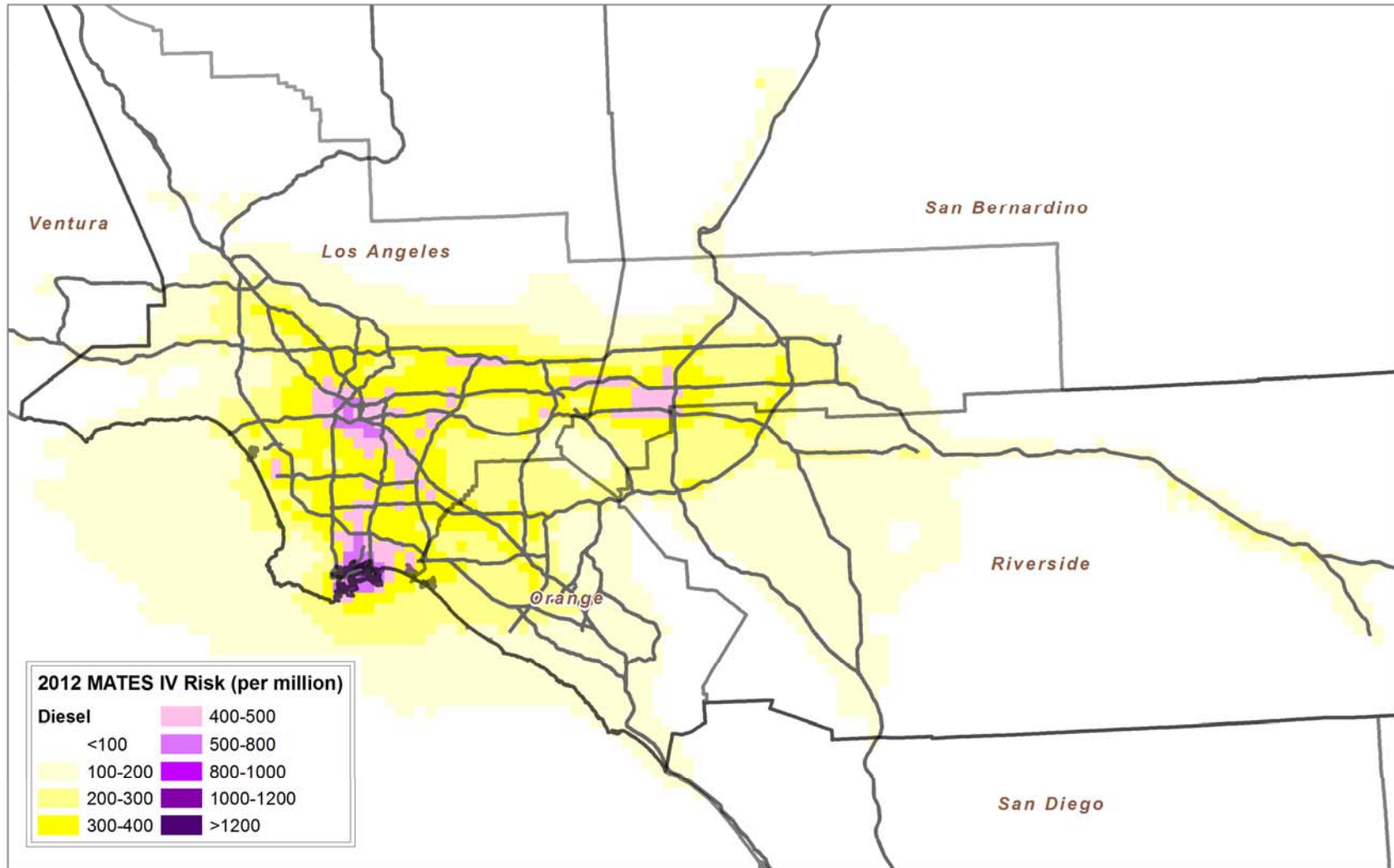
Figure IX-14a
MATES IV Risk from Diesel
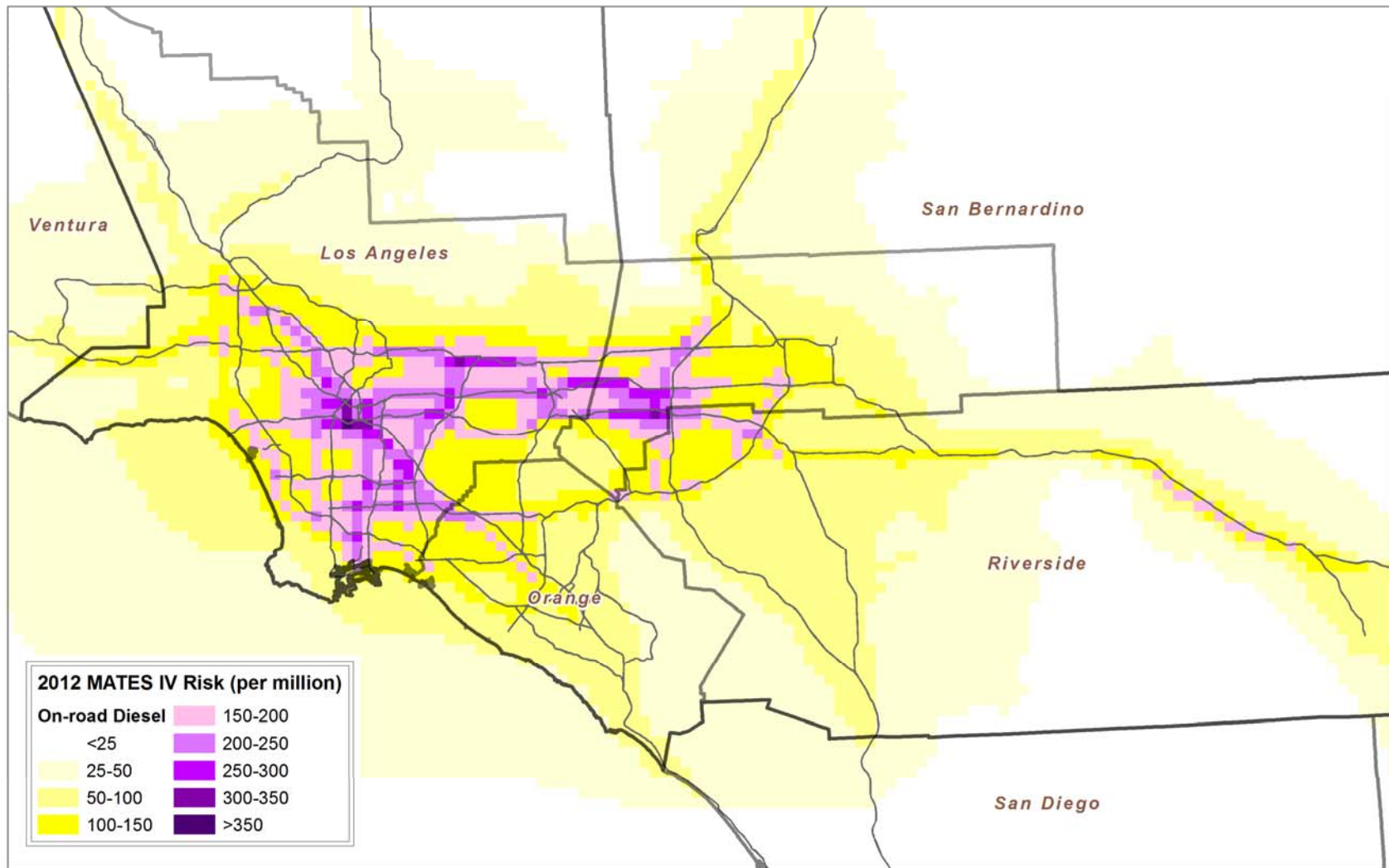
Figure IX-14b
MATES III Simulated Risk from On-Road Diesel.
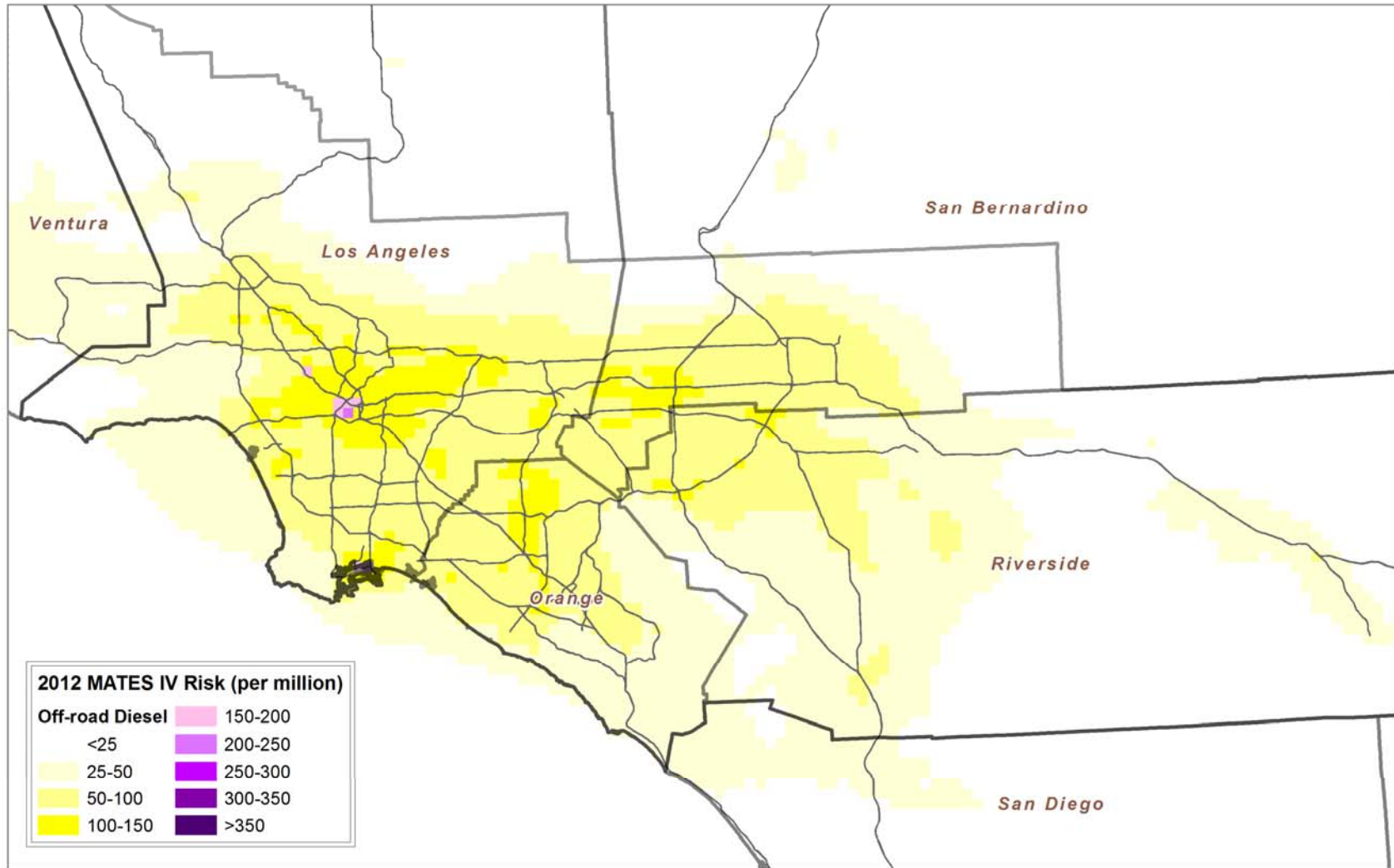
Figure IX-14c
MATES IV Simulated Risk from Off-road Diesel (including railyards but excluding trains and ships).
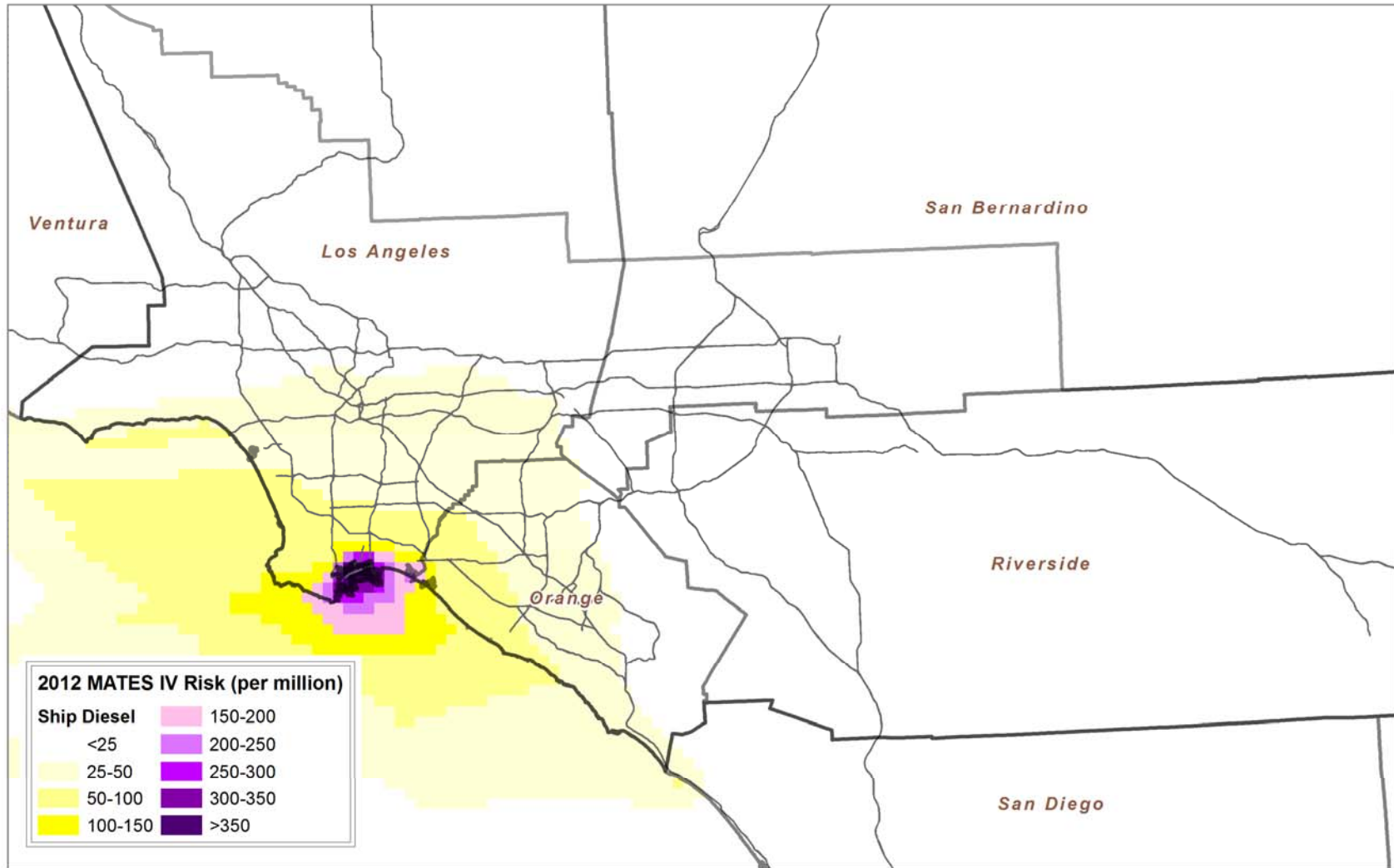
Figure IX-14d
MATES IV Simulated Risk from Ship Diesel.
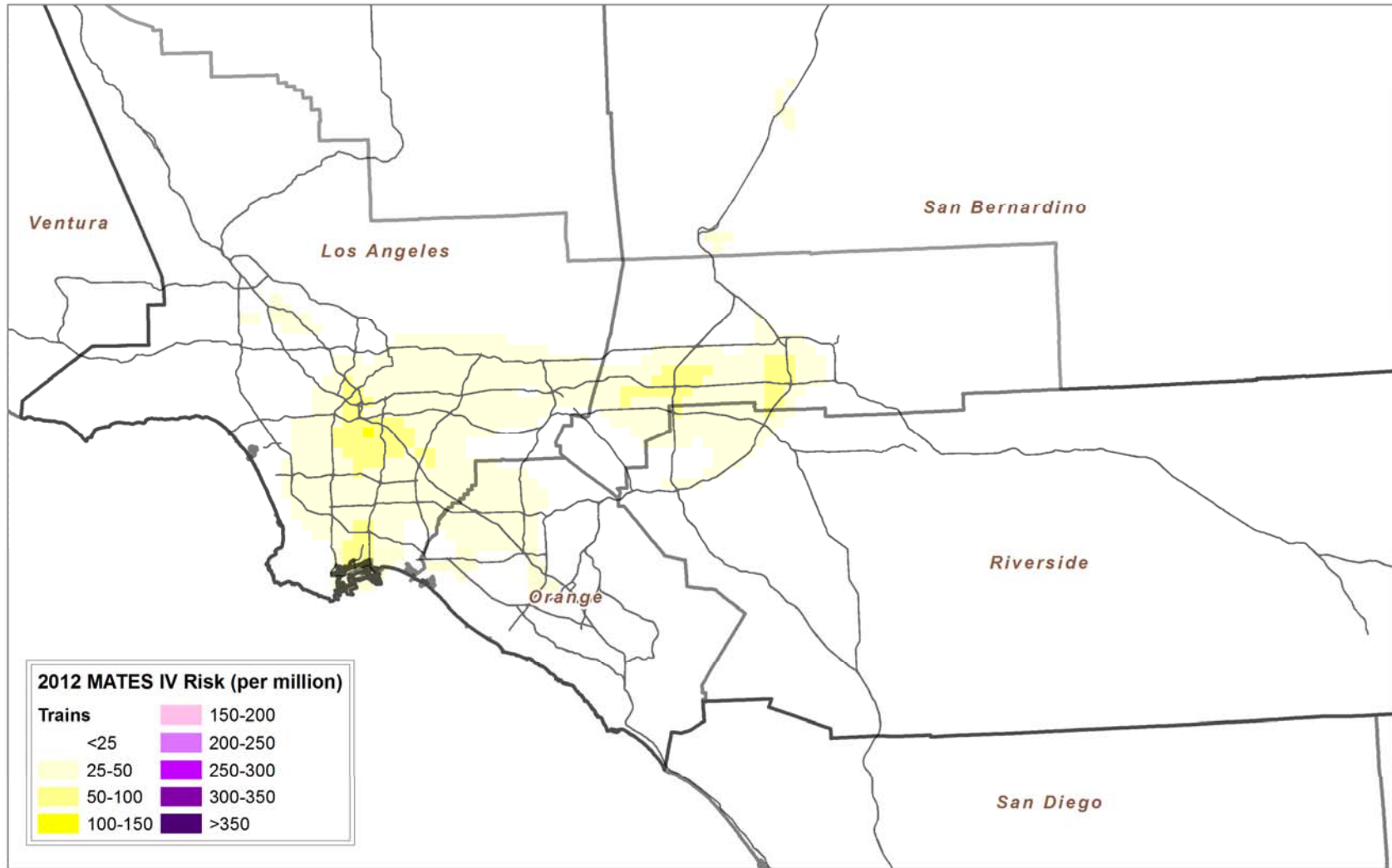
Figure IX-14e
MATES IV Simulated Risk from Trains (Excluding Railyards Equipments).
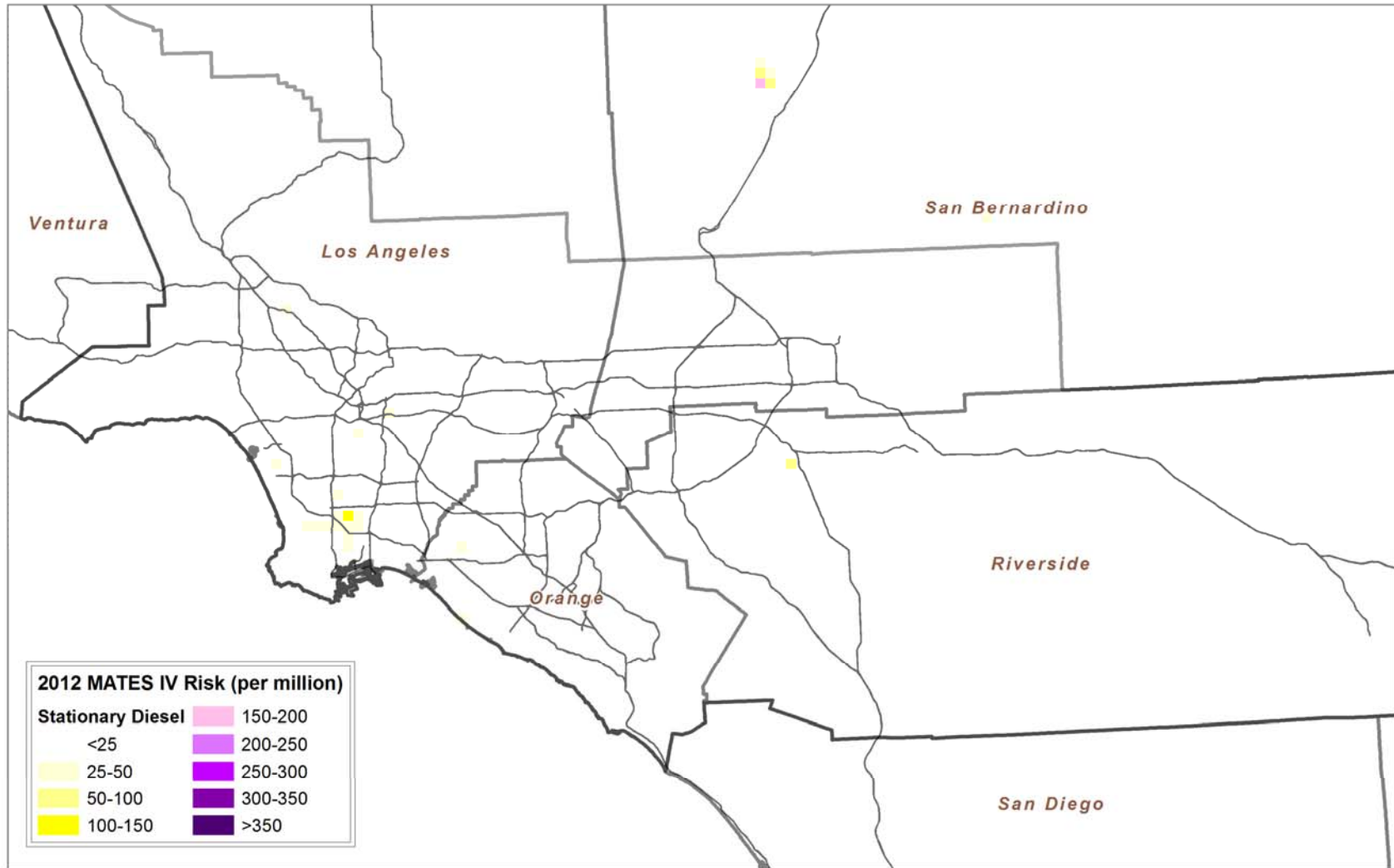
Figure IX-14f
MATES IV Simulated Risk from Stationary Diesel.
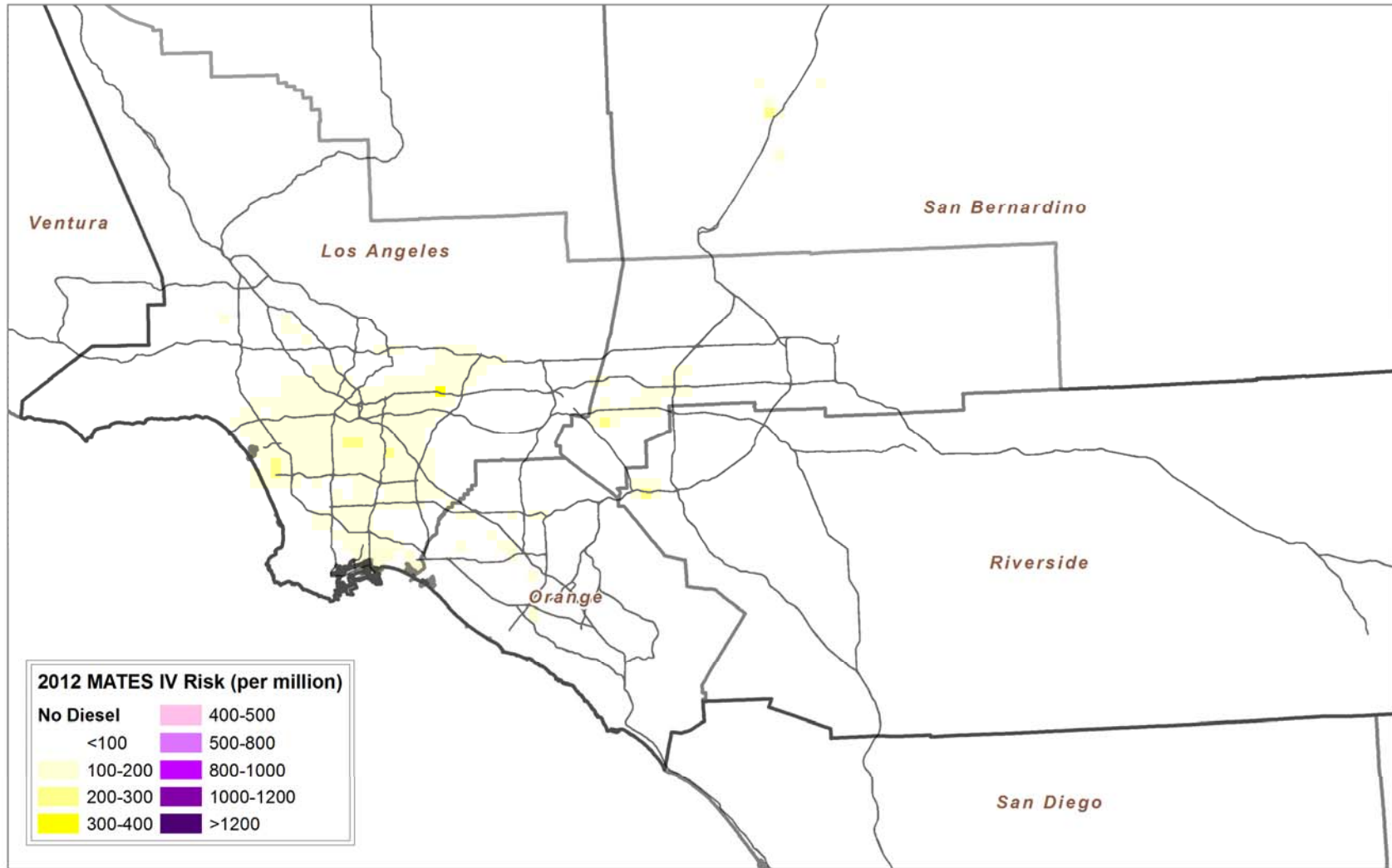
Figure IX-15
MATES IV Simulated Risk No-Diesel.

Figure IX-16 provides a close-up plot of risk in the ports area. Table IX-11 provides a summary risk estimated for the Basin, for the Ports area, and for the Basin excluding the ports area. For this assessment, the ports area includes the populated cells roughly bounded by the Interstate 405 to the north, San Pedro to the west, Balboa Harbor to the east and Pt. Fermin to the south. The 2012-2013 average population-weighted air toxics risk in the ports area (as defined above) was 480 in one million. The Basin average population-weighted air toxics risk, excluding the grid cells in the ports area, was 359 in one million. It is important to note that the downwind impacts resulting from port area activities are reflected in the toxics risk estimates for the grid cells categorized as "Basin minus Ports." Similarly, the MATES III simulations for 2005 indicated that the ports area air toxics risk was 1,415; and the Basin, minus the ports area, was 816 in one million. Overall, the ports area experienced an approximate 66% decrease in risk, while the average population-weighted risk in other areas of the Basin decreased by about 56%.
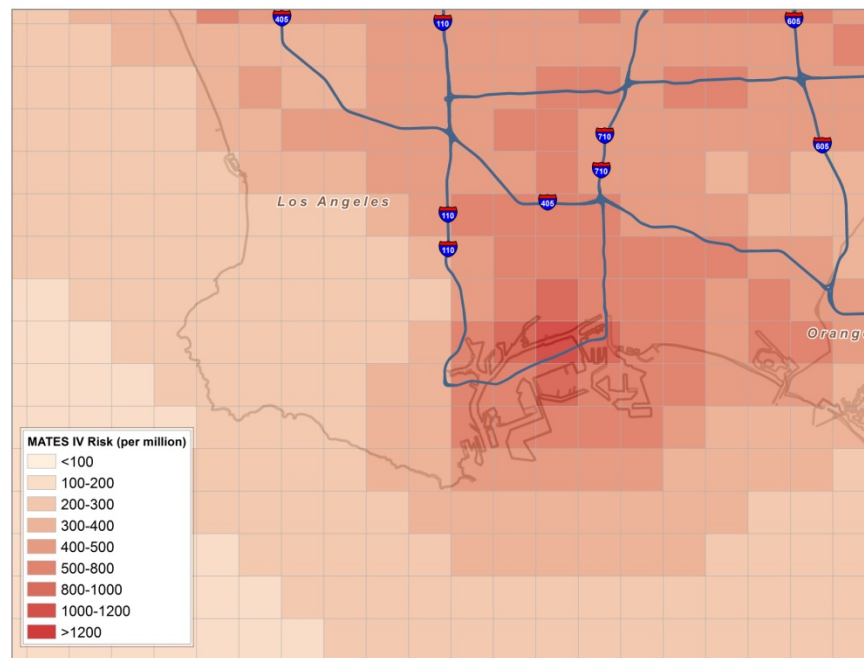
Figure IX-16
2012 Ports area MATES IV Simulated Air Toxic Risk.

Table IX-11
Basin and Port Area Population Weighted Risk

Region	MATES IV		MATES III		Average Percentage Change in Risk
	2012 Population	Average Risk (Per Million)	2005 Population	Average Risk (Per Million)	
Basin	15,991,150	367	15,662,620	853	-57
Ports Area	998,745	480	959,761	1,415	-66
Basin Excluding Ports Area	14,992,806	359	14,702,859	816	-56

IX.18 County Risk Assessment

Figures IX-17 through IX-20 provide close up depictions of air toxics risk to Central Los Angeles, Mira Loma/Colton, Central Orange County and West Los Angeles areas, respectively;, and Table IX-12 provides the county breakdown of air toxics risk to the affected population. As presented in the spatial distribution, Los Angeles County bears the greatest average risk at 415 per one million person population. The SCAB portion of San Bernardino County has the second highest projected risk at 339 per one million person population. The estimated risk for Orange County is 315 per million, and Riverside was estimated to have the lowest population-weighted risk at 223. The Coachella Valley of Riverside County, as expected, has the lowest toxic risk at 139. It should be noted that these are county-wide averages, and individual communities could have higher risks than the average if they are near emissions sources, such as railyards or intermodal facilities.

Comparison of the county-wide population-weighted risk shows that the greatest reduction occurred in Orange County with nominal variations among counties. Reductions in emissions from mobile sources including benzene, 1,3-butadiene, and diesel particulate have contributed to the improved county-wide risk. It is noteworthy that San Bernardino County now has higher population-weighted risk than Orange County. This is because the port area has a proportionally larger impact in Orange County than in San Bernardino County.

Table IX-12
County-Wide Population Weighted Air Toxic Risk

Region	MATES IV		MATES III		Average Percentage Change in Risk
	2012 Population	Average Risk (Per Million)	2005 Population	Average Risk (Per Million)	
Los Angeles	9,578,586	415	9,887,127	951	-56
Orange	3,067,909	315	2,764,620	781	-60
Riverside	1,784,872	223	1,548,031	485	-54
San Bernardino	1,560,183	339	1,462,842	712	-52
SCAB	15,991,550	367	15,662,620	853	-57
Coachella Valley	465,064	139	N/A	N/A	N/A
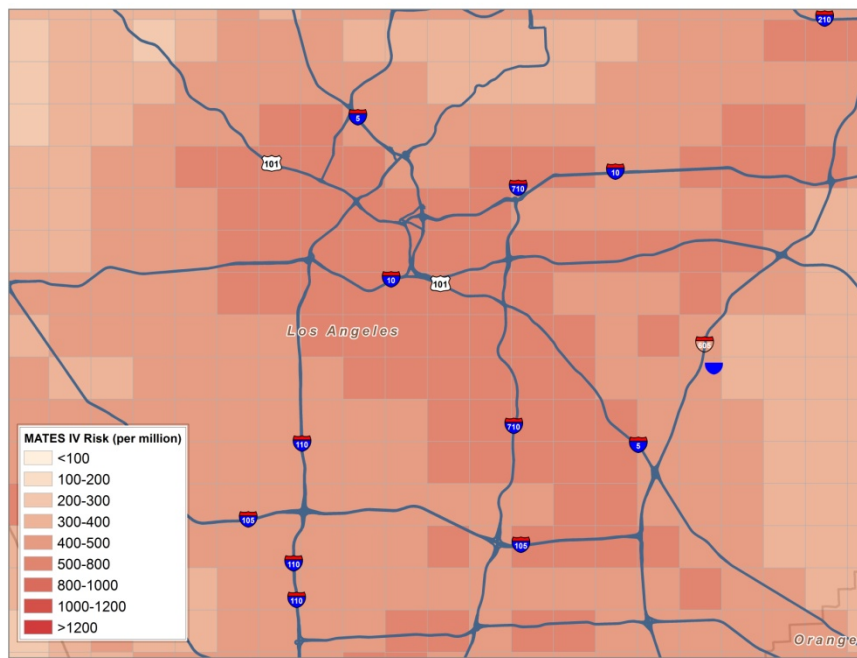
Figure IX-17
2012 Central Los Angeles MATES IV Simulated Air Toxic Risk.
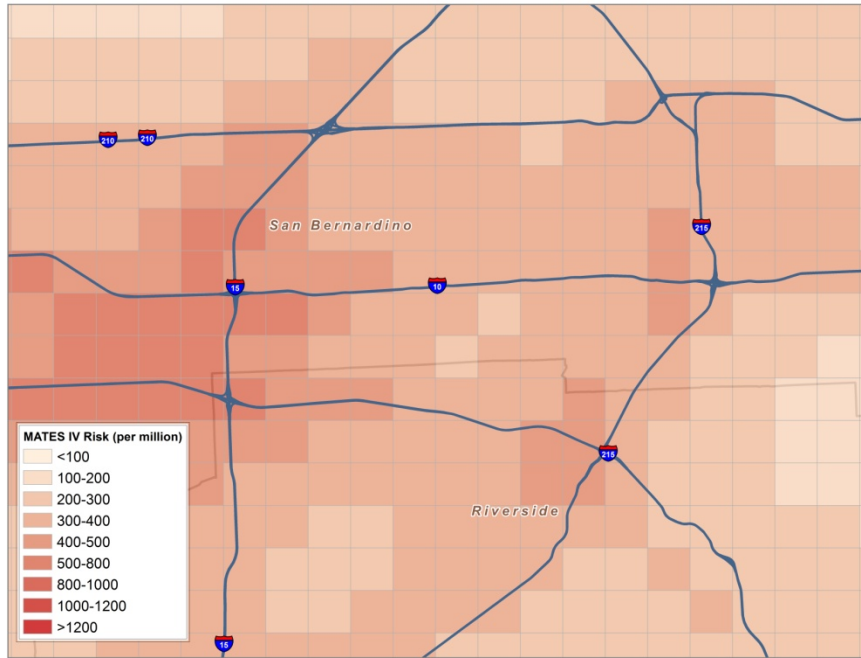
Figure IX-18
2012 Mira Loma/Colton MATES IV Simulated Air Toxic Risk.
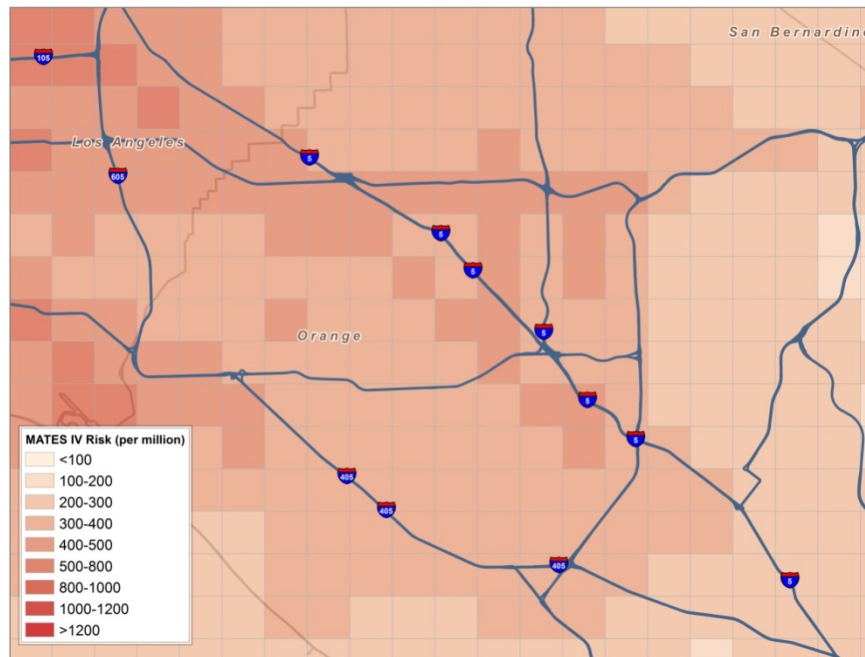
Figure IX-19
2012 Central Orange County MATES IV Simulated Air Toxic Risk.
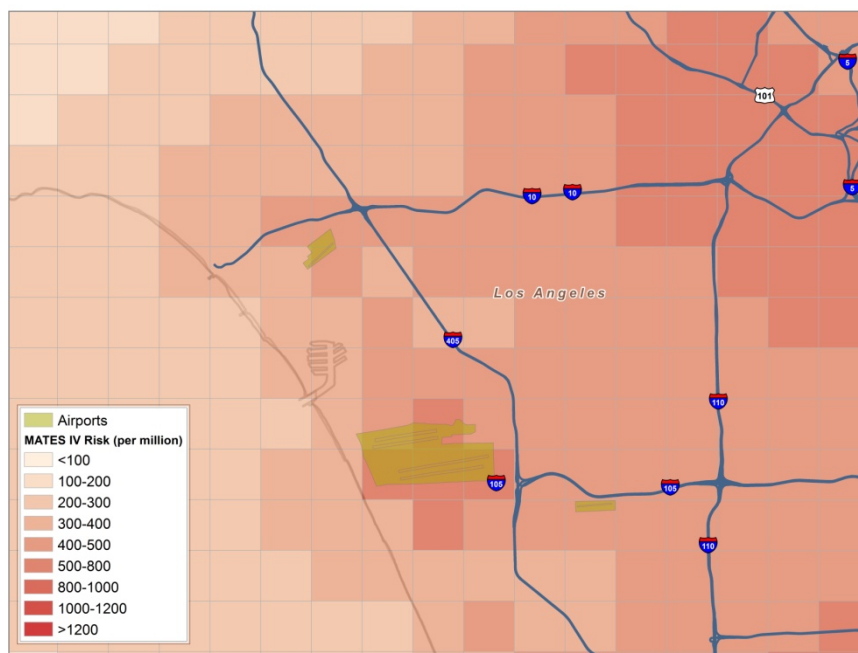
Figure IX-20
2012 West Los Angeles MATES IV Simulated Air Toxic Risk.

IX.19 Risk from Key Compounds

Table IX-13 provides the Basin average breakdown of risk associated with each of the key compounds simulated in the analysis. Diesel particulate ranked highest (76%) as the toxic compound contributing to the overall risk to the population. The next three highest contributors included benzene, hexavalent chromium and 1,3-butadiene. The four top toxic pollutants contribute over 91% toxic risk. Formaldehyde (primary and secondary) and acetaldehyde (primary and secondary) contribute 3.5% and 1.3%, respectively, while the remaining compounds combined accounted for less than 4% of the total.

IX.20 Network Risk Evaluation

Table IX-14 provides the simulated air toxics risk at each of the 10 stations for the three main toxic compounds and the remaining aggregate based on the regional modeling. Risk is calculated using the predicted concentrations of each toxic component for the specific monitoring station location (based on a nine-cell weighted average concentration). The summary also provides the comparison between simulated average risk for the 10 stations combined and the average risk calculated using the annual toxic compound measurements and the estimated diesel concentrations at those sites.

Table IX-13
2012-2013 MATES IV Risk from Simulated Individual Toxic Air Contaminants

Toxic Compound	Risk Factor ($\mu g/m^3$)	Peak Annual Average Concentration	Population Weighted Annual Average Concentration	Units	Cumulative Risk (per million)	% Contribution
Diesel	3.00E-04	17.4	0.93	$\mu g/m^3$	279.67	76.2
Benzene	2.90E-05	0.51	0.25	ppb	22.82	6.2
Hexavalent Chromium	1.50E-01	0.001	1.37E-04	$\mu g/m^3$	20.52	5.6
1,3-Butadiene	1.70E-04	0.58	0.03	ppb	12.54	3.4
Secondary Formaldehyde	6.00E-06	2.35	1.24	ppb	9.12	2.5
Primary Formaldehyde	6.00E-06	2.71	0.50	ppb	3.7	1.0
Secondary Acetaldehyde	2.70E-06	0.93	0.73	ppb	3.56	1.0
Arsenic	3.30E-03	0.043	9.97E-04	$\mu g/m^3$	3.29	0.9
p-Dichlorobenzene	1.10E-05	0.11	4.38E-02	ppb	2.90	0.8
Perchloro-ethylene	5.90E-06	0.356	0.07	ppb	2.71	0.7
Naphthalene	3.40E-05	0.03	9.87E-03	ppb	1.76	0.5
Cadmium	4.20E-03	0.014	3.29E-04	$\mu g/m^3$	1.38	0.4
Nickel	2.60E-04	0.11	3.69E-03	$\mu g/m^3$	0.96	0.3
Primary Acetaldehyde	2.70E-06	0.67	0.16	ppb	0.80	0.2
Methylene Chloride	1.00E-06	0.59	0.21	ppb	0.74	0.2
Trichloroethylene	2.00E-06	0.39	3.08E-02	ppb	0.33	0.1
Lead	1.20E-05	0.065	4.17E-03	$\mu g/m^3$	0.05	<0.1

The highest simulated risk was estimated for West Long Beach followed by Los Angeles, Huntington Park, North Long Beach, and Compton.   The lowest modeled risk was simulated at Anaheim. As previously discussed, simulation performances at those high risk sites showed a tendency for overprediction; consequently, this feature resulted in the higher risk calculation.

Risk averaged over the 10 stations was simulated as 505 in a million, which is approximately 25% higher than the value estimated from measurements. This includes the contribution of diesel particulates. An emission-based adjustment factor, 0.82, was applied to estimate the diesel portion from the $EC_{2.5}$ measurements.

The nondiesel portion of the simulated risk can be directly compared to risk calculated from the toxic compound measurements. Figure IX-21 presents a comparison of the model simulated and measurement estimated nondiesel risk at each monitoring site, as well as the 10-station average. Simulated nondiesel risk is within 30% of measurements at all stations. The simulated 10-station average risk is essentially equal to the risk estimated from the measurements.

Simulated total risk, including the contribution of diesel particulates, taken as an eight-station average, is 505 in a million. The 10-station average simulated risk is approximately 25% lower than the risk calculated from the measured toxic compound concentrations and the estimates of diesel concentrations using the emissions based factor (0.82) applied to the $EC_{2.5}$ average concentration.

Table IX-14
Comparison of Network Averaged CAMx RTRAC 2012-2013 Modeled Risk to Measured Risk
at the 10 MATES IV Sites

Location	2012-2013 MATES IV CAMX RTRAC Simulation				
	Benzene	1,3-Butadiene	Others	Diesel	Total
Anaheim	26	14	54	301	395
Burbank	27	13	59	333	431
Central LA	33	19	78	516	646
Compton	26	17	63	383	489
Inland Valley San Bernardino	21	9	61	309	400
Huntington Park	30	62	96	389	576
North Long Beach	27	16	65	395	503
Pico Rivera	25	13	62	358	459
Rubidoux	20	7	46	296	369
West Long Beach	32	15	69	662	778
10-Station Average Modeled	27	18	65	394	505
10-Station MATES IV Average Measured ($EC_{2.5}$ *0.82 for Diesel)	35	33	47*	287	402

* Including modeled species only, Risk from some species, such as carbon tetrachloride, chloroform and PAHs are excluded.
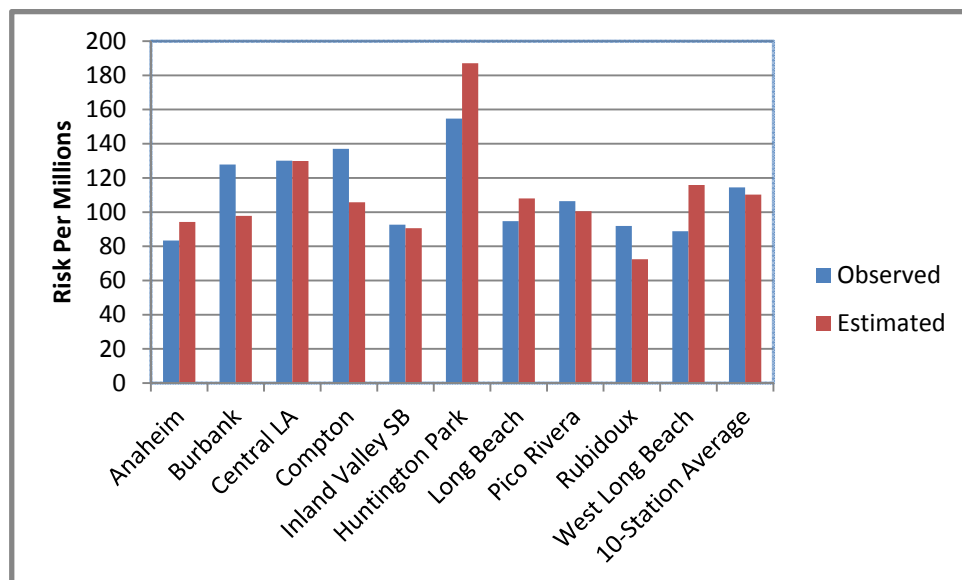
Figure IX-21
2012 MATES IV Simulated vs. Measured Non-Diesel Air Toxics Risk

IX.21 Evaluation

The population-weighted average Basin air toxics risk (367 per million) simulated using CAMx RTRAC for the 2012-2013 MATES IV period was estimated to be 57% lower than estimated (853 in a million) for the MATES III period. The areas of the Basin with the highest risk continued to be the Ports of Los Angeles and Long Beach with a secondary maximum occurring in an area around the railyard in the Los Angeles.

A majority of the risk reduction can be tied to changes in diesel emissions, which were reduced by 66% from 2005 to 2012. The emissions reductions of benzene (11%), 1,3-butadiene (50%), arsenic (43%) and other air toxics contribute to the overall reduction in 2012-2013 simulated risk, as well. A general assessment of the observed meteorological profile suggests that the two monitoring periods were comparable in dispersion potential.

.

IX.22 References

Byun, D.W., and Ching, J.K.S., 1999, Science Algorithms of the EPA Models-3 Community Multiscale Air Quality (CMAQ) Modeling system, U.S. Evironmental Protection Agency, EPA/600/R-99/030

ENVIRON, Inc., 2008, CAMx User's Guide Version 4.5. ENVIRON. Novato, CA 94945

ENVIRON, Inc., 2005, "METSTAT software for MM5 version 3 (02/11/05)," ENVIRON. Novato, CA 94945, http://www.camx.com/down/support.php

ENVIRON, Inc., 2006, "KVPATCH software for CAMx," ENVIRON. Novato, CA 94945, http://www.camx.com/down/support.php

Grell, G.A., Dudhia, J., Stauffer, D.R., 1994, A Description of the Fifth-Generation Penn State/NCAR Mesoscale Model (MM5), NCAR/TN-398+STR, NCAR Technical Note

Mason, R., Dolwick, P., Carey, P., Kinnee, E., Wilson, M., 2008. Emissions processing and sensitivity air quality modeling of category 3 commercial marine vessel emissions. In: Proceedings from 17th Annual International Emission Inventory Conference, Portland, OR.

O'Brien, J.J., 1970, A note on the vertical structure of the eddy exchange coefficient in the planetary boundary layer. J. Atmos. Sci., 27, 1213-1215

Skamarock, W.C., Klemp, J.B., Dudhia, J., Gill, D.O., Barker, D.M., Duda, M.G., Huang, X.-Y., Wang, W., Powers, J.G., 2008. A Description of Advanced Research WRF version 3. NCAR/TN-475+STR, NCAR Technical Note

U.S. EPA, 2006," Guidance on Use of Modeled and Other Analyses for Demonstrating Attainment of Air Quality Goals for Ozone, $PM_{2.5}$ and Regional Haze NAAQS," U.S. EPA, Office of Air Quality Planning and Standards, Emissions, Monitoring, and Analysis Division, Air Quality Modeling Group, Research Triangle Park, North Carolina, September, 2006

WRAP, 2007, Western Regional Air Partnership, Technical Support System, Emissions Method, Offshore Emissions, http://vista.cira.colostate.edu/